Parameterization Schemes: Keys to Understanding Numerical Weather Prediction Models

Comments on Course Development and Chapter Problem Solutions

David J. Stensrud

This book is a compilation and expansion of the course notes developed for a graduate course in parameterization taught within the School of Meteorology at the University of Oklahoma. This course has been taught 7 times within a 15 week semester. There is a lot of material to cover in this short of a time period, and the graduate students are warned at the beginning that they will have to work hard. I am not certain that undergraduate students could handle this pace, and so have not allowed undergraduates to take this course. While I don't think the material is too advanced for senior level undergraduates, the pace would have to be decreased for them to participate fully. Most of the problems found at the end of each book chapter are assigned for homework, yielding a total of 10 problem sets. In addition, I have the students select a journal article at the beginning of the semester on a topic of their own choosing and provide a professional review of that article. The review is intended to mimic the peer-review process and serves two functions: 1) educate the students on how to provide a quality review, and 2) remind them that not everything in the literature is perfect.

The weekly course outline is as follows:

Week 1 – Introductions and Chapter 1: Why study parameterization schemes? I also review a few basics about primitive equation models (especially vertical coordinates) and stress that they need to take a more traditional numerical weather prediction course if they haven't already.

Weeks 2 and 3 – Chapter 2: Land surface-atmosphere parameterizations.

Weeks 4 and 5 - Chapter 3: Soil-vegetation-atmosphere parameterizations.

Week 6 - Chapter 4: Water-atmosphere parameterizations and turbulence closure overview from Chapter 5.

Week 7 - Chapter 5: Planetary boundary layer parameterizations.

Weeks 8 and 9 - Chapter 6: Convective parameterizations.

Weeks 10 and 11 - Chapter 7: Microphysics parameterizations.

Weeks 12 and 13 - Chapter 8: Radiation parameterizations.

Week 14 - Chapter 9: Cloud cover and cloudy sky radiation parameterizations.

Week 15 - Chapter 10: Orographic drag parameterization and final thoughts.

To get through this much material, the lectures need to be very organized and highlight only the most important and fundamental points of each chapter. Thankfully, the book can fill in a lot of details, so the lectures are really only needed to introduce the basic concepts and help dispel any misunderstandings that the students may develop. I typically hear grumbling about the number of problem sets and the amount of material covered, but also have heard from a number of students after they are out of school and gainfully employed who indicate that the class was very valuable.

It would be relatively easy to slow down the pace and offer the course over two successive semesters or quarters. This would allow the students more time to digest the material and projects could be added to have the students work directly with a numerical weather prediction model. During the first few times I taught this course in the mid-1990s, I divided the students into groups of 3 to 5 and had them use the Penn State-NCAR model to produce a simulation of an event of their choice. They would then run sensitivity tests to changes in parameterization schemes, or perhaps grid spacing, and summarize the results in an oral presentation to the class and a written report. However, as the material in the course grew the students no longer had the time to do a project in addition to keeping up with the problem sets, the paper review, and the mid-term and final exams.

I also hope that the reference list will help an instructor expand upon the book chapters and add additional material of importance to their particular students. However, I believe that it is important to introduce the students to these main types of parameterization schemes at some point during the teaching of this course. Thus, I hope that all the chapters will be covered at least briefly by anyone who teaches from this book.

If you find errors in these solutions, which almost certainly is the case, please let me know at David.Stensrud@noaa.gov. The correct answers would also be most welcome!

Table of Contents

Chapter 1 Solutions	4
Chapter 2 Solutions	7
Chapter 3 Solutions	34
Chapter 4 Solutions	58
Chapter 5 Solutions	66
Chapter 6 Solutions	90
Chapter 7 Solutions	108
Chapter 8 Solutions	129
Chapter 9 Solutions	139
Chapter 10 Solutions	146

Chapter 1

1] Do an internet search looking for information on operational and/or research numerical weather prediction models. Read over the outlines of what is available with regard to these systems. Based upon the information available on these web pages, list the positive and any negative aspects of each modeling system. Which one seems most complete and user friendly?

Solution:

There is no right or wrong answer to this question. The hope is that the students will spend some time searching on the web in order to learn something about the numerical models that are either available for use by researchers or are used to make forecasts. As a starting point, the following web sites describe numerical models that could be used for numerical weather prediction. Let's start with some of the larger international providers of numerical forecasts:

European Centre for Medium-range Weather Forecasting

http://www.ecmwf.int/products/

Japan Meteorological Agency

http://www.jma.go.jp/jma/jma-eng/jma-center/nwp/nwp-top.htm

Meteorological Services of Canada

http://www.msc-smc.ec.gc.ca/cmc/op_systems/index_e.html

U. S. National Centers for Environmental Prediction

http://www.emc.ncep.noaa.gov/

U. K. Met Office

http://www.metoffice.com/research/nwp/numerical/unified_model/index.html

One can also look at models developed more for use by researchers:

Advanced Regional Prediction System

http://www.caps.ou.edu/ARPS/index_flash.html

Community Climate System Model

http://www.ccsm.ucar.edu/

High-resolution Limited-Area Model

http://hirlam.org/

Rapid Update Cycle Model

http://maps.fsl.noaa.gov/

Regional Atmospheric Modeling System

http://rams.atmos.colostate.edu/

Regional Spectral Model

http://www.emc.ncep.noaa.gov/mmb/RSM/

The Penn State University - National Center for Atmospheric Research Mesoscale Model

http://www.mmm.ucar.edu/mm5

Weather Research and Forecast Model

http://www.wrf-model.org

There are other modeling systems available as well that have not been listed. Some of these are unknown to me, while others I wanted to list but had a hard time finding a good web site containing useful information. The point is that there are a number of modeling systems being used to make forecasts and being used in research. It is not always easy to find documentation on the details of these models, or to find out if one could download the model and compile it on your local computer. Thus, the intent is that the student see both the breadth of models available but also perhaps become a bit frustrated with the difficulties involved with learning about each model. In some ways, it might be useful to ask this question again at the end of this course and see what the students think after they know more about parameterization.

Chapter 2

1] The following mean wind data, sampled at various heights, occur above a vegetated canopy. Find the displacement depth *d* for this canopy.

Height (m)	Wind speed (m/s)
10	7.11
12	8.01
14	8.63
16	9.11
20	9.81
30	10.92
40	11.63

Typically, if ln(z-d) is plotted versus wind speed, the line will be concave upward if *d* is too small and concave downward if *d* is too large.

Solution:

The easiest way to approach this problem is to use a simple graphing program, such as Excel, to plot ln(z-d) versus wind speed and vary the value of *d*. You may want to suggest to the students that they try varying *d* by 0.5 m starting from 0 and increasing to 9 m. The answer is that a *d* value of 6.5 m yields a straight line and is the correct displacement depth. It may or may not be easy to get this exact value, but from the graph

you can see that values more than 1.5 m away from the true value show considerable curvature in the plots and are clearly not correct.

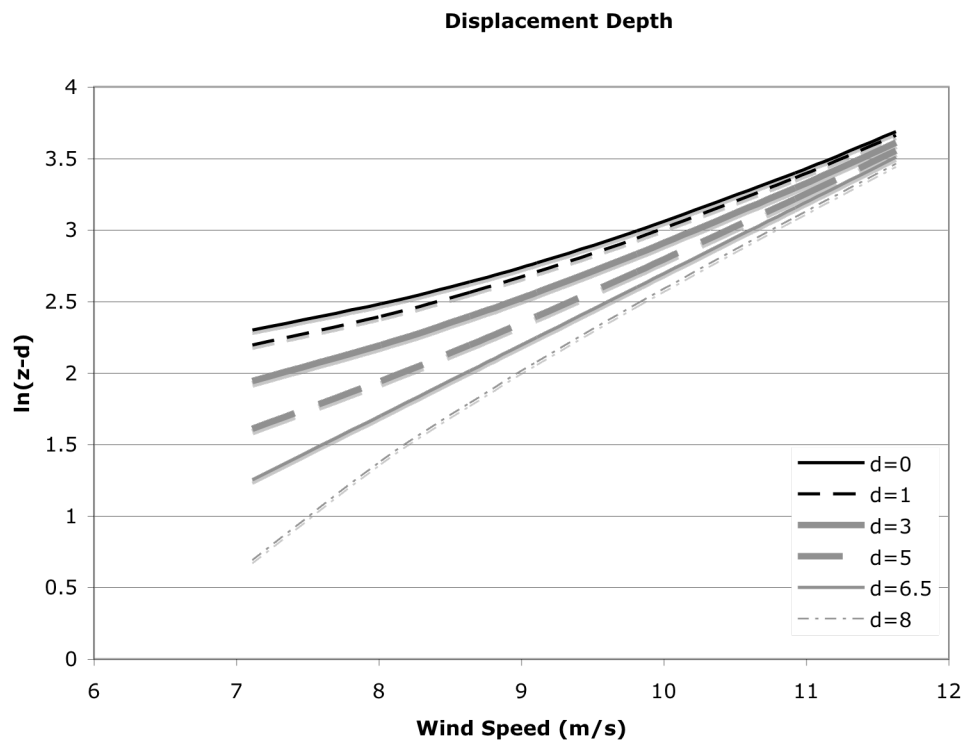

2] Given that T_g = 302K, T_{10m} = 294K, Q_H = 300 W m^{-2}, and ρ = 1.0 kg m^{-3}, calculate the resistance to sensible heat flux in the layer from the surface to 10 m above the surface. Assuming T_{2m} = 294.5K and z_0 = 0.01 m, what is the resistance from the surface to 2 m? Using this knowledge, estimate the resistance to sensible heat flux in the lowest 20 m above the surface and determine the temperature at this level. Is this temperature profile realistic? State any assumptions made and show all work.

Solution:

From (2.23) one can see that all the terms in the equation are defined except for the resistance. Thus, one can simply plug in the values and solve for resistance.

$$(2.23) \Rightarrow r_H = \frac{\rho c_p \Delta T}{Q_H} = \frac{(1)(1004)(8)}{(300)} = 26.77 \ sm^{-1}.$$

It is also wise to always check the units, which you can do and you'll find out that they work out to give resistance in s m^{-1} as needed.

Now the value of temperature at 2 m is given, along with the roughness length, and one is asked to calculate the resistance from the surface to the 2 m height. However, the roughness length really isn't needed to solve the question. Between the surface and 2 m, the temperature changes by 7.5 K. Thus, with knowledge that these heights are within the surface layer, where fluxes are assumed constant, we have

$$(2.23) \Rightarrow r_H = \frac{\rho c_p \Delta T}{Q_H} = \frac{(1)(1004)(7.5)}{(300)} = 25.1 \ sm^{-1}$$

and the resistance from 2 m to 10 m is then 26.77 - 25.1 = 1.67 s m^{-1}.

Finally, estimate the resistance in the lowest 20 m and determine the temperature at 20 m. Here an assumption is required to solve the problem. Assume that the resistance above 2 m is a linear function of height. Since the resistance increased by 1.67 s m^{-1} over 8 m, it will increase to 2.0875 s m^{-1} over 10 m (i.e., 1.67 * 10 / 8). Thus, the total resistance

from the surface to 20 m is 26.77 + 2.0875 = 28.8575 s m^{-1}. Equation (2.23) is then used one more time, assuming that the heat flux is still constant within the 20 m deep surface layer, to get

$$\Delta T = \frac{r_H Q_H}{\rho c_p} = \frac{(28.8575)(300)}{(1)(1004)} = 8.6228$$

which leads to a 20 m temperature of 302 - 8.6228 = 293.3772 K. So is this temperature realistic? Yes, since the 20 m temperature is less than the surface temperature. However, the lapse rate is certainly superadiabatic between 2 m and 20 m which may argue that the temperature profile is unrealistic.

3] Calculate the resistances for sensible heat flux assuming that u(20 m) = 10 m s^{-1} and that there are three different uniform vegetation types: h = 1.6 m for one vegetation height, h = 0.8 m for another, and h = 0.1 m for the third. State any assumptions made. Which resistance is larger? Assuming a 10 K temperature potential, calculate the differences in sensible heat flux from these three resistances. What does this say about the importance of the roughness length in models?

Solution:

The key equation for solving this problem is (2.49) that defines the resistance to sensible heat flux. To make life much easier, and since the question provides no information on stability, assume that the layer has neutral stability. Also assume that z_0 = h/8, that z_{0h} = z_0/7 as shown in (2.50), and that the displacement depth is zero.

Using these assumptions, one finds that for a vegetation height of 1.6 m, z_0 = 0.2 m, for a height of 0.8 m, z_0 = 0.1 m, and for a height of 0.1 m, z_0 = 0.0125 m. If (2.49) is now examined, the only missing term is the friction velocity u_*. This can be calculated using the log wind profile (2.30), where one finds that with a bit of rearranging that

$$u_* = \frac{\bar{u}k}{\ln\left(\frac{z}{z_0}\right)},$$

where z is used instead of z_{eff} since the displacement depth is assumed to be zero. Plugging in the values from the question yields u_* = (10)(0.4)/ln(20/0.2) = 0.8686 m s^{-1}.

Using (2.49), one can now calculate the resistance to heat flux

$$r_H = \frac{1}{ku_*}\ln\left(\frac{z}{z_0}\right) + \frac{1}{ku_*}\ln\left(\frac{z_0}{z_{0h}}\right) = \frac{1}{(0.4)(0.8686)}\ln\left(\frac{20}{0.2}\right) + \frac{1}{(0.4)(0.8686)}\ln(7)$$

$$= 13.25 + 5.6 = 18.85 \;\; sm^{-1}$$

The 7 in the right-most natural logarithm is from the assumption of (2.50) and so is constant for all the calculations. Following this same approach for the other 2 vegetation heights yields friction velocities of 0.755 and 0.542 m s^{-1} for the vegetation heights of 0.8 and 0.1 m, respectively. The resistances are then 24.15 and 43.01, respectively. Thus, the resistances increase as both the roughness length decreases and the roughness length

for heat decrease. This makes sense, since the depth over which the resistance is calculated increases as the roughness lengths decrease. This confirms that resistance is proportional to length.

Finally, one assumes a 10 K potential difference from the surface to the 20 m height and calculates the sensible heat flux using (2.23) or (2.43) to yield for the 1.6 m vegetation height that

$$Q_H = \frac{\rho c_p \Delta T}{r_H} = \frac{(1)(1004)(10)}{18.85} = 532.6 Wm^{-2},$$

assuming a density of 1 kg m^{-3}. For the other 2 vegetation heights, one finds that the sensible heat flux is 415.74 and 233.43 W m^{-2}. Thus, the differences in sensible heat flux from the 1.6 m vegetation height are 117 W and 299.17 W m^{-2} as the vegetation height is first halved and then reduced by another 1/8th. This analysis suggests that roughness lengths are *very important* to specify correctly in numerical models.

4] Using the same three vegetation types as described in 3], calculate the resistances to latent heat flux. Assuming a 0.02 kg kg^{-1} specific humidity potential [$\Delta q = q_s(T_g)-q(z)$] and a canopy resistance of 200 s m^{-1}, what are the latent heat fluxes for the three vegetation heights? Do the changes in the relative values of latent and sensible heat fluxes over the three different vegetation types make sense? What is the value of moisture availability?

Solution:

Begin by noting that the equation for resistance to latent heat flux (2.62) is nearly the same as the equation for resistance for sensible heat flux (2.49), with a difference only in the last term. Thus, portions of the calculations for the previous question can be used to solve this question as well. So we can begin by using the same friction velocities as calculated in the previous problem, and make the same basic assumptions (neutral stability, atmospheric density of 1 kg m^{-3}). Using (2.62) we find that for the 1.6 m vegetation height

$$r_V = \frac{1}{ku_*}\ln\left(\frac{z}{z_0}\right) + \frac{1}{ku_*}\ln\left(\frac{z_0}{z_{0h}}\right)\left(\frac{\kappa}{D_v}\right)^{2/3}$$

$$= \frac{1}{(0.4)(0.8686)}\ln\left(\frac{20}{0.2}\right) + \frac{1}{(0.4)(0.8686)}\ln(7)(0.93)^{2/3} = 13.25 + 5.34 = 18.59\ sm^{-1}$$

Similarly, for the 0.8 and 0.1 m vegetation heights one finds that r_V = 23.82 and 42.58 s m^{-1}, respectively. Note that these resistance values are all slightly smaller than the resistances calculated for sensible heat flux, as expected from (2.62).

The latent heat flux is then defined using (2.64) in which

$$Q_E = \frac{M\rho L_v \Delta q}{r_a + r_{bv}},$$

suggesting that we need to determine the moisture availiability M. This variable is defined in (2.65) where for the 1.6 m vegetation height we find that

$$M = \frac{r_a + r_{bv}}{r_a + r_{bv} + r_c} = \frac{18.59}{18.59 + 200} = 0.085.$$

knowing that the canopy resistance r_c is 200 s m^{-1}. Similar calculations for the 0.8 and 0.1 m vegetation heights yields M values of 0.1064 and 0.176, respectively. Using the equation for latent heat flux, we then find that

$$Q_E = \frac{M\rho L_v \Delta q}{r_a + r_{bv}} = \frac{(0.085)(1)(2.5x10^6)(0.02)}{18.59} = 228.62\ Wm^{-2}.$$

Similarly, for the 0.8 and 0.1 m vegetation heights, one finds that the latent heat flux is 223.34 and 206.67 W m^{-2}. Thus, the latent heat flux increases slightly as the vegetation height increases. In contrast, over the same changes in vegetation height, the sensible heat flux changed by a factor of 2! The difference is that the canopy resistance term in the latent heat flux calculation dominates, and so the latent heat flux is much less sensitive to changes in the atmospheric resistances. So do the changes in the relative values of sensible and latent heat flux make sense? Yes, they do once you realize the importance of the canopy resistance term.

5] Draw a typical diurnal cycle for each of the terms (R_{net}, Q_G, Q_E, and Q_H) of the surface energy budget. Then draw an energy flux diagram and show the magnitudes and signs of

each term at 1200 local noon and 0400 local morning (before sunrise). Why are these values realistic? Explain.

Solution:

This problem is intended to make the students think about the diurnal energy cycle and gain some appreciation for the relative magnitudes of the different terms. While there are no specific answers to this question, there certainly are wrong answers.

A definition is needed to define the signs of the terms. Here it is assumed that positive flux values act to warm the surface, while negative flux values act to cool the surface. Thus, under clear sky conditions in midlatitudes or tropical latitudes, net radiation is generally going to be large and positive during the daytime (owing to incoming solar radiation acting to heat the ground) and small and negative at night (outgoing longwave greater than incoming longwave so cooling of the ground occurs). Sensible and latent heat fluxes tend to follow the net radiation, but with opposite signs. Thus, sensible and latent heat fluxes are large and negative during the daytime (acting to move heat away from the ground surface and hence cool it) and small and positive at night. Ground heat flux follows the sensible and latent heat fluxes, also being larger and negative during the daytime and positive at night. However, ground heat flux usually is not quite in sync with the other heat fluxes and has a slight phase shift to later times of maximum values.

The magnitudes of the fluxes are determined by the net radiation. This term is dominated by the incoming solar radiation, so certainly cannot exceed the solar constant. Depending

upon the latitude under consideration, values could range from small positive numbers to values approaching 1000 W m^{-2}. A student could choose a location above the Arctic Circle during the wintertime, but this has not happened yet. The 3 heat fluxes, since they differ in sign, should sum to the value of the net radiation as indicated by (2.102). If not, then the surface energy budget is not in balance. So the values chosen are realistic if the surface energy budget balances and are not realistic if the energy budget is out of balance.

A typical example of the resulting diurnal cycle is shown below along with the two energy flux diagrams. Remember that arrows pointing toward the ground surface (the horizontal thin line) act to warm the ground, whereas arrows pointing away act to cool the ground surface. Again, there is no specific correct answer, but the general rules discussed above can be used to evaluate the solutions and determine if any of them are obviously incorrect. Also note that the net radiation at night often is less than 100 W m^{-2} in magnitude.

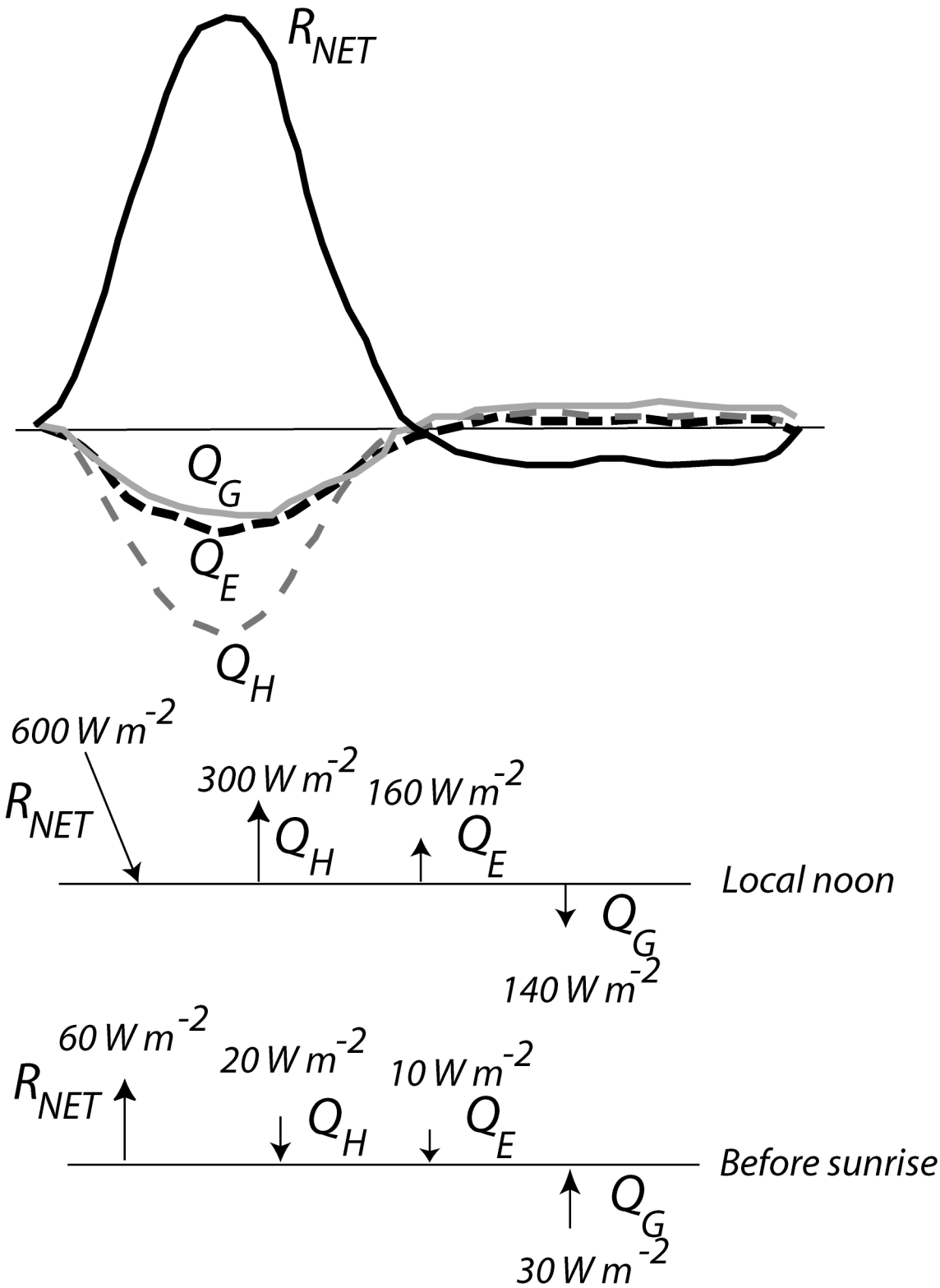
R_{NET}
Q_G
Q_E
Q_H
600 W m^{-2}
R_{NET}
300 W m^{-2}
Q_H
160 W m^{-2}
Q_E
Local noon
Q_G
140 W m^{-2}
60 W m^{-2}
R_{NET}
20 W m^{-2}
Q_H
10 W m^{-2}
Q_E
Before sunrise
Q_G
30 W m^{-2}

6] Write a computer program to calculate the change in surface temperature over an entire daytime heating cycle (sunrise to sunset) using the force-restore method. Assume that the calculation is for near Amarillo, Texas on 30 June, 1999 (35.2 latitude, -102.0 longitude), and begin the calculations at sunrise and end the calculations at sunset. To actually do this without attaching the surface to a boundary layer model, we have to make some pretty stringent assumptions: assume the atmospheric transmissivity is constant at 0.8, the solar constant is 1368 W m^{-2}, the Earth's orbit is circular, the thermal capacity of the slab (c_g) is 1.4×10^5 J m^{-2} K^{-1}, the skies are clear, the Bowen ratio is 0.7, the temperature at 40 hPa above the ground surface is equal to 25°C, the initial temperature of the ground surface (skin temp) is 23°C, the reservoir temperature is 25°C, the precipitable water is 2.5 cm, the emissivity is 0.95, and the albedo is 20%. Run two experiments. First, assume the sensible heat flux is 15% of the net radiation received at the surface, and second assume that the sensible heat flux is 30% of the net radiation received at the surface. Plot the radiation amounts on one graph, show the change in ground (skin) temperature on another, and plot the various surface fluxes (sensible, latent, and ground) on yet another graph. What is the phase relationship between the ground (skin) temperature and the heat flux into the ground? What are the times of sunrise and sunset? What is the maximum value of incoming solar radiation?

Remember that

$$\frac{\partial T_g}{\partial t} = \frac{1}{c_g}\left[Q_S + Q_{Ld} - Q_{Lu} - Q_H - Q_E - \kappa(T_g - T_r)\right]$$

where κ is assumed to be constant at 11 J m^{-2} K^{-1} s^{-1} and T_r is the reservoir temperature (K). It is assumed that the energy loss due to the surface albedo is already included in Q_S.

Solution:

A fortran 77 program to solve this question is shown below. Time of sunrise is 11.6667 UTC (1140 UTC), time of sunset is 26.00 (0200 UTC), and the maximum solar radiation is 856.45 W m^{-2}. Plots also are shown for the 2 cases of sensible heat flux being 15 and 30% of the net radiation. These indicate that the ground heat flux and ground temperature are in phase, while they are slightly offset from the other fluxes that peak earlier in the day.

```
      program homework2_6
c**   Calculate the change in surface temperature at Amarillo, TX, using
c**   basic formulas in Chapter 2.  David Stensrud 2006.
c
c**   Use Monteith formula to calculate downwelling radiation, Stefan-
c**   Boltzmann Law, and formulas for zenith angle from early in Chapter 2.
c**   Assumptions:
c**   1)  Sensible heat flux is 15% of net radiation
c**   2)  Sensible heat flux is 30% of net radiation
c**   and we are given the Bowen ratio to calculate the latent heat flux
c**   and the soil conductivity to calculate the ground heat flux.
c
c**   This program uses NCAR graphics to plot the fields needed to answer the
c**   questions.  If this program is not available on your system, then simply
c**   write out the values and read them in using Excel or some other spreadsheet
c**   software with plotting abilities.
c
c**    Variable names:
c
c**    fact - fraction of rnet for sensible heat flux (0.15 or 0.30)
c**    a - albedo
c**    bowen - bowen ratio
c**    cg - thermal capacity of the slab
c**    delta - declination angle
```

```
c**     dt - time step size (in seconds)
c**     dtr - constant conversion factor for degrees to radians
c**     emiss - emissivity
c**     h  - local hour of the day.  Choose initial value before sunrise.
c**         (below selected 11 UTC as start time)
c**     kappa - soil conductivity
c**     omega - Stefan-Boltzmann constant
c**     pi - pi (3.1415927...)
c**     qe, qeflux - latent heat flux
c**     qgflux - ground heat flux
c**     qh, qhflux - sensible heat flux
c**     qld - downwelling longwave component
c**     qlu - upwelling longwave component
c**     qs - shortwave radiation component
c**     rnet - net radiation
c**     s -  incoming shortwave radiation (including albedo effects)
c**     solar - solar constant
c**     ta - air temperature 40 mb above surface
c**     tau - transmissivity
c**     tg, tgr - ground temperature
c**     time - time (hours)
c**     tm - reservoir temperature of soil
c**     wp - precipitable water
c**     xlat - latitude (degrees)
c**     xlon - longitude (degrees)
c
      real tau,a,omega,emiss,wp,tm,rnet,solar,qh,qs,qld,qlu,kappa
      real time(288),s(288),tgr(288),qgflux(288)
      real qeflux(288),qhflux(288)
c
c       define variables that are fixed in the program
c**
c**     fact must be changed to run the two scenarios.  First, fact=0.15 and
c**     then fact=0.30
c**
c
      fact=0.15
      a=0.20
      bowen=0.7
      cg=1.4e+05
      emiss=0.95
      kappa=11.0
      omega=5.67e-08
      solar=1368.
      ta=298.15
      tau=0.8
```

```
      tg=296.15
      tm=298.15
      wp=2.5
      xlat=35.2
      xlon=-102.
c
      pi=4.*atan(1.)
      dtr=pi/180.
      dt=5.*60.
      xsunrise=-10.
      xsunset=10.
      xmaxrad=0.
c
c**     calculate declination angle for this location
c**     Note that 30 June 1999 is Julian day 181.
c
      delta=23.45*cos( (2.*pi*(181.-173.)) /365.25 )
      print *,'declanation angle is ',delta
c
c*********************************************************************
c*********************************************************************
c       loop over the 24 h day at 5 minute intervals and determine various parameters
c*********************************************************************
c*********************************************************************
c
     do 10 i=1,288
c
      h = ( (11.+ (i-1)*5./60.-12.0)*pi )/12. +xlon*pi/180.
      time(i) = 11.+float(i-1)*5./ 60.
      rnside=sin(xlat*dtr)*sin(delta*dtr)+
     &        cos(xlat*dtr)*cos(delta*dtr)*cos(h)
      zenith=acos(rnside)
      qs=solar*(1.-a)*tau*rnside
      if(qs.lt.0.0) qs=0.0
      s(i) = qs
      if(qs.gt.0.0.and.xsunrise.lt.0.) then
       xsunrise=time(i)
       xsunset=-10.
      end if
      if(qs.lt.0.0.and.xsunset.lt.0.) then
       xsunset=time(i)
      end if
      if(qs.gt.xmaxrad) then
       xmaxrad=qs
      end if
c
```

```
c**    According to question, start calculations at sunrise and end at sunset
c
      if(qs.gt.0.0) then
c
       qlu=emiss*omega*tg**4
       qld=emiss*(0.725+0.17*log10(wp))*omega*ta**4
       rnet=qs+qld-qlu
       qh=fact*rnet
       qe=(1./bowen)*qh
       tgnew=tg + (1./cg) * (rnet - qh - qe
     1         - kappa*(tg-tm) ) * dt
        tg = tgnew
        qhflux(i)=-qh
        qeflux(i)=-qe
        qgflux(i)=-kappa*(tg-tm)
        tgr(i)=tg
       else
        qeflux(i)=0.
        qhflux(i)=0.
        qgflux(i)=0.
        tgr(i)=tg
       end if
c
 10    continue
c
c**     print out time (UTC) of sunrise, sunset, and also maximum value of qs
c
      print *,' sunrise at ',xsunrise
      print *,' sunset at ',xsunset
      print *,' maximum solar radiation (including albedo)',xmaxrad
c
c**   plot time evolution of solar flux, sensible, latent, and ground heat flux,
c**   and ground temperature using NCAR graphics
c
      call opngks
      call gopwk(3,4,3)
      call ezxy(time,s,288,'Solar flux$')
      call ezxy(time,qhflux,288,'Sensible heat flux$')
      call ezxy(time,qeflux,288,'Latent heat flux$')
      call ezxy(time,qgflux,288,'Ground heat flux$')
      call ezxy(time,tgr,288,'Ground temperature$')
      call gclwk(3)
      call clsgks
c
      stop
      end
```

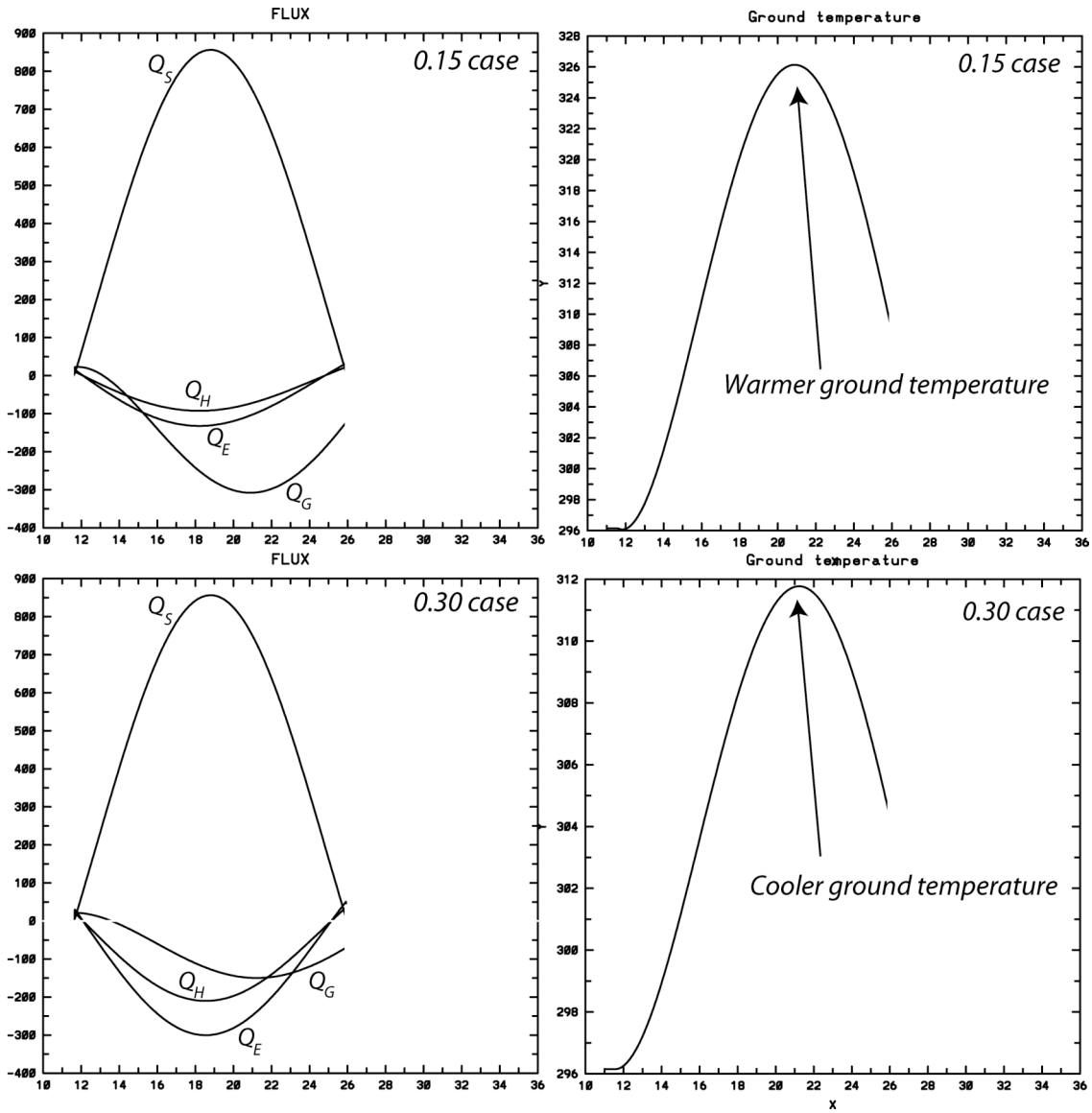

Flux values above are in W m^{-2}, while temperatures for the right side plots are in K. Postive values of flux act to warm the ground surface, negative values act to cool the ground surface. Note that the ground temperature in the 15% sensible heat flux simulation (~326 K) is much warmer than the 30% case (~312 K), owing to the large amount of energy that is available to warm the ground. This is a simple model that is fun to play with, so challenge your students to vary more relationships and see how sensitive the results are to the energy partitioning!

7] Seguin and Gignoux (1974) made wind speed measurements at a number of heights over two adjacent, yet very different, regions. One region consisted of cypress hedges 7 m in height and separated by short grass of roughly 10 cm tall. The other region consisted of grass only with a height of roughly 40 cm (see Fig. 2.25). Both regions were large and separated by sufficient distance to allow them to be considered independent regions. The wind speeds at the top of the surface layer at 50 m above ground level (over which the flux profile laws apply) were virtually identical above both the cypress hedges and the 40 cm grass regions. However, the profiles down to the ground were different. The log-wind profile in the grass-only region simply responded to a surface of grass 40 cm high. The log-wind profile in the hedge region first responded to a vegetation canopy at the height of the cypress hedges (7 m), while the log-wind profile below the hedge top responded to the short grass (10 cm). The height of the hedge top is where they observed this change in the log-wind profile behavior in the region with hedges.

a) Calculate and show graphically the wind speed profiles in the two regions and the difference in wind speed at hedge top level and at 2 m between the hedge and grass-only regions for a wind speed of 10 ms^{-1} at 50 m. Assume neutral static stability. [Note that the two wind regimes in the hedge region must be meshed. The upper regime has a different roughness from the lower.] Calculate the three relevant friction velocities for the problem. Helpful hint: $z_o \approx$ h/8 where h is the average height of the grass or hedge. Comment on the differences in wind speed between the two regions.

Solution:

This exercise is all about using the log wind profile. We will use the suggested relationships between roughness length and displacement depth that are discussed in section 2.4, namely $z_0 \sim h/8$ and $d \sim 3h/4$ where h is the vegetation height. For the grass region, the wind speed follows the same log wind profile from 50 m down to the roughness length. This should be easy to calculate. However, for the winds in the hedge region, the wind speeds follow 2 different log wind profiles. One profile responds to the hedges and is followed from 50 m down to the height of the hedge tops at 7 m. The second wind profile responds to the 10 cm tall grasses and is followed from the top of the hedges at 7 m down to the roughness length for this shorter grass. Thus, to figure out the wind profile below hedge top, one must know the wind speed at hedge top. This wind speed is not provided, and so must be calculated.

Let's begin with the 40 cm tall grass region. Here z_0 = .40/8 = 0.05 m, and d = 0 (one can calculate d and use it in the equation, but to the first two decimal places it has no effect). To determine the wind speed as a function of height, we need to use the log wind profile equation (2.30). However, one immediately noticed that the friction velocity is not specified. Calculate it using the data available at the 50 m height. Thus,

$$u_* = \frac{\bar{u}k}{\ln\left(\frac{z_{eff}}{z_0}\right)} = \frac{(10)(0.4)}{\ln\left(\frac{50}{0.05}\right)} = 0.58ms^{-1}.$$

Then this value of u* can be used to calculate the wind speeds at 7 and 2 m heights. For the 7 m height, this yields

$$\bar{u} = \frac{u_*}{k}\ln\left(\frac{z_{eff}}{z_0}\right) = \frac{0.58}{0.4}\ln\left(\frac{7}{0.05}\right) = 7.17ms^{-1},$$

and using the same expression at a 2 m height yields a wind speed of 5.34 m s^{-1}. If using non-zero *d* values, then the wind speeds decrease to 7.10 and 5.11 m s^{-1}.

In the hedge region, one first must find the wind speed at the hedge top height of 7 m and then define a new log wind profile from this height down to the surface. Above the 7 m tall hedge, z_0 = 7/8 = 0.875 m and *d* = 3*7/4 = 5.25 m. Using the log wind profile to again solve for the friction velocity, one finds that

$$u_* = \frac{\bar{u}k}{\ln\left(\frac{z_{eff}}{z_0}\right)} = \frac{(10)(0.4)}{\ln\left(\frac{50-5.25}{0.875}\right)} = 1.016ms^{-1},$$

and then the wind speed at 7 m height is

$$\bar{u} = \frac{u_*}{k}\ln\left(\frac{z_{eff}}{z_0}\right) = \frac{1.016}{0.4}\ln\left(\frac{7-5.25}{0.875}\right) = 1.76ms^{-1}.$$

Below the hedge, the winds respond to the 10 cm tall grasses. Here $z_0 = 0.10/8 = 0.0125$ m and $d = 0$ m. Once again the first step is to calculate the friction velocity for this log wind profile, namely

$$u_* = \frac{\bar{u}k}{\ln\left(\frac{z_{eff}}{z_0}\right)} = \frac{(1.76)(0.4)}{\ln\left(\frac{7}{0.0125}\right)} = 0.11 ms^{-1}.$$

Finally, the wind speed at 2 m height can be calculated from

$$\bar{u} = \frac{u_*}{k}\ln\left(\frac{z_{eff}}{z_0}\right) = \frac{0.11}{0.4}\ln\left(\frac{2}{0.0125}\right) = 1.4 ms^{-1}.$$

The difference in winds at the 2 m height is 5.34 - 1.4 = 3.94 m s^{-1}, and at hedge top the wind speed difference is 7.17 - 1.76 = 5.41 m s^{-1}. These are pretty large differences, especially when one remembers that stress is proportional to the square of the wind speed. This yields differences in stress between the two regions of more than an order of magnitude!

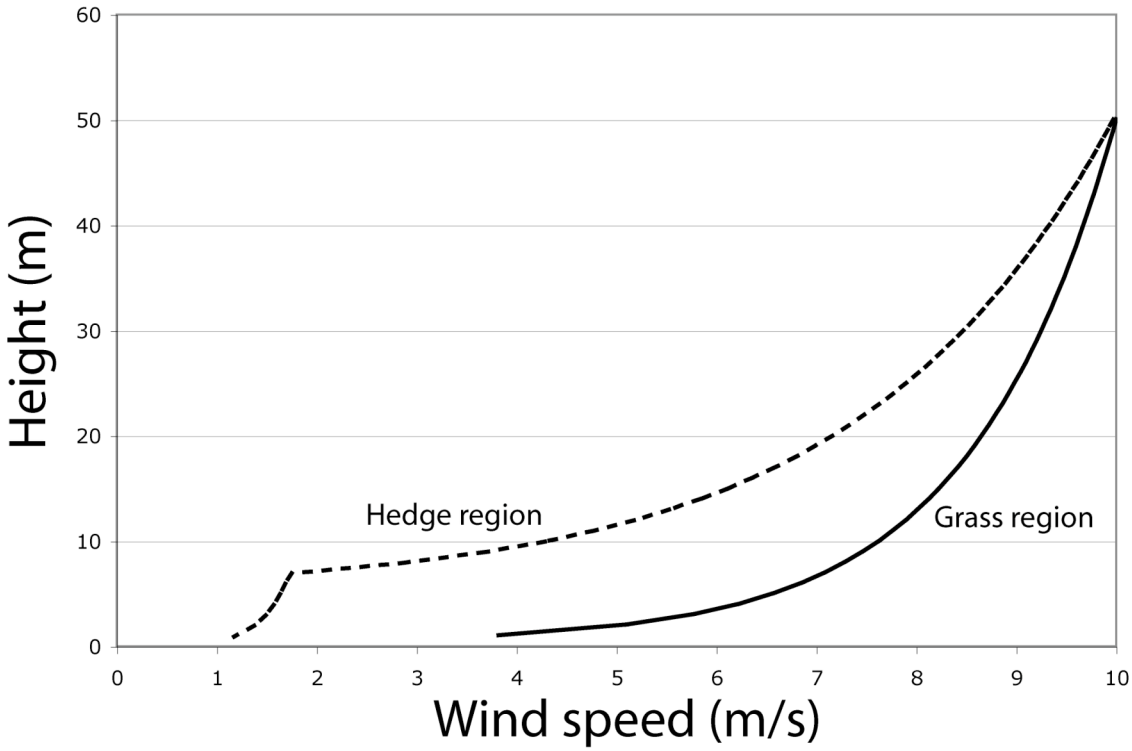

Wind speed profiles for the hedge and 40 cm tall grass regions.

b) Calculate the values of resistance to sensible heat flux from the surface to 50 m for the two regions. Assuming a potential difference of 10 K, what are the values of heat flux over these two regions? If the grass-only region, as depicted at the far right of Fig. 2.25, has the cypress hedge internal boundary layer above it, how might one estimate the change in resistance to heat flux above the grass-only region? Using this estimation technique, how big of a difference in the value of resistance does this make?

Solution:

Recall that the resitance equation for sensible heat flux is

$$r_H = \frac{1}{ku_*}\ln\left(\frac{z_{eff}}{z_0}\right) + \frac{1}{ku_*}\ln\left(\frac{z_0}{z_{0h}}\right).$$

The difference in the calculations over the 40 cm grass and the hedge region is that the first term in the resistance equation has two parts in the hedge region: from the roughness length to hedge top and from hedge top to 50 m. Above the hedge region we know that $u_* = 1.016$ and $d = 5.25$, while below the hedge top we know that $u_* = 0.11$ and $z_0 = 0.0125$. Thus, we find that

$$r_H = \frac{1}{(0.4)(1.016)}\ln\left(\frac{50-5.25}{7-5.25}\right) + \frac{1}{(0.4)(0.11)}\ln\left(\frac{7}{0.0125}\right) + \frac{1}{(0.4)(0.11)}\ln(7)$$

$$= 7.98 + 143.82 + 44.22 = 196.02$$

The sensible heat flux is then

$$Q_H = \frac{\rho c_p \Delta T}{r_H} = \frac{(1)(1004)(10)}{196.02} = 51.22 Wm^{-2}.$$

Over the 40 cm grass region,

$$r_H = \frac{1}{(0.4)(0.58)}\ln\left(\frac{50}{0.05}\right) + \frac{1}{(0.4)(0.58)}\ln(7) = 29.77 + 8.39 = 38.16 sm^{-1},$$

and the sensible heat flux is then

$$Q_H = \frac{(1)(1004)(10)}{38.16} = 263.1 Wm^{-2}.$$

Thus, the sensible heat fluxes differ by a factor of 5 between the hedge region and the 40 cm grass region! This is because the resistances differ by a factor of 5, which is a very large difference with obvious consequences in the calculation of flux.

To estimate changes in the resistance due to the cypress hedge internal boundary layer being above the grass-only region, one needs to estimate the depth of this internal boundary layer. Starting from the 50 m height, replace the resistance for the grass-only region with the resistance from the hedge region over successively larger depths. If z_1 is the height above the ground at which the hedge internal boundary layer is reached, then the resistance can be estimated using

$$r_H = \frac{1}{(0.4)(1.016)} \ln\left(\frac{50 - 5.25}{z_1 - 5.25}\right) + \frac{1}{(0.4)(0.58)} \ln\left(\frac{z_1}{0.05}\right) + \frac{1}{(0.4)(0.58)} \ln(7).$$

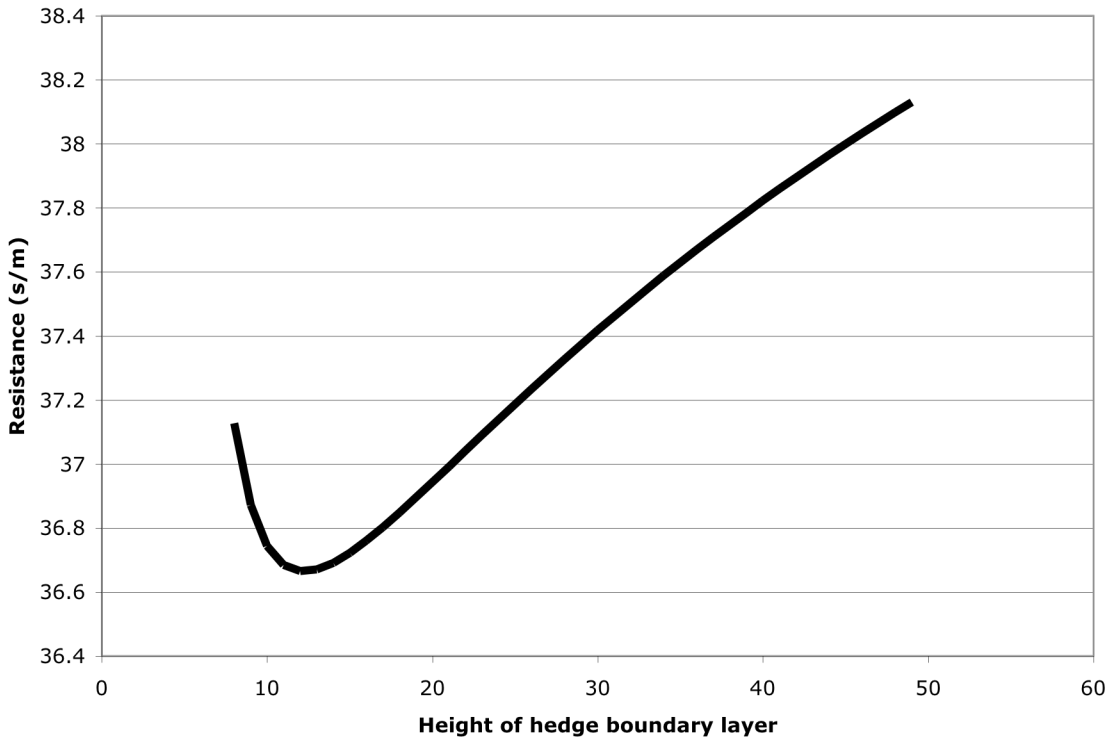

Resistance from mixed grass-only and cypress hedge boundary layers as a function of the height at which the bottom of the cypress hedge internal boundary layer is reached. While the variation is not large, the shape of the resistance profile is curious and reaches a minimum at a height of 12 m.

[This question 7 is based upon course notes from a bioclimatology class taught by Dr. Toby Carlson at The Pennsylvania State University in the late 1980s. I thought the question was excellent at the time and still think it illustrates many important points.]

8] At a given surface observing site, the roughness length is 0.1 m, and at a particular time during the daytime the friction velocity $u_* = 0.85$. The site has two heights at which temperature is observed: 10 and 2 m. The 10 m temperature is 295.4 K and the 2 m

temperature is 298.0 K. Determine the ground temperature and the surface sensible heat flux.

Solution:

This question returns again to using the equation for sensible heat flux and resistance. Recall that fluxes are constant in the surface layer, and that the sensible heat flux is defined as

$$Q_H = \frac{\rho c_p \Delta T}{r_H}.$$

With the information given one can determine the sensible heat flux from the temperature difference if we can calculate the needed resistance. Unlike the earlier problems, the friction velocity and roughness length are provided. Thus, assuming neutral stability the resistance in the layer from 2 to 10 m is given by

$$r_H = \frac{1}{ku_*}\ln\left(\frac{z_2}{z_1}\right) = \frac{1}{(0.4)(0.85)}\ln\left(\frac{10}{2}\right) = 4.73 sm^{-1}.$$

Thus, the sensible heat is found to be

$$Q_H = \frac{\rho c_p \Delta T}{r_H} = \frac{(1)(1004)(298-295.4)}{4.73} = 551.88 Wm^{-2}.$$

To solve for the ground temperature, we need to determine the resistance from 10 m down to the roughness length for heat. This is calculated from

$$r_H = \frac{1}{ku_*}\ln\left(\frac{z_{eff}}{z_0}\right) + \frac{1}{ku_*}\ln\left(\frac{z_0}{z_{0h}}\right) = \frac{1}{(0.4)(0.85)}\ln\left(\frac{10}{0.1}\right) + \frac{1}{(0.4)(0.85)}\ln(7)$$

$$= 13.54 + 5.72 = 19.26 sm^{-1}$$

The sensible heat flux equation is then used to solve for the ground temperature, such that

$$T_g = \frac{Q_H * r_H}{\rho c_p} + T_{10m} = \frac{(551.88)(19.26)}{(1)(1004)} + 295.4 = 305.99K.$$

Chapter 3

1] The following data were taken over a tall grass field at Norman, Oklahoma on 17 May 2004 at local noon.

IR Surface Temperature:	37°C
Air Temperature:	28°C at 2 m
Specific Humidity of air:	14 g kg^{-1} at 2 m
Wind Speed:	7.0 m s^{-1} at 10 m
Vegetation height:	1.0 m
Leaf Area Index:	2.0
Net Radiation:	600 W m^{-2}
Ground Heat Flux:	100 W m^{-2}

Rainfall totals of slightly more than 0.25 inch occurred the day before.

a) Calculate the sensible heat flux, assuming neutral stability for the log profile laws. Using the surface energy balance and the calculated sensible heat flux, solve for the evapotranspiration flux.

Solution:

We know that $z_0 = h/8 = 1./8. = 0.125$ m for this case. Using the neutral stability assumption and further assuming a zero displacement depth, one can then calculate the friction velocity from the information provided. Thus,

$$u_* = \frac{\overline{u}k}{\ln\left(\frac{z_{eff}}{z_0}\right)} = \frac{(7)(0.4)}{\ln\left(\frac{10}{0.125}\right)} = 0.64 ms^{-1}.$$

If the displacement depth is assumed to be non-zero, then the friction velocity is 0.64 m s^{-1}. Once the friction velocity is known, then it is easy to calculate the resistance using (2.49), such that

$$r_H = \frac{1}{ku_*}\left[\ln\left(\frac{z_{eff}}{z_0}\right) + \ln\left(\frac{z_0}{z_{0h}}\right)\right] = \frac{1}{(0.4)(0.64)}\left[\ln\left(\frac{2}{0.125}\right) + \ln(7)\right] = 18.43 \text{ sm}^{-1}.$$

It is important to note that this resistance is calculated from the surface to the 2 m height, since this is where we have a temperature observation. The wind observation is at 10 m, which allows us to calculate the friction velocity, but the only way to calculate the sensible heat flux is with knowledge of the temperature difference and this information is only available at the 2 m height!

Now one can calculate the sensible heat flux from

$$Q_H = \frac{\rho c_p \Delta T}{r_H} = \frac{(1)(1004)(9)}{(18.43)} = 490.3 Wm^{-2}.$$

The surface energy balance then yields

$$R_{NET} - Q_H - Q_E - Q_G = 0$$

$$\Rightarrow Q_E = R_{NET} - Q_H - Q_G = 600 - 490.3 - 100 = 9.7 Wm^{-2}$$

But this doesn't make sense! The information given indicates that the data were taken over a 1 m tall grass field in May (during the warm season) and that it rained more than 0.25 inches the day before. One would expect more latent heat flux than a small value of 9.7 W m^{-2} at local noon! Looking back at our assumptions, the one variable that has several expressions is the roughness length for heat, z_{0h}. Let's try another formula for this roughness length and see how much difference it makes and if the results become more realistic.

A second expression for the roughness length for heat is (2.51), which indicates that

$$z_{0h} = \frac{\alpha \kappa_m}{k u_*},$$

where $\kappa_m = 0.18 \times 10^{-4}$ m^2 s^{-1} is the molecular thermal diffusivity of air, and α is a fudge factor that is typically set to 1. Using this expression, one finds that

$$z_{0h} = \frac{\alpha \kappa_m}{k u_*} = \frac{(1)(0.18x10^{-4})}{(0.4)(0.64)} = 7.0x10^{-5} m.$$

Using this roughness length to calculate the resistance yields

$$r_H = \frac{1}{ku_*}\left[\ln\left(\frac{z_{eff}}{z_0}\right) + \ln\left(\frac{z_0}{z_{0h}}\right)\right] = \frac{1}{(0.4)(0.64)}\left[\ln\left(\frac{2}{0.125}\right) + \ln\left(\frac{0.125}{7x10^{-5}}\right)\right] = 40sm^{-1}!$$

This is nearly double the value originally calculated. Replacing the value for resistance in the sensible heat flux equation above yields Q_H = 226 W m^{-2} and then surface energy balance requires that Q_E = 600 - 226 - 100 = 274 W m^{-2}. This value of latent heat flux makes a lot more sense given the observations.

This question is intended to help the students learn that one needs to always be thinking about whether or not the answers are reasonable. It also illustrates that the formulas used for roughness length for heat can make a large difference in the answers one calculates! For this problem, the sensible heat flux differs by a factor of 2 depending upon how the roughness length is calculated. One could also use (2.52) to calculate the resistance, arriving at yet a third answer.

b) Calculate the Monin-Obukhov length using the value of u_* calculated above. Note that Stull (1988) shows that

$$\overline{w'\theta_v'} = \overline{w'\theta'}\left[1 + 0.61\overline{q}\right] + 0.61\overline{\theta}(\overline{w'q'}).$$

Solution:

To answer this question, one must be able to convert from sensible heat flux units of W m^{-2} to K m s^{-1} and latent heat flux values from W m^{-2} to (kg/kg) m s^{-1}. For sensible heat flux, simply divide by ρc_p. For latent heat flux, divide by ρL_v. Thus, assuming a surface pressure of 1000 hPa, the buoyancy flux is simply

$$\overline{w'\theta_v'} = \frac{Q_H}{\rho c_p}(1+0.61\overline{q}) + 0.61\overline{\theta}\frac{Q_E}{\rho L_v}$$

$$= \frac{226}{(1)(1004)}(1+0.61(0.014)) + 0.61(273.15+28)\frac{274}{(1)(2.5x10^6)}$$

$$= 0.225(1.00854) + 183.70(0.0001096) = 0.247 Kms^{-1}$$

Now one can calculate the Monin-Obukhov length using (2.41) which yields

$$L = -\frac{\overline{\theta}_v u_*^3}{kg(\overline{w'\theta_v'})_{sfc}} = -\frac{(303.72)(0.64)^3}{(0.4)(9.81)(0.247)} = -82.15 < 0.$$

A negative value of L indicates unstable conditions, which fits our expectations for a sunny day at local noon.

c) Recalculate the value of u_* for non-neutral conditions. How much does it change from the value determined for neutral conditions? Recalculate the sensible heat flux, and note how much it changes. How much would u_* have to change to alter the sensible heat flux by 50 W m^{-2}?

Solution:

To recalculate the value of friction velocity for unstable conditions, (2.37) indicates that we need to determine the value of ψ_m. For unstable conditions, the equation to use is (2.39). Thus, one finds that

$$x = \left(1 - 15\frac{z_{eff}}{L}\right)^{1/4} = \left(1 - 15\frac{(10)}{(-82.15)}\right)^{1/4} = (1 + 1.83)^{1/4} = 1.297 ms^{-1}$$

and then

$$\psi_m = 2\ln\left(\frac{2.297}{2}\right) + \ln\left(\frac{2.6822}{2}\right) - 2\tan^{-1}(1.297) + \frac{\pi}{2} = 0.313 > 0.$$

This again agrees with the expectation that the value of ψ_m should be greater than zero for unstable conditions. Then we can recalculate u_* using

$$u_* = \frac{\bar{u}k}{\left[\ln\left(\frac{z_{eff}}{z_0}\right) - \psi_m\right]} = \frac{(7)(0.4)}{\left[\ln\left(\frac{10}{0.125}\right) - 0.313\right]} = .69 ms^{-1}.$$

Thus, the value of u_* increases from 0.64 to 0.69 under non-neutral conditions, or a 8% change.

The same equations as previously can be used to calculate the sensible heat flux using this new value of friction velocity, which yields Q_H = 243.10 W m^{-2}. We could also include the non-neutral effects in our calculation of r_H from the surface to the 2 m height, yielding a value of x = 1.08, ψ_H = 0.16, r_H =39.41 s m^{-1} and Q_H = 229.3 W m^{-2} or a 3.3 W m^{-2} difference from the original value. To obtain a change in Q_H of 50 W m^{-2}, one can calculate the needed resistance and find that r_H = 32.74 would yield a sensible heat flux of 276 W m^{-2} (50 more than the original value of 226). The resistance equation can then be used to find that under non-neutral conditions a friction velocity of 0.783 m s^{-1} is needed to get a 50 W m^{-2} change in sensible heat flux. This is a 22% change from the original friction velocity.

2] Using the same data as in 1], examine the calculations for bare soil evaporation when the green vegetation fraction is zero. Assume that the Richardson number is zero, Θ_l = 0.35, Θ_{fc} = 0.45, and Θ_w = 0.18. Use (3.6)-(3.7) to calculate bare soil evaporation. Then use (3.8)-(3.9) instead to calculate bare soil evaporation. Comment on the differences in the calculated fluxes.

Solution:

There are a number of equations that are needed to finish this problem. The first challenge for using (3.6)-(3.7) is to calculate the potential evaporation. Since the measurements above the surface are at the 2 m height, we first need to determine the wind speed at this level. Since a zero Richardson number implies neutral stability, we use

$$\bar{u}(2m) = \frac{u_*}{k}\ln\left(\frac{z_{eff}}{z_0}\right) = \frac{0.64}{0.4}\ln\left(\frac{2}{0.125}\right) = 4.44ms^{-1}.$$

From this we can determine the value of the coefficient C_q in (3.13) as

$$C_q = \left[k/\ln((z+z_0)/z_0)\right]^2 = \left[(0.4)/\ln((2+0.125)/0.125)\right]^2 = (0.14118)^2 = 0.01993.$$

From this, we can calculate $r_a = 1/(C_q u) = 1./(0.01993*4.44) = 11.30$. Next the value of Δ is needed. Using the Clausius-Clapeyron equation, one can rewrite (3.12) as

$$\Delta = \frac{0.622L_v L_v e_s(T)}{pc_p R_v T^2} = \frac{(0.622)(2.5x10^6)^2(39.39)}{(1000)(1004)(461)(301.15)^2} = 3.648,$$

assuming a surface pressure of 1000 hPa and using a Skew-T log p diagram to determine the saturation mixing ratio at 28°C and 1000 hPa and then converting to vapor pressure in hPa. We now have all that is needed to calculate the potential evaporation using (3.11). Thus,

$$E_p = \frac{\Delta(R_{net} - Q_G)}{1+\Delta} + \frac{\rho L_v(q_s(T_a) - q_a)}{(1+\Delta)r_a} = \frac{(3.648)(600-100)}{1+3.648} + \frac{(1)(2.5x10^6)(0.0245-0.014)}{(1+3.648)(11.30)}$$

$$= 392.43 + 499.79 = 892.22Wm^{-2}$$

Finally, the bare soil evaporation is

$$Q_{EB} = (1-\sigma_f)\left(\frac{\Theta_1 - \Theta_w}{\Theta_{fc} - \Theta_w}\right)E_p = (1-0)\left(\frac{0.35-0.18}{0.45-0.18}\right)(892.22) = (1)(0.629)(892.22) = 561.2Wm^{-2}$$

which some may note is greater than the net radiation. Since the "observations" that form the basis of these questions are fictional, one should not make too big of a deal about this flux value being greater than the net radiation. However, this is an opportunity to remind the students that most land surface schemes do not force closure of the surface energy budget. The results are often close to balancing, but the flux values are not required to do so.

If we turn to (3.8) and (3.9) to calculate the bare soil evaporation, then the results are different. The first step is to calculate *h*, where

$$h = \frac{1}{2}\left[1-\cos\left(\frac{\Theta_1 \pi}{1.6\Theta_{fc}}\right)\right] = (0.5)\left[1-\cos\left(\frac{(0.35)(3.1415927)}{(1.6)(0.45)}\right)\right] = 0.5\left[1-0.0436\right] = 0.4782.$$

Then from a Skew-*T* log *p* we find that the saturation mixing ratio at 37°C is 0.043 kg kg^{-1}, and from question 1] we know that a realistic resistance in the surface layer for neutral conditions is 40.0 s m^{-1}, so the bare soil evaporation is

$$Q_{EB} = \rho L_v\left(\frac{hq_s(T_g) - q_a}{r_a}\right) = (1)(2.5x10^6)\left(\frac{(0.4782)(0.043)-(0.014)}{40.0}\right) = 410.16Wm^{-2}$$

which is slightly less than the net radiation. Thus, the difference in the bare soil evaporation from these two approaches is 151.04 W m^{-2}. This is a fairly large number, and indicates the very different values one can get when using different parameterizations for bare soil evaporation.

3] Again, using the same data as in 1], examine the calculations for evapotranspiration from vegetation when the vegetation fraction is 1. Assume that the Richardson number is zero, $\Theta_1 = 0.35$, $\Theta_2 = 0.25$, $\Theta_{fc} = 0.45$, and $\Theta_w = 0.18$. The first soil layer is 10 cm deep, and the second soil layer that incorporates that rest of the root zone is 40 cm deep. Assume that $W_c = 0$, so that the canopy surface is dry. Use (3.24)-(3.25) to calculate the evapotranspiration. If one further assumes that $Q_S = 700$ W m^{-2}, $Q_{GL} = 50$ W m^{-2}, $r_{cmin} =$ 100 s m^{-1}, and $\alpha = 40$ in the definition of F_2, then use (3.38)-(3.41) to calculate evapotranspiration assuming $r_r = 15$ s m^{-1}. Comment on the differences in the calculated fluxes.

Solution:

Thankfully, we already calculated the potential evaporation in 3] and so can use it in the following question as well. So to begin with $E_p = 892.22$ W m^{-2}. Now, using the values for volumetric water content given, one can go ahead and use (3.24) and (3.25) to calculate the answer. One potential item of uncertainty is the value to use for Θ_{ref} in the question. The discussion after (3.25) indicates that Pan and Mahrt use a value of 0.25, but the question indicates a field capacity value of 0.45. However, since the intent is to scale g based upon the volumetric water content in between its largest and smallest

values, using 0.45 for Θ_{ref} makes the most sense. This value is used in the calculations below.

$$Q_{EV} = E_p k_v \sigma_f \left[\frac{z_1}{z_2} \left(\frac{\Theta_1 - \Theta_w}{\Theta_{fc} - \Theta_w} \right) + \frac{(z_2 - z_1)}{z_2} \left(\frac{\Theta_2 - \Theta_w}{\Theta_{fc} - \Theta_w} \right) \right] \left(1 - \left(\frac{W_c}{S} \right)^n \right)$$

$$= 892.22(1)(1) \left[\frac{10}{40} \left(\frac{0.35 - 0.18}{0.45 - 0.18} \right) + \frac{(40 - 10)}{40} \left(\frac{0.25 - 0.18}{0.45 - 0.18} \right) \right] (1) = 892.22 \left[0.25(0.6296) + 0.75(0.259259) \right]$$

$$= 892.22(0.35184) = 313.92$$

Using (3.38)-(3.41) to calculate evapotranspiration is a bit more complicated, since more equations are involved. We begin by calculating the *F* factors from Noilhan and Planton (1989) that are found in (3.28) - (3.34). Thus,

$$f = 0.55 \frac{Q_S}{Q_{GL}} \frac{2}{LAI} = 0.55 \frac{700}{50} \frac{2}{2} = 7.7$$

from which

$$F_1 = \frac{f + \frac{r_{c\min}}{r_{c\max}}}{1 + f} = \frac{7.7 + \frac{100}{5000}}{1 + 7.7} = 0.8874 .$$

The second *F* factor is from (3.31), such that

$$F_2 = \frac{1}{1+\alpha[q_s(T_a)-q_a]} = \frac{1}{1+40\left[0.0245-0.014\right]} = 0.7042,$$

where the value of $q_s(T_a)$ is found using a Skew-T log p. One could also calculate it if desired. Then the third factor is

$$F_3 = 1-1.6x10^{-3}(T_{ref}-T_a)^2 = 1-1.6x10^{-3}(298-301.15)^2 = 0.9841.$$

The fourth and last F factor is deals with the soil water content and is defined following

$$F_4 = \sum_{i=1}^{2} \frac{(\Theta_i - \Theta_w)d_{z_i}}{(\Theta_{fc}-\Theta_w)(d_{z_1}+d_{z_2})} = \frac{(0.35-0.18)(10)}{(0.45-0.18)(40)} + \frac{(0.25-0.18)(30)}{(0.45-0.18)(40)} = 0.1574 + 0.1944 = 0.35184$$

Now we can finally calculate the canopy resistance using (3.27), with

$$r_c = \frac{r_{c\min}}{LAI \cdot F_1F_2F_3F_4} = \frac{100}{(2)(0.8874)(0.7042)(0.9841)(0.35184)} = 231.07\,\mathrm{sm}^{-1}.$$

The equation for the evapotranspiration is given by (3.38), namely

$$Q_{EV} = \sigma_f E_p B_c \left[1-\left(\frac{W_c}{S}\right)^n\right],$$

and we see from (3.39) that

$$B_c = \frac{1 + \frac{\Delta}{r_r}}{1 + r_c C_h u_a + \frac{\Delta}{r_r}}$$

where we already calculated Δ in the previous problem and r_c above, r_r is given, which leaves C_h for calculation. With a zero Richardson number, this reduces to

$$C_h = \frac{k^2}{R} \frac{F2}{\ln\left(\frac{z}{z_0}\right)\ln\left(\frac{z}{z_{0h}}\right)} = \frac{(0.4)^2}{1} \frac{1}{\ln\left(\frac{2}{0.125}\right)\ln\left(\frac{2}{0.01788}\right)} = 0.1223,$$

assuming that $z_{0h} = z_0/7$. Thus, we can calculate B_c with knowledge of the 2-m wind speed of 4.44 ms^{-1} from 1], yielding

$$B_c = \frac{1 + \frac{\Delta}{r_r}}{1 + r_c C_h u_a + \frac{\Delta}{r_r}} = \frac{1 + \frac{3.6559}{15}}{1 + (231.07)(0.01223)(4.44) + \frac{3.6559}{15}} = .0902.$$

Finally,

$$Q_{EV} = \sigma_f E_p B_c \left[1 - \left(\frac{W_c}{S}\right)^n\right] = (1)(892.22)(0.0902)(1) = 80.47 Wm^{-2} .$$

Thus, the difference in the flux values is 233.44 W m^{-2}. While the "observations" given in 1] are fictional, they are not by any means unrealistic. This suggests that the additional

F factors used to calculate this last value of evapotranspiration also are realistic, yet the resulting flux differences are large. This comparison highlights the challenges to accurate surface flux calculations. Recall that observations are few and far between, and the formulations for evapotranspiration are rather crude. It should not be surprising that this magnitude of difference occurs, although it makes one wonder about the accuracy of fluxes from operational models.

4] Using the same data as in 1] and the results of 2] and 3], calculate the total latent heat flux as a function of the vegetation fraction as the vegetation fraction varies from 0 to 1 in increments of 0.1. If one assumes that errors of 10% in vegetation fraction are reasonable, how large is the uncertainty in latent heat flux?

Solution:

Choose a value for the bare soil evaporation and a value for transpiration from vegetation. The results will vary depending upon the values selected, but the general conclusions should be similar. Here I choose Q_{EB} = 410.16 and Q_{EV} = 80.47 W m^{-2} which then need to be scaled by the vegetation fraction. Recall that the above questions assumed either completely bare soil or a fully vegetated surface, such that the flux values calculated represent these conditions. Thus, for this question we only need to use

$$Q_E = (1-\sigma_f)Q_{EB} + \sigma_f Q_{EV}$$

and vary the value of σ_f from 0 to 1 to get the answer. This yields using a spreadsheet program

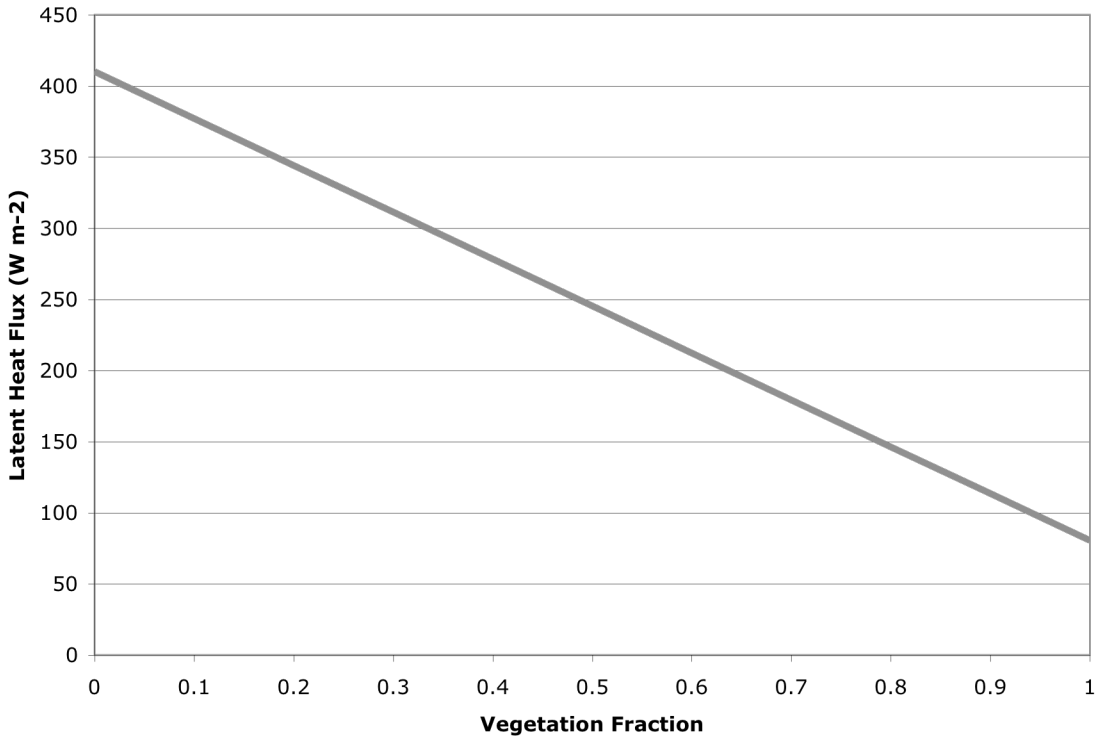

Thus, an error of 10% in vegetation fraction yields differences in latent heat flux of approximately 33 W m^{-2}. As the differences in the fluxes between the bare soil and vegetated surfaces increase, then this error also increases. This last conclusion is probably the most important one, that as the differences in flux values from bare soil and vegetated surfaces get larger, then errors in vegetation fraction have a larger impact.

5] For a 50% vegetation fraction at a particular grid cell, assume errors of 10% in vegetation fraction and errors of 0.05 m^3 m^{-3} in volumetric soil moisture measurements.

Using (3.6)-(3.7) for the bare soil evaporation and (3.24)-(3.25) for evapotranspiration from the vegetation, determine the range in uncertainty for the total latent heat flux owing to these two factors. Comment on the importance of these two measurements.

Solution:

This question again looks at uncertainties in the flux values due to errors in both soil moisture and vegetation fraction. One way to approach this question is to evaluate the uncertainties separately, and then combined, to more fully explore the sensitivies to these errors. Recall that both expressions use a function *g* where

$$g(\Theta) = \begin{cases} 1, & \Theta > \Theta_{ref} \\ \dfrac{\Theta - \Theta_w}{\Theta_{ref} - \Theta_w}, & \Theta_w \le \Theta \le \Theta_{ref} \\ 0, & \Theta \le \Theta_w \end{cases}$$

Thus, one can rewrite the total latent heat flux, assuming zero canopy water, as

$$\begin{aligned} Q_E &= E_p \left\{ \sigma_f \left[\frac{z_1}{z_2} \frac{(\Theta_1 - \Theta_w)}{(\Theta_{fc} - \Theta_w)} + \frac{(z_2 - z_1)}{z_2} \frac{(\Theta_2 - \Theta_w)}{(\Theta_{fc} - \Theta_w)} \right] + (1 - \sigma_f) \frac{(\Theta_1 - \Theta_w)}{(\Theta_{fc} - \Theta_w)} \right\} \\ &= E_p \left\{ \sigma_f \gamma + (1 - \sigma_f) \beta \right\} \end{aligned}$$

where γ represents the contribution to transpiration from soil moisture and β represents the contribution to bare soil evaporation from soil moisture. Start with the default values for soil moisture and vegetation fraction, and knowing that E_p = 892.22 W m^{-2} from

question 2]. Vary the soil moisture in the two vertical levels by plus and minus 0.05 and recalculate the values of γ and β. Then use these values with the 2 different vegetation fractions (40% and 60%). This leads to a table of results, such that

	γ	β	QE	QE with 40%	QE with 60%
initial	0.35184	0.62962	437.8391206	462.6232078	413.0550334
-0.05	0.16666	0.4444	272.5999766	297.3804949	247.8194583
0.05	0.537	0.8148	603.051498	627.8373696	578.2656264

where initial is the default value for soil moisture and vegetation fraction.

From this table, one can see that the latent heat flux varies from a low value of 247.8 to a high value of 627.8 W m^{-2}, yielding a maximum flux difference of 380 W m^{-2} for these size errors in soil moisture and vegetation fraction. Errors in vegetation fraction of 30% are reported in studies when the model uses a climatology for vegetation fraction (Kurkowski et al. 2003). Uncertainty in volumetric water content of 0.05 m^3 m^{-3} are not uncommon. Thus, this problem highlights that errors in flux values due to improper specification of the land surface can be quite large.

6] Calculate the values of soil potential for sand, loam, and sandy clay from $\Theta = 0.05$ to 0.40 with $\Theta_s = 0.40$ assumed for all three soil textures. Assume that $\kappa_s = 1\text{x}10^{-5}$ m s^{-1} and that $\psi_s = -0.5$ J kg^{-1}. Using the results in Table 3.1, incorporate one standard deviation in the values of b and recalculate the values of soil potential. Using (3.67), calculate the values of diffusivity D for these 9 values of soil potential. Comment.

Solution:

The equation for soil potential is (3.56), which states that

$$\psi_{soil} = \psi_s \left(\frac{\Theta}{\Theta_s} \right)^{-b},$$

such that if we know the saturation matric potential, the porosity, and the exponential *b* factor, then it is easy to calculate the soil potential. The question provides the porosity and the saturation matric potential, so all we need to do is look up the value of *b* for the 3 soil types. The table shows that the values of b and its standard deviation for sand are 2.79 and 1.38, for loam are 5.25 and 1.66, and for sandy clay are 10.73 and 1.54. Thus, using a spreadsheet program, one can generate the following chart using the above equation for soil potential.

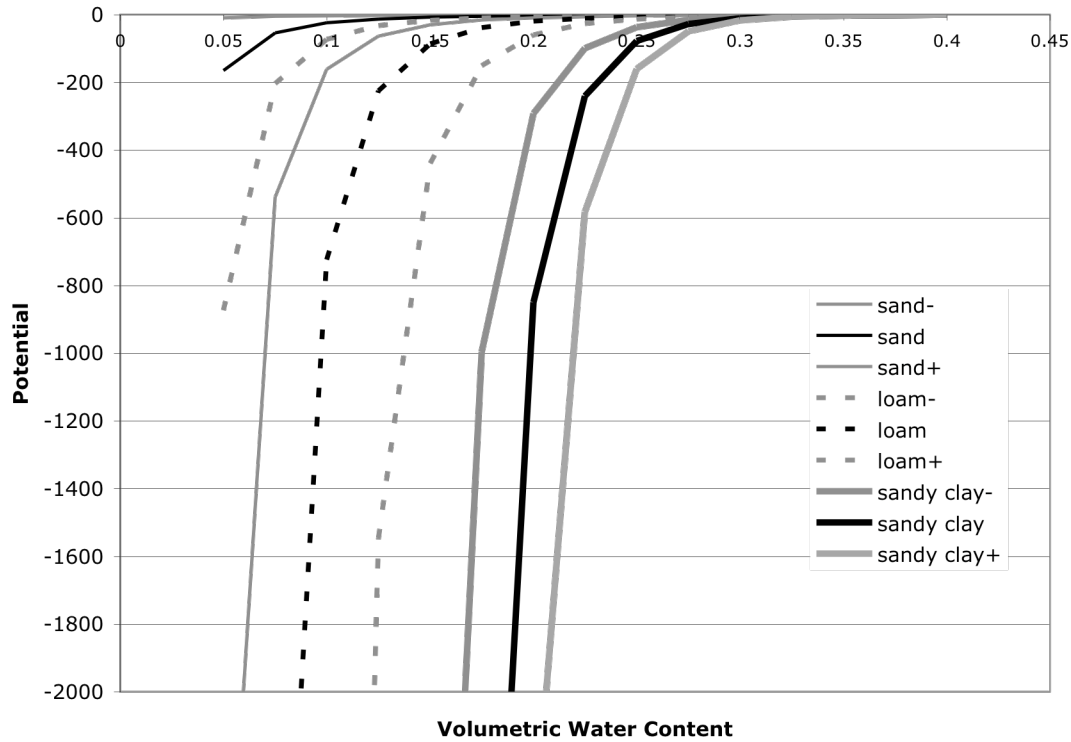

This chart shows a few common behaviors. First, as the value of *b* increases, the curves shift to the right (i.e., the potentials become negative faster as volumetric water content decreases). Second, if one chooses a volumetric water content, the differences in potential for the 3 values of *b* for each soil type can be large. Take loam soil with a volumetric water content of 0.125 $m^3\ m^{-3}$ and one finds that for the 3 values of *b*, the potential varies from -32 to -1547 J kg^{-1}! Finally, the potential curves from different soil types overlap in their range (loam and sand in the above chart).

To calculate the value of the diffusivity D, we use (3.67) as indicated. This equation states that

$$D = \frac{\kappa(\Theta)}{g}\frac{\partial\psi}{\partial\Theta},$$

and we further know from (3.57) that

$$\kappa_{soil} = \kappa_s \left(\frac{\Theta}{\Theta_s} \right)^{2b+3}.$$

This yields

$$D = \frac{\kappa_s}{g} \left(\frac{\Theta}{\Theta_s} \right)^{2b+3} \frac{\partial \psi}{\partial \Theta},$$

in which we can calculate the derivative of potential with respect to volumetric water content from the spread sheet we created to produce the graphs. This yields a chart of diffusivity as a function of volumetric water content for the 3 soils.

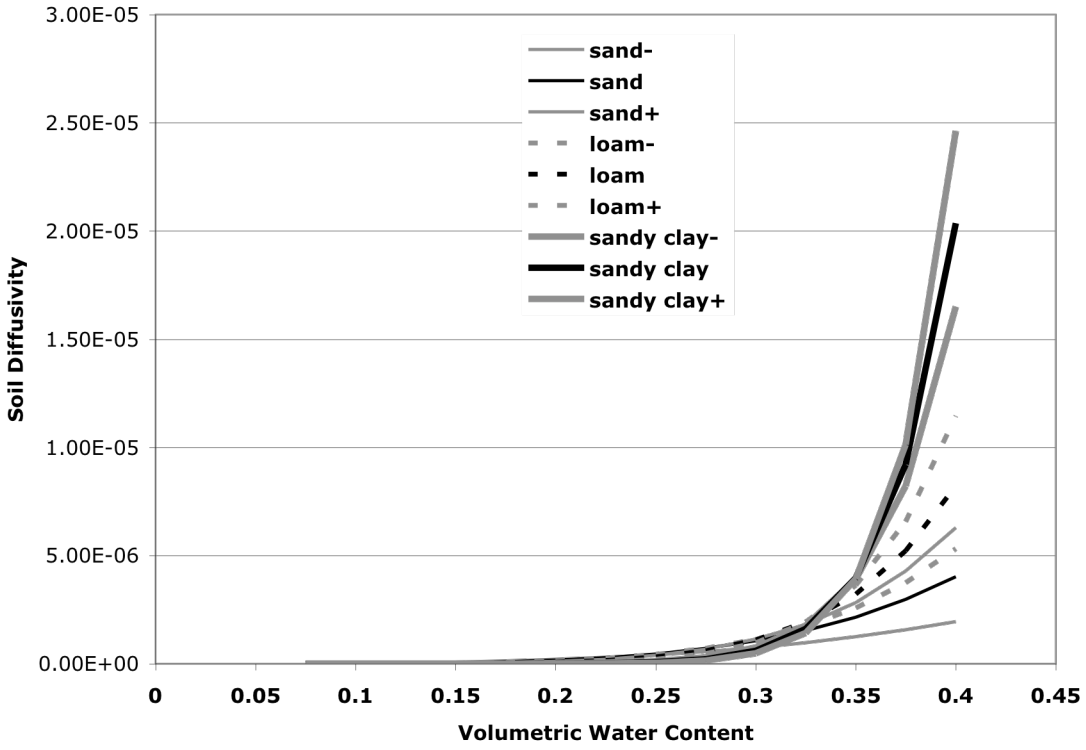

Again, as with potential, one sees that the values of diffusivity can overlap for different soil types when their range of values is taken into consideration. Also note that diffusivity values are small and remain fairly constant for volumetric water contents below 0.25, but increase fairly rapidly for volumetric water contents above 0.3. Minimum values of diffusivity are roughly 10^{-11}.

7] Using the same basic data as in 1], examine the benefits of mosaic tiling. The latent heat flux for 1 m tall grasses has already been calculated. Now assume that 70% of the model grid cell is represented by these grasses, but that 30% of the model grid cell is represented by oak trees that are 8 m tall and have a *LAI* of 10. Determine the latent heat flux using the tiling approach of (3.44). Comment on the differences in the values of latent heat flux for a homogeneous versus heterogeneous land surface as described.

Solution:

This is a really open-ended question that can be solved in a number of ways, depending upon the assumptions one makes. For example, in previous problems we always calculated the fluxes at the 2 m height where the data are available. However, this is not so simple for oak trees that are 8 m tall. For these trees, the displacement depth is 6 m, below which the winds are light but not exactly zero. The notes provide no formulas for calculating the wind speed at heights below the displacement height. Thus, one needs to make a guess or hunt for another formula. This question challenges the students to think about the problem and how to solve it in a way that makes sense, but without breaking any important rules or making really, really bad assumptions.

One option is to begin by assuming that the value of E_p calculated in 2] still applies and using equations (3.38)-(3.41) with the F-factors to calculate a new transpiration over the oak tree region. Use the same assumptions as in questions 2] and 3] to make life easier. The next step is to see if any of the F-factors need to be calculated with different input values. With identical soil moisture and incoming radiation levels, and assuming the same resistances, the big differences are the value of LAI and the wind profile due to the height of the trees.

The F_1 factor will be different than the earlier calculation. Recall that

$$f = 0.55 \frac{Q_S}{Q_{GL}} \frac{2}{LAI} = 0.55 \frac{700}{50} \frac{2}{10} = 1.54$$

from which

$$F_1 = \frac{f + \frac{r_{c\,\min}}{r_{c\,\max}}}{1+f} = \frac{1.54 + \frac{100}{5000}}{1+1.54} = 0.6142.$$

However, the other 3 F-factors are all the same. Thus, the canopy resistance becomes

$$r_c = \frac{r_{c\,\min}}{LAI \cdot F_1 F_2 F_3 F_4} = \frac{100}{(10)(0.6154)(0.7042)(0.9841)(0.35184)} = 66.77.$$

Next, the value of Δ is the same, but the values of C_h and u_a are going to be different. Calculating the wind speed is problematic, as we need to provide values of roughness lengths that we don't have from the question. So again we guess. We know that the winds below the displacement height are light, perhaps much less than 1 m s^{-1}. Assume a value of 0.2 m s^{-1} below the displacement height. Further guess a small roughness length of 0.1 m and estimate that the roughness length for heat is 1/7 of this value. This leads to an estimate of

$$C_h = \frac{k^2}{\ln\left(\frac{z}{z_0}\right)\ln\left(\frac{z}{z_{0h}}\right)} = \frac{(0.4)^2}{\ln\left(\frac{2}{0.1}\right)\ln\left(\frac{2}{0.0143}\right)} = 0.011$$

from which one can calculate B_c once again. This yields

$$B_c = \frac{1+\frac{\Delta}{r_r}}{1+r_c C_h u_a + \frac{\Delta}{r_r}} = \frac{1+\frac{3.6559}{15}}{1+(66.77)(0.011)(0.2)+\frac{3.6559}{15}} = .894.$$

Finally, we can calculate the latent heat flux over the oak region to be

$$Q_{EV} = \sigma_f E_p B_c \left[1-\left(\frac{W_c}{S}\right)^n\right] = (1)(892.22)(0.894)(1) = 797.64 Wm^{-2}$$

assuming a vegetation fraction of 1. For a grid cell that is 70% grasses with a latent heat flux of 80.47 W m^{-2} and 30% oak trees with a latent heat flux of 797.64 W m^{-2}, one can combine these to get an estimate for the latent heat flux from the total grid cell using (3.46) or simply

$$Q_E = \frac{70 * Q_{E_grass} + 30 * Q_{E_oak}}{100} = \frac{70(80.47)+30(797.64)}{100} = 295.62 Wm^{-2}.$$

Compared to the original flux value over the grass region of less than 100 W m^{-2}, the flux that represents both the grass and oak tree region is over 3 times larger! Even though the oak trees represent only 30% of the grid cell area. Thus, under the right conditions subgrid variability of vegetation type can have a large role in determining the flux values.

Chapter 4

1] Go onto the world-wide web and search for a site that provides daily or weekly global SST analyses or regional SST analyses appropriate for your location and available over at least a 1-year period. Explore these data for a 1-year period and describe the SST evolution nearest to where you live. What is the typical range of SST values? Are there any features or structures that you can describe (e.g., currents, anaomlies such as warm rings)? How do you think the oceans influence the weather where you live?

Solution:

The hope is that this question will encourage the students to see what information is available on the internet, and challenge them to think about how the oceans influence the weather where they live. A quick search on Google with the words "SST analyses" leads to several candidate sites. One is the NOAA Optimum Interpolation Sea Surface Temperature page at http://www.emc.ncep.noaa.gov/research/cmb/sst_analysis/ that has archived images from 2000 onward that can be downloaded as images. While the images do not have a lot of small-scale structure, they definitely paint a picture of the general evolution of ocean SSTs.

Much greater detail can be found with the RTG_SST analysis from the NCEP/EMC Marine Modeling and Analysis Branch. The web page for this is http://polar.ncep.noaa.gov/sst/ but it does not appear to have archived imagery available as images (it may have data from a few months back available in GRIB files).

2] Using the sensible heat flux equation (4.1), examine the sensitivity to roughness lengths z_0 and z_{0h}. First, assume ρ = 1.0 kg m^{-3}, T_{SST} = 303 K, T *(10 m)* = 300 K, L = -50 m, w^* = 1.0 ms^{-1}, the 10 m wind speed is 10 m s^{-1}, u_* = 0.8 m s^{-1}, and viscosity ν = 1.46x10^{-5} m^2 s^{-1}. Determine z_0 using (4.7) and then z_{0h} from (4.13) and (4.14). Calculate Q_H using both values of z_{0h}. How sensitive are the results to the formulas used?

Solution:

This question again explores the differences one finds when using various formulas to calculate the sensible heat flux. In particular, the information provided focuses the question on the sensitivity to the roughness length calculations. To begin, use (4.7) to calculate the roughness length over water. Thus,

$$z_0 = \alpha_c u_*^2 / g + 0.11\nu / u_* = \frac{(0.011)(0.8)^2}{9.81} + \frac{(0.11)(1.46x10^{-5})}{(0.8)} = 0.000718m.$$

Next, to determine z_{0h} from (4.13) one first must calculate the roughness Reynolds number R_r. We know that

$$R_r = \frac{u_* z_0}{\nu} = \frac{(0.8)(0.000718)}{1.46x10^{-5}} = 39.34,$$

so from Table 4.1 we see that a_h = 34.904 and b_h = -2.067. Then (4.13) yields

$$z_{0h} = \frac{\nu}{u_*} a_h R_r^{\,b_h} = \frac{1.46x10^{-5}}{0.8}(34.904)(39.34)^{-2.067} = 3.22x10^{-7} m\,.$$

Using the resistance formula (4.2), we have that

$$r_H = \frac{1}{ku_*}\left[\ln\left(\frac{z}{z_0}\right) - \psi_h\left(\frac{z}{L}\right)\right] + \frac{1}{ku_*}\ln\left(\frac{z_0}{z_{0h}}\right),$$

so we still need to calculate the value for ψ_h. Thus, we look back to Chapter 2 for the definition of this function and note that it requires us to calculate x first. The expression is from (2.40) and states

$$x = \left(1 - 15\frac{z_{eff}}{L}\right)^{1/4} = \left(1 - 15\frac{10}{(-50)}\right)^{1/4} = (4)^{1/4} = 1.4142,$$

and so from (2.46)

$$\psi_h = 2\ln\left[\frac{\left(1 + x^2\right)}{2}\right] = 2\ln\left(\frac{1+2}{2}\right) = 0.8109\,.$$

Finally, we can calculate the resistance and then the sensible heat flux over the water, using

$$r_H = \frac{1}{ku_*}\left[\ln\left(\frac{z}{z_0}\right) - \psi_h\left(\frac{z}{L}\right)\right] + \frac{1}{ku_*}\ln\left(\frac{z_0}{z_{0h}}\right)$$

$$= \frac{1}{(0.4)(0.8)}\left[\ln\left(\frac{10}{0.000718}\right) - 0.8109\right] + \frac{1}{(0.4)(0.8)}\left[\ln\left(\frac{0.000718}{3.22x10^{-7}}\right)\right]$$

$$= 27.283 + 24.093 = 51.376$$

and

$$Q_H = \frac{\rho c_p (T_{SST} - T(z))}{r_H} = \frac{(1)(1004)(303-300)}{51.376} = 58.62Wm^{-2}.$$

Now we turn to calculating the roughness length for heat from (4.14). The value of the roughness Reynolds number was already found to be 39.34, so we use the rough surface formula. This yields

$$z_{0h} = ae^{-bu_*^{1/4}} = 0.169e^{-1.53(0.8)^{1/4}} = 0.03976m.$$

However, this roughness length for heat is larger than the roughness length of 0.000718 m. I have double checked the formulas for both roughness length and roughness length for heat, and they appear correct. While the observations used to start this problem are fictitious, they do not appear unrealistic. Thus, I include this as a problem to illustrate to the students that not everything you read in the literature can be immediately translated into code without a bit of testing. I am not certain that the roughness length for heat should be larger than the roughness length, but perhaps this can occur and is realistic.

Regardless, it raises a question that should be answered before these two formulas are used together in a model. Here, I simply choose to use the roughness length calculation for smooth surfaces instead, which states that

$$z_{0h} = \frac{d\nu}{u_*} = \frac{(0.395)(1.46x10^{-5})}{0.8} = 7.2x10^{-6}m.$$

The roughness length for heat is now smaller than the roughness length, which is consistent with expectations. This value is then plugged into the equation for resistance, noting that only the last term is influenced by this change in z_{0h}, and we calculate that r_H = 41.66. Using this value it is simple to calculate the sensible heat flux again, yielding Q_H = 72.3 W m^{-2}. While this is only a 13.6 W m^{-2} difference from the first calculated value, in percent the change from the original value of 52.6 is 26%! So a larger air-sea temperature difference could lead to a significant change in flux values. Think about those cases in the fall when cold continental air surges southward and out over the Gulf of Mexico or off the east coast of the United States.

3] Using the results from 2], now calculate z_0 using (4.8) and assume that the neutral wind speed is equal to the assumed 10 m wind speed given. Recalculate the values of z_{0h} using (4.13) and (4.14) and again determine the values for Q_H. How sensitive is the value of Q_H to the values of z_{0h} and to the values of z_0?

Solution:

To answer this question, one just moves through equations (4.9)-(4.11). Start with the equation for the significant wave height $h = 0.0248u$ where u is the 10 m wind speed. Thus, $h = 0.0248(10) = 0.248$ m. Next move to the domaint wave period calculation, such that $T_p = 0.729u = 0.729(10) = 7.29$. From the wave period one calculates the wave length of the peak energy spectrum $L_p = gT_p^2/2\pi = (9.81)(7.29)^2/(2\pi) = 82.97$. Finally, we can calculate the roughness length using (4.8) such that

$$z_0 = 1200h_s\left(\frac{h_s}{L_p}\right)^{4.5} = 1200(0.248)\left(\frac{0.248}{82.97}\right)^{4.5} = 1.3x10^{-9}m.$$

To calculate z_{0h} we use (4.13) and (4.14). To use (4.13) we need to recalculate the roughness Reynolds number

$$R_r = \frac{u_* z_0}{\nu} = \frac{(0.8)(1.3x10^{-9})}{1.46x10^{-5}} = 7.1x10^{-5}.$$

From Table 4.1 we find that $a_h = 0.177$ and $b_h = 0$. Thus,

$$z_{0h} = \frac{\nu}{u_*}a_h R_r^{b_h} = \frac{1.46x10^{-5}}{0.8}(0.177)(1) = 2.6x10^{-6}m,$$

which is larger than the roughness length z_0! If one instead uses (4.14) then you see that the calculation does not change and the roughness length $z_{0h} = 7.2\text{x}10^{-6}$ m. Thus, both of

these calculated values of z_{0h} are larger than the roughness length z_0. Thus, I will assume that $z_0/z_{0h} = 1$ in the heat flux calculations.

The two resistances for heat flux are then the same, since the roughness lengths for heat are identical to the roughness length, with $r_H = 68.6$. This yields a sensible heat flux value of $Q_H = 43.9$ W m-2. This is smaller than the other calculated values by slightly less than 10 W m^{-2}, but the differences remain a large fraction of the total flux.

These questions are not intended to cast stones at the formulas used. However, it is important for students (and the rest of us) to learn that one must be careful in applying formulas from studies to models where the formulas will be applied over a wide range of values. One must first test the results using these formulas and make sure they are reasonable. There probably is a simple explanation for why the results behave as they do, but I have yet to find it. Perhaps your students will find the answers!

4] We know that SST varies slowly in comparison to changes the atmospheric surface layer, even over the tropical oceans far away from land. What processes could produce variability in the atmospheric surface layer over the oceans?

Solution:

This is another open ended question designed to make the students think a bit. Over the tropical oceans, convection is obviously one phenomena that can influence the surface layer. Cold downdrafts from convection descend into the boundary layer and surface

layer, dramatically changing the conditions within these layers, producing cooler and often drier conditions. Winds within cold downdrafts also can be quite strong, leading to the generation of sea spray.

Chapter 5

1] Following the outline provided by the section on Reynolds averaging and turbulence closure, derive the equations for the perturbation velocity and potential temperature

$$\frac{\partial u_i'}{\partial t} = \ldots$$

$$\frac{\partial \theta'}{\partial t} = \ldots$$

the equations for the turbulent fluxes

$$\frac{\partial(\overline{u_i' u_j'})}{\partial t} = \ldots$$

$$\frac{\partial(\overline{u_i' \theta'})}{\partial t} = \ldots$$

and the equations for the variances

$$\frac{\partial \overline{u_i'^2}}{\partial t} = \ldots$$

$$\frac{\partial \overline{\theta'^2}}{\partial t} = \ldots$$

Begin by expanding the variables into a mean and a perturbation component and use the Boussinesq equation (5.3) and

$$\frac{\partial \theta}{\partial t} + u_j \frac{\partial \theta}{\partial x_j} = \nu \frac{\partial^2 \theta}{\partial x_j^{\,2}}.$$

Show all work.

Solution:

The first part of the solution for the momentum term simply follows the equation development in section 5.3, however, I have found it important for the students to work through this derivation on their own. See Stull (1988) and other boundary layer textbooks for further details. Thus, beginning with (5.3) we have

$$\frac{\partial u_i}{\partial t} + u_j \frac{\partial u_i}{\partial x_j} = -\delta_{i3}\left[g - \frac{\theta_v'}{\overline{\theta}_v} g\right] + f\varepsilon_{ij3} u_j - \frac{1}{\overline{\rho}} \frac{\partial p}{\partial x_i} + \nu \frac{\partial^2 u_i}{\partial x_j^{\,2}}.$$

The next step is to expand each variable into a mean and perturbation, yielding

$$\begin{aligned} \frac{\partial(\overline{u}_i + u_i')}{\partial t} + \frac{(\overline{u}_j + u_j')\partial(\overline{u}_i + u_i')}{\partial x_j} &= -\delta_{i3}\left[g - \frac{\theta_v'}{\overline{\theta}_v} g\right] \\ &+ f\varepsilon_{ij3}(\overline{u}_j + u_j') - \frac{1}{\overline{\rho}} \frac{\partial(\overline{p} + p')}{\partial x_i} + \nu \frac{\partial^2(\overline{u}_i + u_i')}{\partial x_j^{\,2}}. \end{aligned}$$

Now all the terms are multiplied out and separated to obtain

$$\frac{\partial \overline{u}_i}{\partial t} + \frac{\partial u_i'}{\partial t} + \overline{u}_j \frac{\partial \overline{u}_i}{\partial x_j} + \overline{u}_j \frac{\partial u_i'}{\partial x_j} + u_j' \frac{\partial \overline{u}_i}{\partial x_j} + u_j' \frac{\partial u_i'}{\partial x_j} = -\delta_{i3}\left[g - \frac{\theta_v'}{\overline{\theta}_v} g\right] + f\varepsilon_{ij3}\overline{u}_j + f\varepsilon_{ij3}u_j' - \frac{1}{\overline{\rho}}\frac{\partial \overline{p}}{\partial x_i} - \frac{1}{\overline{\rho}}\frac{\partial p'}{\partial x_i} + \nu \frac{\partial^2 \overline{u}_i}{\partial x_j^{\,2}} + \nu \frac{\partial^2 u_i'}{\partial x_j^{\,2}}.$$

However, this equation represents the evolution of both the mean and turbulent portions of the momentum equation. So average over the entire equation to obtain an equation for the time rate of change of the mean, yielding

$$\frac{\partial \overline{u}_i}{\partial t} + \overline{u}_j \frac{\partial \overline{u}_i}{\partial x_j} + \overline{u_j' \frac{\partial u_i'}{\partial x_j}} = -\delta_{i3} g + f\varepsilon_{ij3}\overline{u}_j - \frac{1}{\overline{\rho}}\frac{\partial \overline{p}}{\partial x_i} + \nu \frac{\partial^2 \overline{u}_i}{\partial x_j^{\,2}}.$$

We can then subtract this equation for the mean from the equation just prior to it in order to get an equation for the turbulent gust, namely

$$\frac{\partial u_i'}{\partial t} + \overline{u}_j \frac{\partial u_i'}{\partial x_j} + u_j' \frac{\partial \overline{u}_i}{\partial x_j} + u_j' \frac{\partial u_i'}{\partial x_j} = \delta_{i3}\left[\frac{\theta_v'}{\overline{\theta}_v} g\right] + f\varepsilon_{ij3}u_j' - \frac{1}{\overline{\rho}}\frac{\partial p'}{\partial x_i} + \nu \frac{\partial^2 u_i'}{\partial x_j^{\,2}} + \frac{\partial \overline{(u_i' u_j')}}{\partial x_j}.$$

This equation already contains the rewritten Reynolds stress term developed in section 5.3.

To develop an equation for the turbulent fluxes, recall that

$$\frac{\partial\overline{(u_i'u_k')}}{\partial t} = \overline{u_i'\frac{\partial u_k'}{\partial t}} + \overline{u_k'\frac{\partial u_i'}{\partial t}}.$$

So to obtain the evolution of the Reynolds stress term, simply multiply the equation for the turbulent gust by u_k' to produce the second term on the right hand side of the above equation. The first term on the right hand side can be determined by taking the equation for the turbulent gust, changing all the *i*-indices to *k*-indices and then multiplying by u_i'. This is a messy process, but is not difficult and the end result is

$$\begin{aligned}\frac{\partial\overline{(u_i'u_k')}}{\partial t} + \overline{u}_j\frac{\partial\overline{(u_i'u_k')}}{\partial x_j} &= -\overline{(u_i'u_j')}\frac{\partial\overline{u}_k}{\partial x_j} - \overline{(u_k'u_j')}\frac{\partial\overline{u}_i}{\partial x_j} - \frac{\partial\overline{(u_i'u_j'u_k')}}{\partial x_j} \\ &+ \frac{g}{\overline{\theta}_v}\left[\delta_{k3}\overline{u_i'\theta_v'} + \delta_{i3}\overline{u_k'\theta_v'}\right] + f\left[\varepsilon_{kj3}\overline{u_i'u_j'} + \varepsilon_{ij3}\overline{u_k'u_j'}\right] \\ &- \frac{1}{\overline{\rho}}\left[\frac{\partial\overline{(p'u_k')}}{\partial x_i} + \frac{\partial\overline{(p'u_i')}}{\partial x_k} - \overline{p'\left(\frac{\partial u_i'}{\partial x_k} + \frac{\partial u_k'}{\partial x_i}\right)}\right] \\ &+ \nu\frac{\partial^2\overline{(u_i'u_k')}}{\partial x_j^{\,2}} - 2\nu\frac{\overline{\partial u_i'\partial u_k'}}{\partial x_j^{\,2}}\end{aligned}.$$

This represents 9 different equations, including equations for $\overline{u'u'}, \overline{u'v'}, \overline{u'w'}, \overline{v'v'}, \overline{v'w'}$, and $\overline{w'w'}$. However, the total number of equations is reduced to 6 owing to symmetry (e.g., $\overline{u'v'} = \overline{v'u'}$).

Next, for the momentum variance equation, recall from the product rule of calculus that

$$\frac{\partial(u_i')^2}{\partial t} = 2u_i'\frac{\partial u_i'}{\partial t}.$$

So multiply the equation for the turbulent gust by $2u_i'$. This yields

$$2u_i'\frac{\partial u_i'}{\partial t} + 2u_i'\overline{u}_j\frac{\partial u_i'}{\partial x_j} + 2u_i'u_j'\frac{\partial \overline{u}_i}{\partial x_j} + 2u_i'u_j'\frac{\partial u_i'}{\partial x_j} =$$
$$2u_i'\delta_{i3}\left[\frac{\theta_v'}{\overline{\theta}_v}g\right] + 2u_i'f\varepsilon_{ij3}u_j' - 2u_i'\frac{1}{\overline{\rho}}\frac{\partial p'}{\partial x_i} + 2u_i'\nu\frac{\partial^2 u_i'}{\partial x_j^{\,2}} + 2u_i'\frac{\partial\overline{(u_i'u_j')}}{\partial x_j}.$$

Apply the product rule again to combine terms where possible, yielding

$$\frac{\partial (u_i')^2}{\partial t} + \overline{u}_j\frac{\partial (u_i')^2}{\partial x_j} + 2u_i'u_j'\frac{\partial \overline{u}_i}{\partial x_j} + u_j'\frac{\partial (u_i')^2}{\partial x_j} =$$
$$2u_i'\delta_{i3}\left[\frac{\theta_v'}{\overline{\theta}_v}g\right] + 2u_i'f\varepsilon_{ij3}u_j' - 2u_i'\frac{1}{\overline{\rho}}\frac{\partial p'}{\partial x_i} + 2u_i'\nu\frac{\partial^2 u_i'}{\partial x_j^{\,2}} + 2u_i'\frac{\partial\overline{(u_i'u_j')}}{\partial x_j}.$$

Now Reynolds average the entire equation to obtain

$$\overline{\frac{\partial (u_i')^2}{\partial t}} + \overline{\overline{u}_j\frac{\partial (u_i')^2}{\partial x_j}} + \overline{2u_i'u_j'\frac{\partial \overline{u}_i}{\partial x_j}} + \overline{u_j'\frac{\partial (u_i')^2}{\partial x_j}} =$$
$$\overline{2u_i'\delta_{i3}\left[\frac{\theta_v'}{\overline{\theta}_v}g\right]} + \overline{2u_i'f\varepsilon_{ij3}u_j'} - \overline{2u_i'\frac{1}{\overline{\rho}}\frac{\partial p'}{\partial x_i}} + \overline{2u_i'\nu\frac{\partial^2 u_i'}{\partial x_j^{\,2}}},$$

where the only term that averages to zero is the last term on the right-hand-side, since a perturbation is multiplying an averaged quantity. This equation is often rewritten using knowledge that the perturbation continuity equation equals zero [see equations (5.7) through (5.10)]. Thus, multiplying the perturbation continuity equation by $(u_i')^2$ and

averaging it will still yield zero, allowing the fourth term on the left-hand-side of the above equation to be rewritten, yielding

$$\overline{\frac{\partial (u_i')^2}{\partial t}} = -\overline{u}_j \overline{\frac{\partial (u_i')^2}{\partial x_j}} - 2\overline{u_i' u_j'} \frac{\partial \overline{u}_i}{\partial x_j} - \overline{\frac{\partial (u_j'(u_i')^2)}{\partial x_j}} + 2\delta_{i3} \overline{u_i' \left[\frac{\theta_v'}{\overline{\theta}_v} g \right]} + 2 f \varepsilon_{ij3} \overline{u_i' u_j'} - \frac{2}{\overline{\rho}} \overline{u_i' \frac{\partial p'}{\partial x_i}} + 2\nu \overline{u_i' \frac{\partial^2 u_i'}{\partial x_j^2}}.$$

For the potential temperature equations, we start with

$$\frac{\partial \theta}{\partial t} + u_j \frac{\partial \theta}{\partial x_j} = \nu \frac{\partial^2 \theta}{\partial x_j^2},$$

and expand into mean and perturbations, yielding

$$\frac{\partial \overline{\theta}}{\partial t} + \frac{\partial \theta'}{\partial t} + \overline{u}_j \frac{\partial \overline{\theta}}{\partial x_j} + u_j' \frac{\partial \overline{\theta}}{\partial x_j} + \overline{u}_j \frac{\partial \theta'}{\partial x_j} + u_j' \frac{\partial \theta'}{\partial x_j} = \nu \frac{\partial^2 \overline{\theta}}{\partial x_j^2} + \nu \frac{\partial^2 \theta'}{\partial x_j^2}.$$

Reynolds average to obtain an equation for the mean, namely

$$\frac{\partial \overline{\theta}}{\partial t} + \overline{u}_j \frac{\partial \overline{\theta}}{\partial x_j} = \nu \frac{\partial^2 \overline{\theta}}{\partial x_j^2} - \frac{\partial \overline{(u_j' \theta')}}{\partial x_j},$$

where we used the shallow Boussinesq assumption (incompressibility) to rewrite the Reynolds flux term. Finally, subtract the equation of the mean from the equation above it to obtain the equation for the perturbation potential temperature tendency,

$$\frac{\partial \theta'}{\partial t} + u'_j \frac{\partial \overline{\theta}}{\partial x_j} + \overline{u}_j \frac{\partial \theta'}{\partial x_j} + u'_j \frac{\partial \theta'}{\partial x_j} = \nu \frac{\partial^2 \theta'}{\partial x_j^{\,2}} + \frac{\partial \overline{(u'_j \theta')}}{\partial x_j}.$$

To calculate the turbulent flux, note that

$$\overline{\frac{\partial (u'_i \theta')}{\partial t}} = \overline{\frac{\partial u'_i}{\partial t} \theta'} + \overline{u'_i \frac{\partial \theta'}{\partial t}},$$

so one simply multiplies the turbulent gust equation by θ' and the perturbation potential temperature tendency equation by u'_i, yielding

$$\begin{aligned} &\theta' \frac{\partial u'_i}{\partial t} + \theta' \overline{u}_j \frac{\partial u'_i}{\partial x_j} + \theta' u'_j \frac{\partial \overline{u}_i}{\partial x_j} + \theta' u'_j \frac{\partial u'_i}{\partial x_j} + u'_i \frac{\partial \theta'}{\partial t} + u'_i u'_j \frac{\partial \overline{\theta}}{\partial x_j} + u'_i \overline{u}_j \frac{\partial \theta'}{\partial x_j} + u'_i u'_j \frac{\partial \theta'}{\partial x_j} = \\ &\theta' \delta_{i3} \left[\frac{\theta'_v}{\overline{\theta}_v} g \right] + \theta' f \varepsilon_{ij3} u'_j - \theta' \frac{1}{\overline{\rho}} \frac{\partial p'}{\partial x_i} + \theta' \nu \frac{\partial^2 u'_i}{\partial x_j^{\,2}} + \theta' \frac{\partial \overline{(u'_i u'_j)}}{\partial x_j} + \nu u'_i \frac{\partial^2 \theta'}{\partial x_j^2} + u'_i \frac{\partial \overline{(u'_j \theta')}}{\partial x_j} \end{aligned}.$$

Reynolds average, use the product rule to combine terms, and find that the resulting equation is

$$\frac{\partial(\overline{u'\theta'_i})}{\partial t} + \overline{u}_j \frac{\partial(\overline{u'_i\theta'})}{\partial x_j} + \overline{u'_j\theta'}\frac{\partial \overline{u}_i}{\partial x_j} + \frac{\partial(\overline{u'_i u'_j \theta'})}{\partial x_j} + \overline{u'_i u'_j}\frac{\partial \overline{\theta}}{\partial x_j} =$$
$$\delta_{i3}\left[\frac{\overline{\theta'\theta'_v}}{\overline{\theta}_v} g\right] + f\varepsilon_{ij3}\overline{u'_j\theta'} - \frac{1}{\overline{\rho}}\overline{\theta'\frac{\partial p'}{\partial x_i}} + \nu\overline{\theta'\frac{\partial^2 u'_i}{\partial x_j^{\,2}}} + \nu\overline{u'_i\frac{\partial^2\theta'}{\partial x_j^2}} \quad ,$$

where again the perturbation continuity equation is used to produce the triple correlation term.

Last, the potential temperature variance equation is calculated by starting with the equation for the perturbation potential temperature and multiplying it by $2\theta'$, yielding

$$2\theta'\frac{\partial\theta'}{\partial t} + 2\theta' u'_j\frac{\partial\overline{\theta}}{\partial x_j} + 2\theta'\overline{u}_j\frac{\partial\theta'}{\partial x_j} + 2\theta' u'_j\frac{\partial\theta'}{\partial x_j} = 2\theta'\nu\frac{\partial^2\theta'}{\partial x_j^{\,2}} + 2\theta'\frac{\partial(\overline{u'_j\theta'})}{\partial x_j}.$$

Use the produce rule to simplify terms and Reynolds average, to obtain

$$\frac{\partial\overline{\theta'^2}}{\partial t} = -2\overline{\theta' u'_j}\frac{\partial\overline{\theta}}{\partial x_j} - \overline{u}_j\frac{\partial\overline{\theta'^2}}{\partial x_j} - \frac{\partial(\overline{u'_j\theta'^2})}{\partial x_j} + 2\nu\overline{\theta'\frac{\partial^2\theta'}{\partial x_j^{\,2}}}.$$

As done previously, the continuity equation is used to develop the flux term (the third term on the right-hand-side of the equation).

2] Using knowledge of turbulence closure, discuss the pros and cons to going to higher-order closure schemes (i.e., third-order closure).

Solution:

This question is intended to cement the ideas covered in section 5.3 on turbulence closure. The reasoning behind this parameterization philosophy is stated nicely by Lumley and Khajeh-Nouri, namely, that if a relatively crude assumption for second moments predicts first moments adequately, then perhaps a relatively crude assumption for third moments will predict second moments adequately - yielding even better predictions for the first moments. The farther we move the assumptions away from the terms of most interest (typically the mean quantities), then the more realistic the model and hopefully the less effect the assumptions play in determining the resulting behavior of the parameterization.

3] One set of equations for a mixed layer model are

$$\frac{d\overline{\theta}}{dt} = \frac{(1+k_e)C_T V_S\left(\theta_S - \overline{\theta}\right)}{H},$$

$$\frac{dH}{dt} = k_e C_T V_S \frac{(\theta_S - \overline{\theta})}{\Delta\theta},$$

$$\frac{d\overline{q}}{dt} = C_T V_S \frac{M(q_S - \overline{q}) + \left[k_e(\theta_S - \overline{\theta})\Delta q/\Delta\theta\right]}{H},$$

where M denotes the moisture availability, C_T is a transfer coefficient, and V_S is the surface wind speed. Let us now examine the consequences of changing both the entrainment parameter k_e and the moisture availability. Assume the following:

$C_T = 0.015$

$V_S = 10$ m s^{-1}

$M = 0.5$

$\theta_S = 311$ K + 10 *Δt (3 hours)$^{-1}$ (potential temperature increases linearly with time to 321 K at 3 hours and 331 K at 6 hours)

$q_S = 17$ g/kg - 2.5*Δt (3 hours)$^{-1}$ (mixing ratio decreases by 2.5 g kg^{-1} over 3 hours)

and the initial environmental potential temperature and mixing ratio profiles look like:

$\theta = 310$ K + 5K*z (1000 m)$^{-1}$

$q = 11$ g kg^{-1} at and below $z = 1000$ m

$q = 3$ g kg^{-1} above $z = 1000$ m

where $H = 30$ m at time zero (if H is zero at time zero, then the model blows up). Develop a finite difference version of these mixed layer equations and integrate the equations for 3 hours and 6 hours using three different values of k_e: 0.1, 0.3, and 0.5. Then answer the following questions. What are the final values of θ and q in the mixed layer? What are the final values of mixed layer depth H? What do these results say about the importance of choosing an appropriate value for the entrainment coefficient when using a PBL model? Do these differences increase or decrease over longer time periods?

One simple integration scheme is to define $x'_{i,n} = f(x_{i,n})$, where *i* denotes the variable (*i*=1, 2, 3) and *n* is the time level, and then integrate forward one time step to *n+1* using $x_{i,n+1} = 0.5 * \left[x_{i,n} + \tilde{x}_{i,n+2} \right]$, where one first determines $\tilde{x}_{i,n+1} = x_{i,n} + f(x_{i,n}) * \Delta t$ and then determines $\tilde{x}_{i,n+2} = \tilde{x}_{i,n+1} + f(\tilde{x}_{i,n+1}) * \Delta t$. This simple time integration scheme is stable for the mixed layer model, but requires a time step of about 1 second.

Solution:

First, below is a fortran77 code that integrates the mixed layer equations forward in time.

```
c*****************************************
      program mixed_model
c
c**    simple mixed layer model program
c
      real ct,vs,ke,h,ts,tbar,qs,qbar,dq,dtheta,m
      real tbar2,qbar2,h2
c
      ke=0.5
      m=0.5
c
      ct=0.015
      vs=10.
      tbar=310.
      qbar=11.
      h=30.
c
      dt=1.0
      itime=int(6.*3600./dt)
c
      do i=1,itime
c
       ts=310.+10.*i/(3.*3600.)
       qs=17.-2.5*i/(3.*3600.)
c
       dtheta=(310.+h*5./1000.)-tbar
```

```
      if(h.le.1000.) then
       dq=11.-qbar
      else
       dq=3.-qbar
      end if
c
      tbar2=tbar+dt*(1.+ke)*ct*vs*(ts-tbar)/h
      qbar2=qbar+dt*ct*vs*( m*(qs-qbar) + ke*(ts-tbar)*dq/dtheta )/h
      h2=h+dt*ke*ct*vs*(ts-tbar)/dtheta
c
      tbar=tbar2
      qbar=qbar2
      h=h2
c
c**  print out model data every hour.
c
      if(mod(i,3600).eq.0) print *,(dt*i)/3600.,tbar,h,qbar,ts,qs
c
      end do
c
      stop
      end
```

The results from this model run using a 1 second timestep are shown in the following table.

	$k_e = 0.1$	$k_e = 0.3$	$k_e = 0.5$
3-h θ (K)	315.9	315.9	316.0
3-h q (g/kg)	11.1	10.3	9.8
3-h H (m)	1277.8	1457.6	1602.5
6-h θ (K)	321.7	321.9	322.0
6-h q (g/kg)	8.3	7.9	7.6
6-h H (m)	2555.6	2915.6	3205.1

These results show that while the potential temperature does not change very much as the entrainment coefficient changes (although note the decrease in mixing ratio as entrainment increases), the mixed layer depth varies from 2556 to 3205 m and the mixing ratio varies from 8.3 to 7.6 g kg^{-1}! This is a change of 25% in height and 10% in mixing ratio. The smaller sensitivity of mixing ratio may be due in part to the initial profile chosen and the specified decrease in q_s with time. However, just the change in mixed layer depth alone indicates how important the entrainment coefficient is for mixed layer models. The differences increase in absolute value, but the fractional change in mixed layer depth is constant between 3 and 6 h at just over 25%. This is due in part to the simple environmental potential temperature profile specified that increases linearly with height. The change in mixing ratio actually is a little larger at 3 h than at 6 h, again likely due to the specified initial profile of constant mixing ratio below 1 km.

4] Using the program developed in question 3, assume that the land surface scheme has a bias of +1 K in the temperature forecast over a 3-h period. Thus, θ_S = 311 K + 11 *Δt/(3 hours). Rerun the mixed layer scheme with this surface temperature evolution and with k_e = 0.3. What are the values of mixed layer depth H at 3 and 6 hours? How do these changes compare to changes in the entrainment coefficient?

Solution:

In the computer program, select the proper value for the entrainment coefficient and then modify the definition of variable ts in the code, such that

```
ts=311.+11.*i/(3.*3600.)
```

and rerun. The results are as follows:

	ts = 310+10*i/(3*3600)	ts=311+11*i/(3*3600)
3-h θ (K)	315.9	316.8
3-h q (g/kg)	10.3	9.6
3-h H (m)	1457.6	1691.6
6-h θ (K)	321.9	323.1
6-h q (g/kg)	7.9	7.7
6-h H (m)	2915.6	3241.9

As expected, the warmer surface temperatures lead to a deeper, warmer, and drier mixed layer. The differences in the variables is generally around 10% and the warmer surface temperature produces roughly the same results at 6 h as using an entrainment coefficient of 0.5. Thus, one can imagine that errors in both entrainment coefficient and surface temperatures could lead to fairly substantial and operationally relevant errors in boundary layer depth, temperature, and mixing ratio.

5] Using the same initial potential temperature and mixing ratio profiles as in question 3, and with the same time rate of change of surface potential temperature and mixing ratio, develop a simple finite difference model of the lowest 10,000 m of the atmosphere based only upon *K*-theory mixing. Use

$$\frac{\partial \overline{\theta}(z)}{\partial t} = K_H \frac{\partial^2 \overline{\theta}(z)}{\partial z^2},$$

and

$$\frac{\partial \overline{q}(z)}{\partial t} = K_H \frac{\partial^2 \overline{q}(z)}{\partial z^2},$$

and set up a vertical grid starting at the surface [z=0 so that $\theta_s = \overline{\theta}(0)$] with 50 m vertical increments. Here $\overline{\theta}$ is the mean potential temperature of a given model layer and is allowed to vary with height. Assume that K_H is a constant. The time evolution of potential temperature and mixing ratio at z=0 is then specified. Try the finite difference approximation

$$F_{m,n+1} = F_{m,n} + \frac{K_H \Delta t}{(\Delta x)^2}\left[F_{m+1,n} + F_{m-1,n} - 2F_{m,n}\right],$$

where m is the vertical grid level, and n is the time level. Try time steps of 1 second. Integrate the model out to 6 h and examine the potential temperture and mixing ratio profiles. Try using several values of K_H between 10 and 200. What behaviors are seen? Is this result realistic?

Solution:

Below is a simple fortran77 program to integrate the PBL forward in time using a K-theory approach. It uses the same time specification for surface potential temperature and

mixing ratio as the mixed layer model, but then uses *K*-theory to mix from the surface upward.

```
c***********************************
      program kdiff
c
c**    simple K-theory model for PBL
c
      real kh,tbar,qs,qbar,dq,dtheta,m
      real tbar2,qbar2,h2
      real t(200),q(200)
      real ti(200),qi(200)
      real t2(200),q2(200)
c
      kh=10.0
      dx=50.
c
      dt=1.0
      itime=int(6.*3600./dt)
c
      do i=1,200
       z=dx*(i-1)
       t(i)=310.+z*5./1000.
       ti(i)=310.+z*5./1000.
       if(z.le.1000.) then
        q(i)=11.
        qi(i)=11.
       else
        q(i)=3.
        qi(i)=3.
       end if
      end do

      do i=1,itime
c
       time = time + dt

       t(1)=310.+10.*time/(3.*3600.)
       q(1)=17.-2.5*time/(3.*3600.)
c
       do k=2,199
        if(k.le.5) kh1=kh+kh*(5-k)
        t2(k)=t(k)+kh1*dt*(t(k+1)+t(k-1)-2.*t(k))/(dx**2)
        q2(k)=q(k)+kh1*dt*(q(k+1)+q(k-1)-2.*q(k))/(dx**2)
       end do
```

```
      do k=2,199
       t(k)=t2(k)
       q(k)=q2(k)
      end do

      end do
c
      do k=1,100
       print *,(k-1)*dx,t(k),q(k),t(k)-ti(k),q(k)-qi(k)
       write(10,100) (k-1)*dx,t(k),q(k)
      end do
100     format(3f12.3)

      stop
      end
```

Results for values of K_H = 10, 50, 100, and 200 are shown on the graphs below.

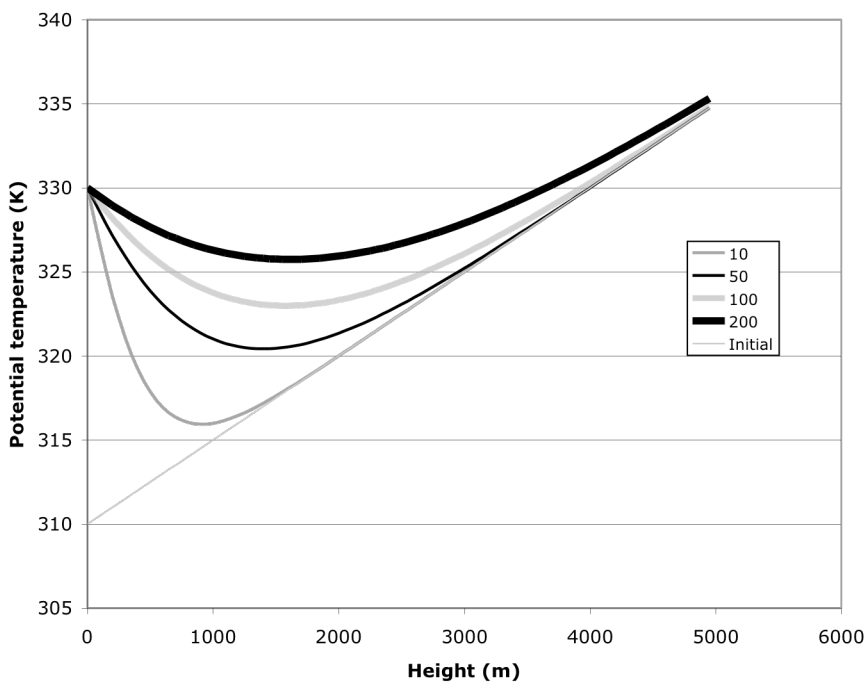

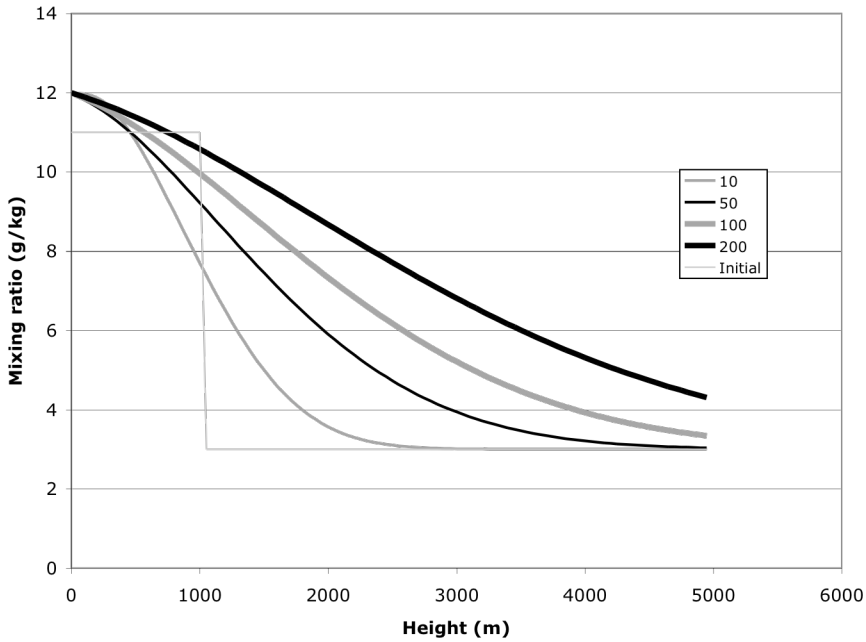

This exercise is used to help the students learn about *K*-theory mixing. Although in a real PBL model, the value of *K* will change with height based upon various assumptions, some behaviors are commonly seen from parameterizations that use *K*-theory.

First, note that off the surface the potential temperature decreases with height to a fairly large depth. This layer is a superadiabatic layer and has been seen over fairly deep layers in models that use this type of approach, although not to the large depths seen above. Second, note the smooth profiles, which make it hard to determine the top of the boundary layer. As the value of K_H is decreased, the vertical depth of the estimated boundary layer is less and the structures are better defined (i.e., easier to find the top of the boundary layer). However, the decrease in potential temperature with height just above the ground to the middle of the boundary layer is larger and quite unrealistic for these lower values of K_H.

While this example is extreme, it does provide a general idea of how *K*-theory works and the challenges to using it to describe PBL evolution.

6] Obtain an observed sounding from near local noon or late afternoon (0000 UTC in the USA is fine) and a corresponding 2-m temperature and mixing ratio. Determine the positive and negative areas of this sounding, as defined from the penetrative convection non-local closure scheme, and the boundary layer top. Using the diffusion scheme, calculate the surface value of $\theta_v + \theta_T$ and from this value also the boundary layer top. Finally, using the observed wind and thermodynamic profiles, estimate values for K_H within this boundary layer using mixing length theory as in (5.59) and (5.61). How does the implied mixing from the local closure scheme compare to the implied mixing from the non-local closure schemes? Explain.

Solution:

Begin with the penetrative convection scheme found in section 5.4.2. Note that the positive area in the boundary layer produced by a thermal rising from the surface conditions is related to the negative area by the entrainment coefficient. For our purposes, the positive area in the sounding is simply the integral of the potential tempeature difference between the rising thermal and the environmental temperature ($\Delta\theta$) multiplied by the change in depth Δz. Thus, for each observation height we calculate the value of $\Delta\theta$ and then multiply it by the change in height Δz between this level and the one below.

I grabbed the 0000 UTC 3 January 2007 sounding from Norman, Oklahoma, for this exercise. I converted the temperature data into potential temperature and list them below.

Pressure (hPa)	Height(m)	Potential temperature(K)	Wind speed(m/s)
984.	345	282.4	1.54
976.	412	282.9	2.06
962.	531	282.9	2.57
952.8	610	282.9	3.08
928.	826	283.1	2.06
925.	852	283.2	2.06
918.	914	283.2	2.06
905.	1029	283.3	2.57
901.	1065	283.7	2.57
899.	1083	283.9	2.57
890.	1164	284.3	3.08
886.	1200	284.8	3.08
883.9	1219	287.1	3.08
870.	1348	289.6	3.08
850.	1538	292.8	2.57

The Norman surface observations from the time of the sounding launch indicate conditions that are cooler than the boundary layer from the sounding, so I choose instead conditions from 2 hours earlier. These conditions are used to determine a surface potential temperature of 283.8 K.

As indicated in Figure 5.13, the positive area in the boundary layer is the area over which a rising thermal from the surface layer (defined using surface conditions) is warmer than the environment. For this example, our surface layer has a potential temperature of 283.8 K as indicated by the surface observations at 2 m height. Thus, the positive area can be calculated simply by calculating the difference in potential temperature between the surface and each observed height in the sounding and multiplying this difference by the change in height. Thus,

Pres(hPa)	Height(m)	Potential (K)	Δθ (K)	Δz (m)
984.	345	282.4	1.5	0
976.	412	282.9	1.0	67
962.	531	282.9	1.0	119
952.8	610	282.9	1.0	79
928.	826	283.1	0.8	216
925.	852	283.2	0.7	26
918.	914	283.2	0.7	62
905.	1029	283.3	0.6	115
901.	1065	283.7	0.2	36
899.	1083	283.9	0.0	18
890.	1164	284.3	-0.4	81
886.	1200	284.8	-0.9	36
883.9	1219	287.1	-1.5	19
870.	1348	289.6	-5.7	129
850.	1538	292.8	-8.9	190

One can immediately tell that the inversion height z_i is at 1083 m or 899 hPa sicne this is where the surface parcel has the same temperature as the sounding. Multiply $\Delta\theta$*Δz from the surface to the inversion height and add them together. The result is 575.6 Km. Assuming an entrainment coefficient of 0.2, yields a negative area of -115.12 Km. Now repeat this process above the inversion height until you match the assumed negative area of -115.12 Km. To do this, you need to use partial layers. The result is a calculated PBL top of 1223 m. This is 140 m above the inversion height.

The next part of the question involves an examination of the non-local diffusion scheme described in section 5.4.3. If one examines (5.44), then you might notice that the results of the exercise above provide information on all the variables except for θ_s. Thus, one can rewrite (5.44) to solve for this variable, which yields

$$\theta_s = \theta(h) - Ri_c \frac{\theta_{va}|U(h)|^2}{gh}.$$

We know that h = 1223 m, $\theta(h)$ = 285.4 K (taking the value from the closest temperature observation to the calculated boundary layer height), Ri_c = 0.25, $U(h)$=3.08 m s^{-1}, θ_{va} = 283.9, and g=9.81 m s^{-2}. Plug these values into the above equation and find that θ_s = 285.34 K. Using the definition of θ_s in (5.45), then θ_T = 1.44 K which is well within the range specified (not to exceed 3.0). Last, since we used the boundary layer depth calculated earlier to obtain a value for θ_s, the boundary layer depth from this approach will be the same value of 1223 m.

Finally, estimate values for K_H using mixing length theory from (5.59) and (5.61). Note that to answer this question a value for mixing length l is needed. We will assume a value of 100 m for l, although values between 50 and 100 are certainly reasonable. Then we see that (5.61) indicates that

$$K_H = l^2 \left| \frac{\partial \overline{u}}{\partial z} \right|.$$

Going back to the sounding, we have

Pres (hPa)	Height(m)	Wind speed(m/s)	ΔU	Δz	K_H
984.	345	1.54	1.54	0	0
976.	412	2.06	0.52	67	77.6
962.	531	2.57	0.51	119	42.9
952.8	610	3.08	0.51	79	64.6
928.	826	2.06	-1.02	216	47.2

925.	852	2.06	0.0	26	0.0
918.	914	2.06	0.0	62	0.0
905.	1029	2.57	0.51	115	44.3
901.	1065	2.57	0.0	36	0.0
899.	1083	2.57	0.0	18	0.0
890.	1164	3.08	.51	81	63.0
886.	1200	3.08	0.0	36	0.0
883.9	1219	3.08	0.0	19	0.0
870.	1348	3.08	0.0	129	0.0
850.	1538	2.57	-0.51	190	26.8

First, note that the values of K_H calculated here are within the range of values used in question 5. Second, to address the question about the implied mixing from these values, one first recognizes that there are several layers for which there is no mixing suggested by mixing-length theory. There is mixing suggested over the bottom four observation levels, nearer the ground surface where wind shear is larger, but in the rest of the boundary layer only sporadic mixing occurs. In contrast, the non-local schemes assume that mixing occurs throughout the boundary layer depth, and as such the implied mixing structures are very different between a mixing-length local closure and a non-local closure approach.

7] Choose a single observed sounding location site and compare the observed soundings against model forecast soundings at all available observation times for a 7 day period. Construct a table comparing boundary layer depth, mean boundary layer potential temperature, and mean boundary layer mixing ratio from both the model and observational data. Separate the data based upon observation time. Summarize the results.

Solution:

This question may or may not be possible to answer, depending upon the resources available at your location. It is not hard to analyze soundings to get the numbers needed for these calculations, but most model web pages do not provide sounding plots as part of their standard output. This is an unfortunate situation and one that I think should be remedied. Sounding structure is so important that I am continually amazed that these vertical profiles are not routinely plotted and shown.

I have found one web site that plots soundings for the Rapid Update Cycle model. This site is located at http://rucsoundings.noaa.gov/ and could be used for this type of project. However, as of early 2007 the data were only available for roughly a 36 h period, so one could not look at an entire week worth of model data in one sitting.

I typically like to ask this question and offer bonus points to students who can actually find the data and complete the analysis. Just having them recognize that these data are not easily available, and yet are so important, is worthwhile.

Chapter 6

1] Plot the sounding data below on a Skew-*T* log-*p* diagram.

HT	P	TC	TD	SPD	DIR	U	V
791.0	920.5	36.7	16.3	11.0	180.	0.0	11.0
965.1	903.0	31.9	12.7	13.0	187.	1.6	12.9
1503.9	850.0	26.1	12.2	15.0	196.	4.1	14.4
2132.6	791.0	20.4	11.9	14.0	191.	2.7	13.7
2819.5	730.0	13.8	10.4	7.0	214.	3.9	5.8
2889.4	724.0	16.0	1.7	5.0	218.	3.1	3.9
3175.4	700.0	15.2	-8.2	1.0	204.	0.4	0.9
5098.8	554.0	-0.9	-15.9	1.0	290.	0.9	-0.3
5906.3	500.0	-8.4	-19.0	5.0	304.	4.1	-2.8
6713.2	450.0	-15.4	-24.4	7.0	269.	7.0	0.1
7091.2	428.0	-16.3	-34.5	12.0	267.	12.0	0.6
7597.0	400.0	-19.7	-37.3	12.0	264.	11.9	1.3
8409.8	358.0	-26.4	-43.0	13.0	270.	13.0	0.0
8960.1	329.8	-30.0	-34.0	14.2	284.	13.8	-3.5
9387.1	310.6	-30.4	-32.9	17.5	273.	17.5	-1.0
9630.6	300.1	-32.7	-35.5	17.4	270.	17.4	0.1
10501.1	264.7	-40.2	-40.0	18.0	259.	17.6	3.3
10888.0	250.0	-43.8	-50.0	18.5	255.	17.8	4.8
12355.9	200.0	-53.3	-60.0	33.2	251.	31.4	10.8

13723.4	161.0	-62.5	-70.0	24.9	282.	24.3	-5.1
14160.5	150.0	-62.1	-75.0	20.8	294.	18.9	-8.6
15157.9	127.4	-67.1	-80.0	25.8	300.	22.4	-12.8

Solution:

Either graph on a Skew-T log p diagram by hand, or use one of many plotting programs. The result is a classic high plains sounding from the USA with an elevated mixed layer. This particular sounding is from Dodge City, Kansas, at 0000 UTC 24 June 1985.

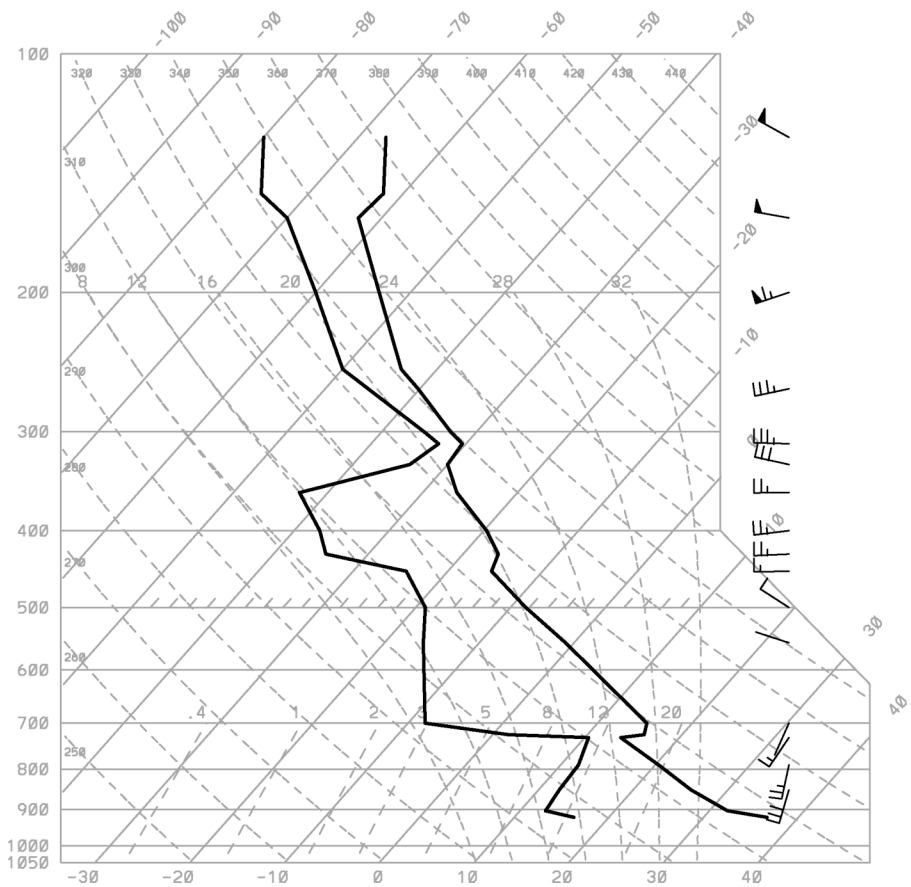

Sounding plotted on Skew-T log p diagram.

2] Calculate the saturation points (SPs) of the sounding (use different colored pencils).

Solution:

Saturation points (SPs) are calculated by lifting parcels dry adiabatically to their lifting condensation level (LCL). Thus, select a particular pressure level and identify the appropriate temperature and dewpoint values at this pressure level. From the selected temperature value, draw a line upward along a dry adiabat. From the corresponding dewpoint temperature value, draw a line upward along a line of constant mixing ratio. Where these two points meet is the SP for this parcel. Repeat this procedure for a number of the observed values along the sounding. This process is illustrated graphically below.

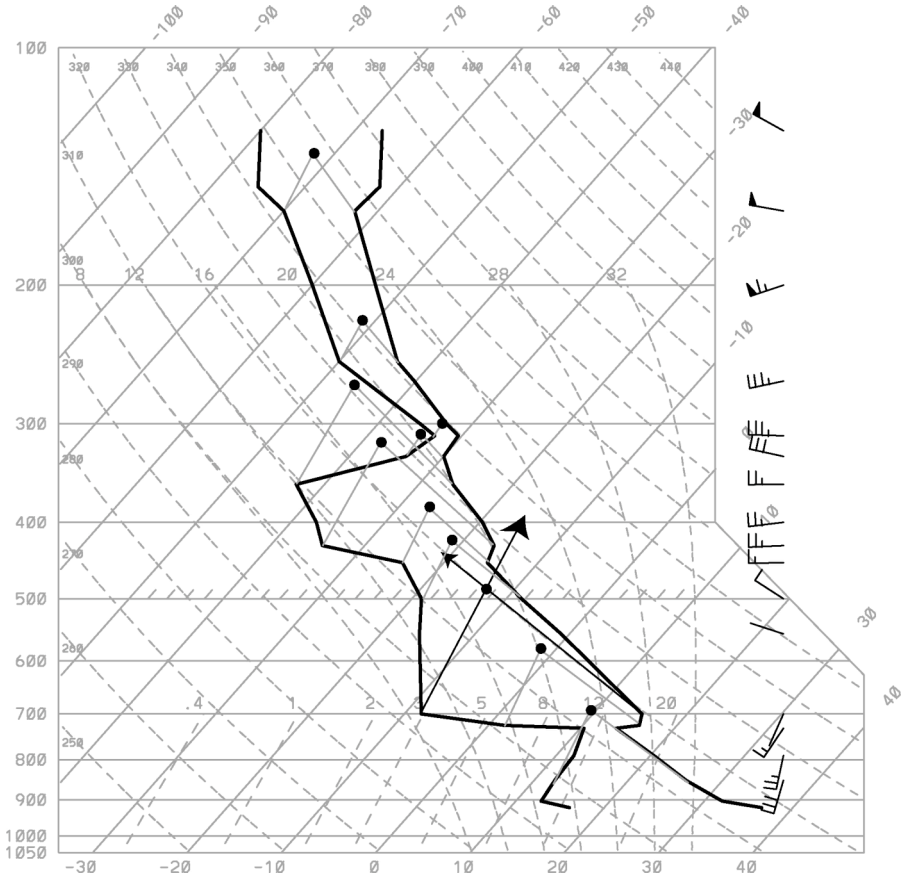

SPs indicated by black dots. Gray lines connect these SPs to their originating points. Arrows show how the SP is calcluated for the 700 hPa conditions.

3] Label any distinct mixing lines that occur over layers at least 100 hPa deep (if any) and calculate the value of β for those mixing lines. Do at most three of these layers, if there are that many.

Solution:

Mixing lines are identified when you can connect SPs with a straight line on a thermodynamic diagram. Three mixing lines are shown on this sounding plot below. The first is not really a line, but a bunch of SPs that cluster in the same location. These SPs are all from the well-mixed boundary layer and end up in the same location. Thus, the value of β for these points is zero, since

$$\beta = \frac{\partial p^*}{\partial p}$$

and the p^* values do not change for these parcels even though their original levels (p value) do change from the bottom to the top of the mixed boundary layer.

The second mixing line connects the SPs from the top of the mixed layer at 730 hPa to the top of the warm layer at 700 hPa. Thus, p^* changes from 700 hPa at the bottom to 490 hPa at the top, while p varies from 730 to 700 hPa. This yields a β value of (210/30) or 7! This indicates that the temperature and dewpoint temperature profiles are diverging in this shallower layer, which is certainly true.

The third mixing line is from 490 to 310 hPa and is shown in black. The original parcels at the top and bottom of this mixing line start at 700 and 428 hPa, respectively. This yields a β value of 0.66, indicating that the temperature and dewpoint temperature lines are moving closer together.

While one could argue that other mixing lines exist, or take issue with the fit of the mixing lines I have selected, the general idea and process should be clear.

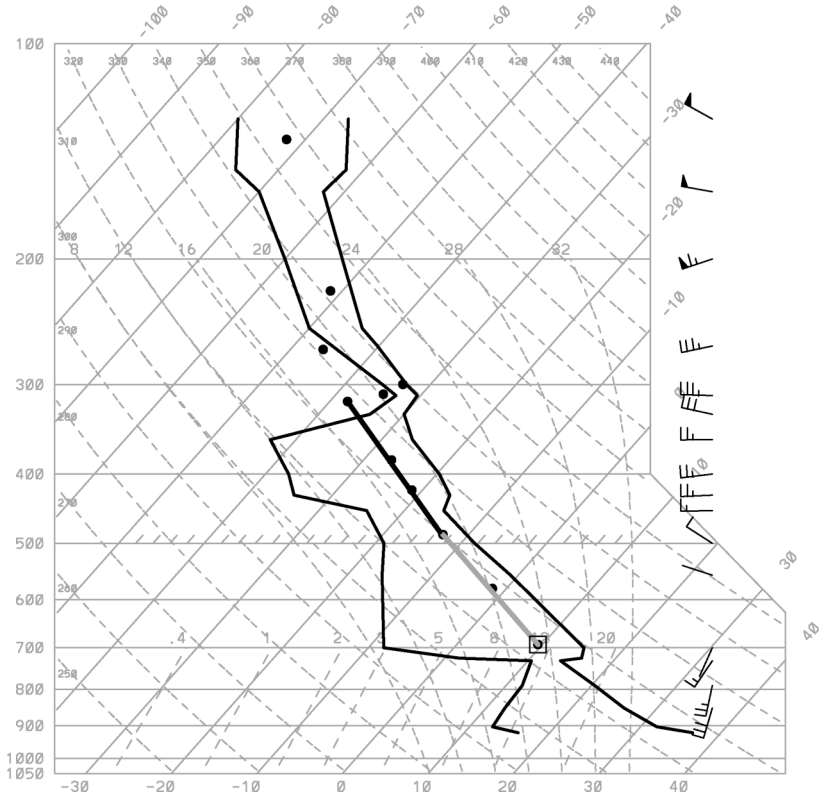

Three mixing lines (box, thick gray, and thick black lines) identified on this sounding. The box indicates that all the SPs from the boundary layer have the same SP, since the boundary layer is very close to being perfectly well mixed. The gray mixing line is for the 730 to 700 hPa originating layer, while the black mixing line is for the 700 to 428 hPa originating layer.

4] Calculate cloud base (LCL) and cloud top (equilibrium temperature level) for a representative parcel. How is this parcel defined? Discuss why the way in which this parcel is defined is important.

Solution:

Cloud base is typically defined by taking an average parcel in the low levels. However, one could also take the parcel with the highest equivalent potential temperature (which for this sounding would be the parcel from the surface). I have selected a parcel from the boundary layer, especially since it is fairly well mixed. This is used to define a moist adiabatic that is shown starting at the LCL of a typical boundary layer parcel. When this moist adiabat intersects the environmental sounding again in the upper levels, this is cloud top or the equilibrium level.

Choose the surface parcel instead and see how far it moves the moist adiabat to the right on this sounding. It certainly makes a big difference in the location of the moist adiabat, but will not dramatically affect the outcome of the BMJ scheme. It will change the height of the equilibrium level, however, which does influence the scheme closure to some extent.

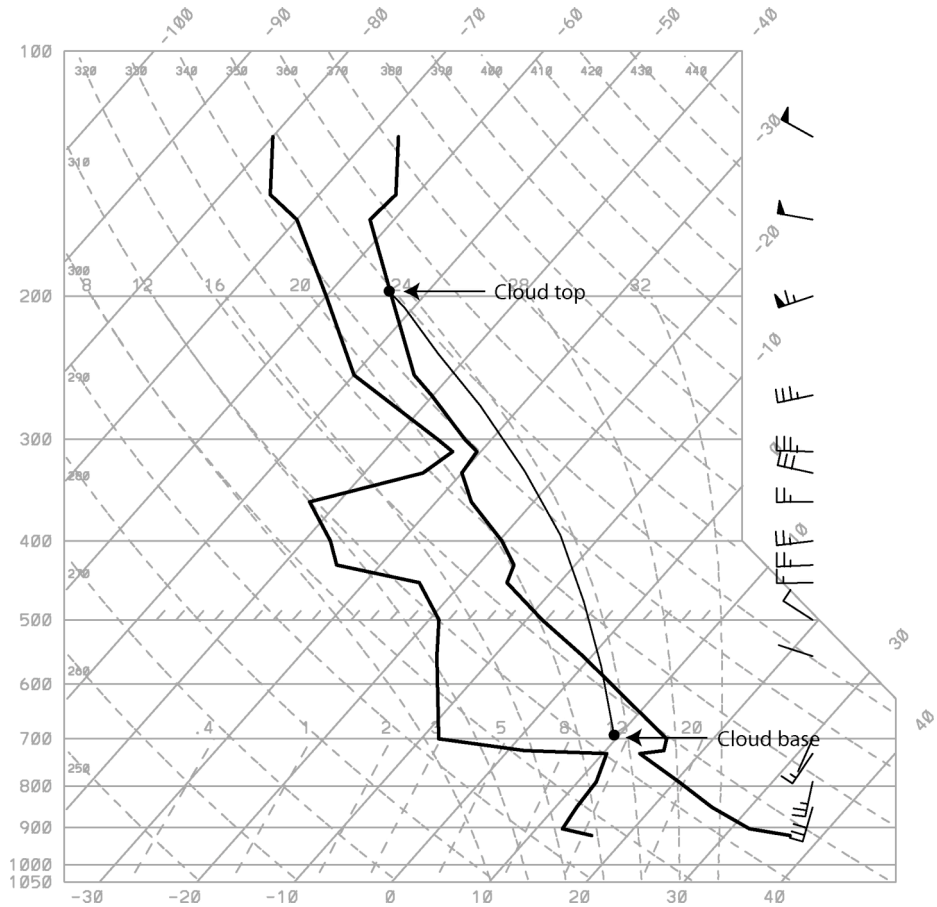

Cloud base is defined by an average parcel from the boundary layer, and cloud top is defined as the level at which the moist adiabat from cloud base equals the environmental temperature above the level where this adiabat is warmer than the environmental temperature.

5] Draw the first-guess reference temperature and humidity profiles for the Betts-Miller convective scheme. Please use a second Skew-*T* log-*p* diagram for this plot. Using knowledge of this scheme, adjust the BMJ profiles to conserve enthalpy and plot the resulting profiles. Will the scheme activate? Discuss how this decision was made. If the scheme will not activate, then what would it take to make the scheme activate? [Note

that a more general, approximate answer is desired. There is no need to code up the entire scheme!]

Solution:

Recall that the BMJ scheme creates a reference temperature profile that has a lapse rate 85% of the moist adiabatic lapse rate between cloud base and the freezing level and then asymptotes to the cloud base moist adiabat (sketched in question 4) between the freezing level and cloud top. For this exercise, a simple estimate of this profile is sufficient. An example is shown in the sounding below. For the reference mixing ratio profile, note that Figure 6.13 shows the saturation pressure departure assumed by the scheme. This is the pressure difference between the parcel LCL and its originating level. The pressure departure is -25 hPa at cloud base, -40 hPa at 500 hPa, and -15 hPa at cloud top. A sketch of this profile, defined using these pressure departures and calculated using the same SP methods as in questions 1-3, is also shown on the sounding below. Note the characteristic shape of this reference profile.

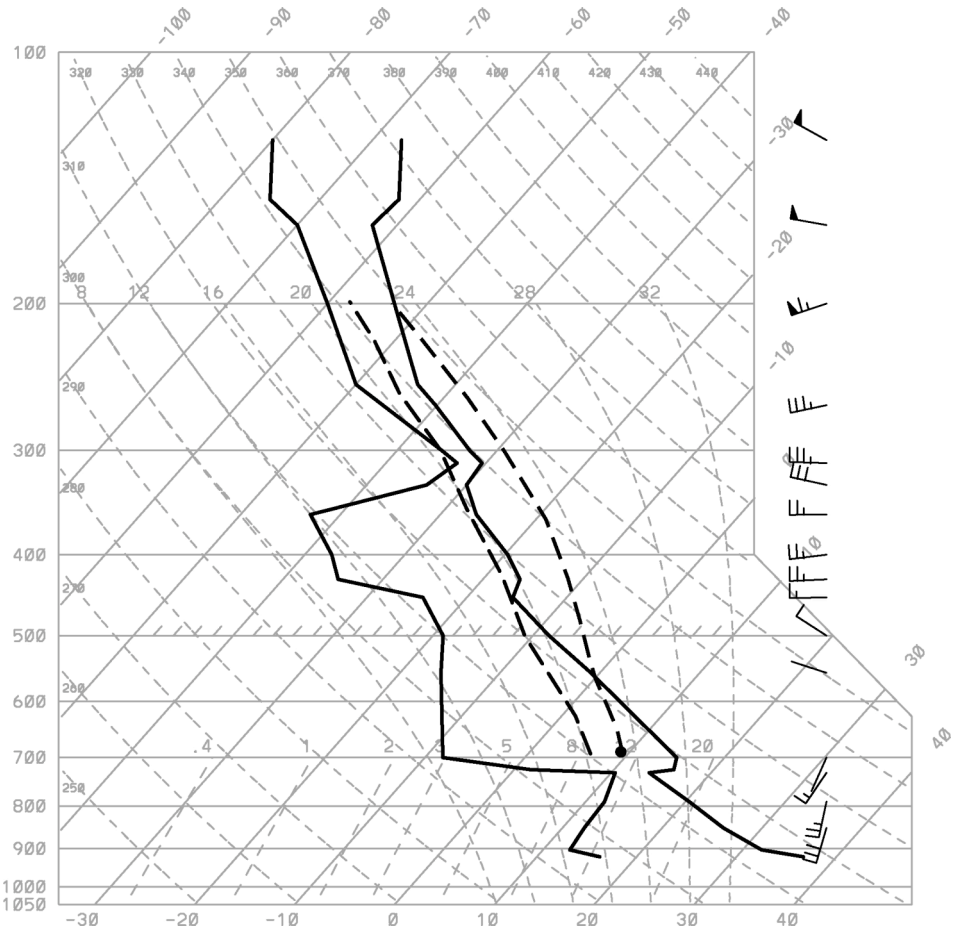

Estimated reference temperature and mixing ratio profiles (dashed) for the BMJ scheme.

The next step is to shift the profile to the left (in this case) to conserve enthalpy. I use an approximate technique by dividing the cloud layer into 3 parts, from 700 to 500 hPa, from 500 to 300 hPa, and from 300 to 200 hPa. For each layer I estimate an average temperature and mixing ratio value for both the original sounding and from the BMJ reference profile. In order to conserve the total enthalpy, one needs

$$\int_{p_{cb}}^{p_{ct}} \left[\left(c_p T_R + L_v q_R \right) - \left(c_p \overline{T} + L_v \overline{q} \right) \right] dp = 0,$$

which is not true for the initial first-guess reference profile. In this case the above integral is much greater than zero. One can crudely estimate a correction by taking the total enthalpy and dividing by the difference in pressure between cloud base and cloud top and then dividing again by c_p. My calculations indicate a shift to the left of roughly 5 K should come pretty close to conserving enthalpy for this case. I make the shift, estimate again the layer-average values of temperature and mixing ratio and recalculate the total enthalpy. It is not quite zero, but it is pretty small. Good enough for this question.

Looking at the final reference profile after enthalpy conservation, it is clear that the adjusted sounding is more moist than the original sounding. You can verify this with a few simple calculations if you like. This means that the scheme if activated would add moisture to the atmosphere, whereas we know convection removes moisture (and moisture removal is required by the BMJ scheme). Thus, the scheme will NOT activate. Greater cloud layer moisture in the environment would be needed to activate the scheme.

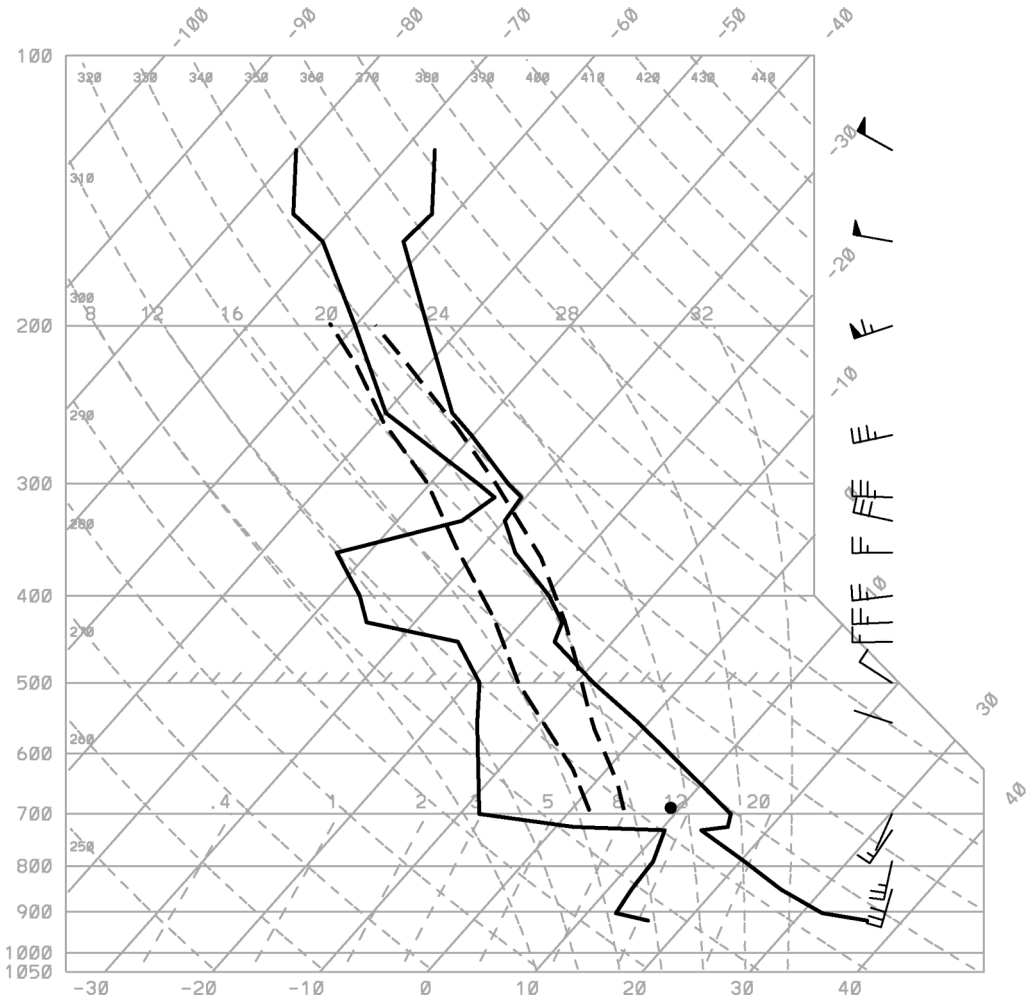

Estimated final temperature and mixing ratio profiles for the BMJ scheme after total enthalpy is conserved. Note the significant shift to the left compared to the first-guess profiles shown earlier. In addition, the final mixing ratio profile is moister than the environment, indicating that the BMJ scheme will NOT activate. The dot indicates the original cloud base SP.

6] Assume that the Kain-Fritsch scheme activates at this grid point. Draw an undilute updraft profile and an undilute downdraft profile. Knowing that the final profile is a mixture of the updraft, downdraft, and environmental profiles, estimate a final reference profile for the scheme. Draw these estimated reference temperature and moisture profiles

for the KF scheme, and explain how the three contributing profiles are mixed. Please use a third Skew-*T* log-*p* diagram for this plot. [Note the details on how to do this calculation were not provided formally, and since the KF scheme uses a buoyancy sorting procedure, one cannot reproduce the resultant profiles exactly without writing a lengthy computer program. However, several examples were provided and the general working of the KF scheme was summarized, so it is possible to provide a general sketch of what the reference profiles look like.]

Solution:

Approximation and a few facts are needed to solve this question. First, we know that the KF scheme defines a 60 hPa deep updraft source layer and evaluates these layers starting from the ground. So define an updraft source layer as the first 60 hPa above ground and lift the average parcel defined by this layer to it's LCL. Then construct a moist adiabat starting at this LCL and use it to determine the equilibrium level or cloud top. This moist adiabat is a crude approximation to the updraft profile in the KF scheme.

The downdraft is determined by the average conditions within the first 150 to 200 hPa above the updraft source layer. I choose to use a value of 200 hPa for this example. Once this layer is defined, then calculate the average conditions within this layer (average temperature, mixing ratio, and pressure), and bring this parcel up to it's LCL. This defines the wet bulb potential temperature of the downdraft parcel. We know that the downdraft remains saturated above cloud base, but the become unsaturated below cloud base. Construct an estimated downdraft profile using this knowledge.

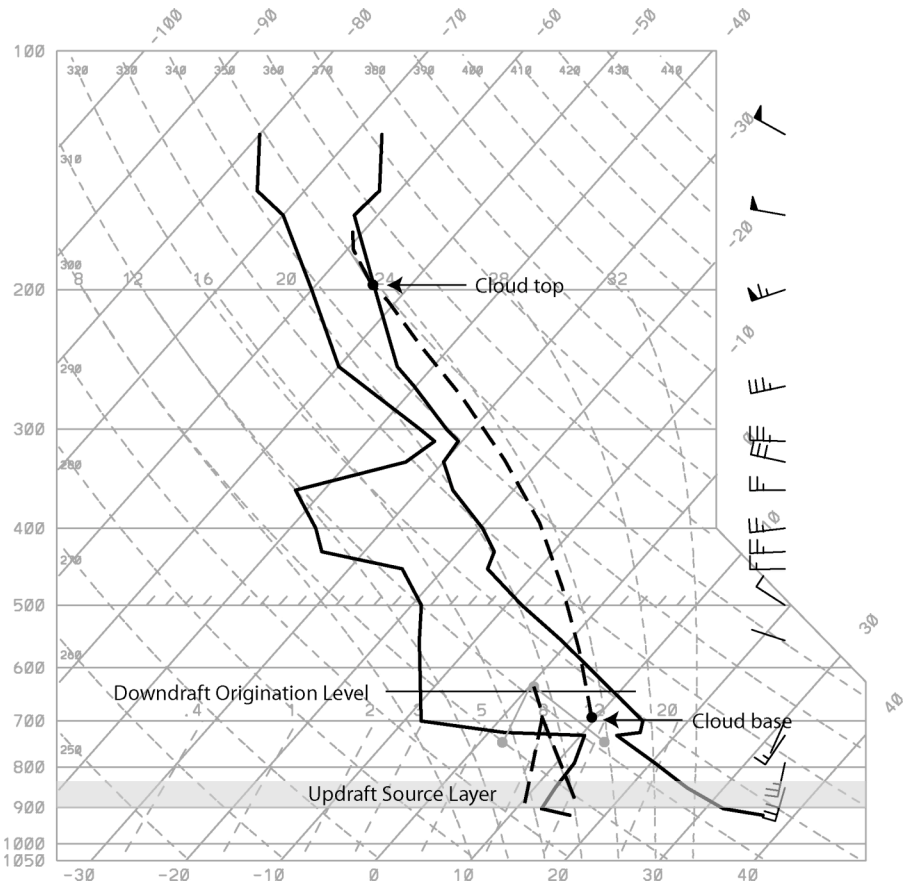

Estimated updraft and downdraft profiles (dashed thick black lines) for the KF scheme. Updraft source layer and downdraft origination level are shown. The updraft is assumed to be saturated, while the downdraft is assumed to be saturated only above cloud base.

The final profile from the KF scheme must lie between the downdraft, updraft, and environmental profiles. It also needs to remove most of the CAPE in the environment and also should be slightly drier than the environment. Using these conditions, estimate a final adjusted profile from the KF scheme. One could spend a lot of time making sure moisture is removed by the scheme, but the main point is to focus on how the updraft,

downdraft, and environmental profiles all combine to produce the final result. It is a much different process than used by the BMJ scheme. Also emphasize that the BMJ scheme only directly influences the cloud layer, whereas the KF scheme influences the boundary layer as well.

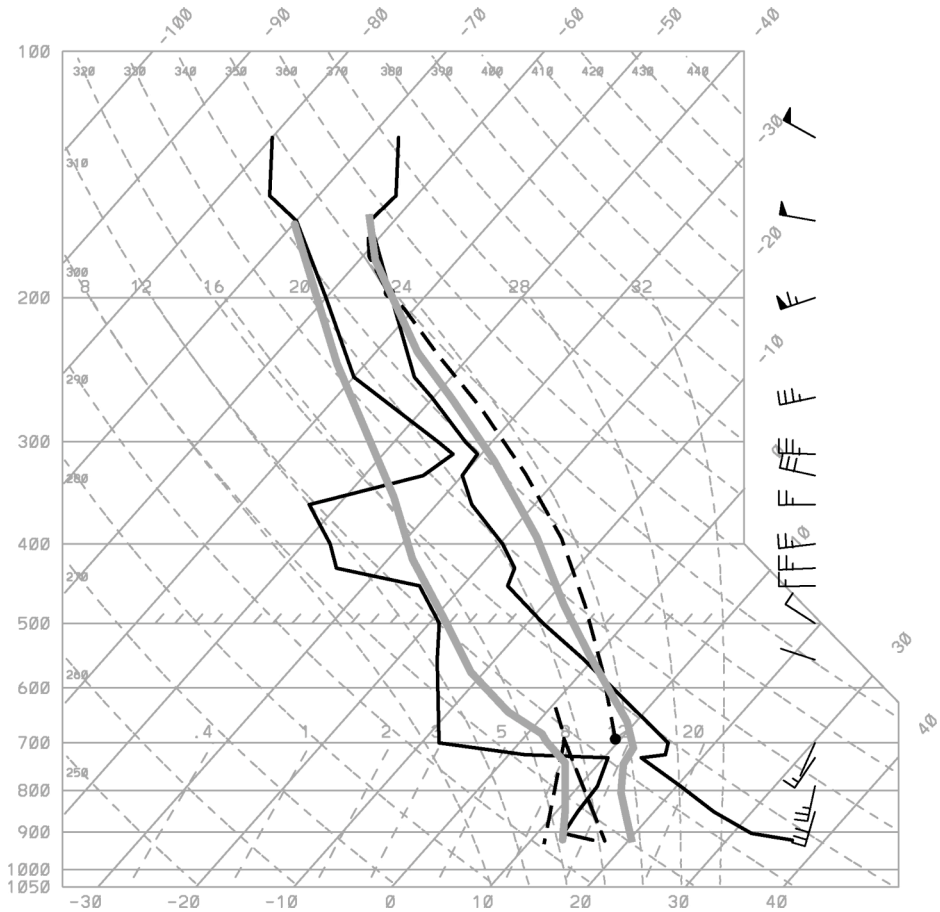

Estimated final adjusted profiles of temperature and mixing ratio (thick gray lines) produced by the KF scheme for this sounding. The updraft and downdraft profiles are still shown (thick black dashed lines). Note that CAPE is very small and that the final profile reduces the boundary layer moisture a lot, even though it moistens the cloud layer. The net result is a very small decrease in moisture when the scheme activates. In this type of environment, the KF scheme likely will not produce much rainfall.

7] How do the adjusted profiles from the Betts-Miller and Kain-Fritsch schemes compare? Under what circumstances would one be preferred over the other? Why?

Solution:

As mentioned previously, one main difference between the two schemes is that the BMJ scheme does not directly influence the environment below cloud base. This is clearly seen when the two final profiles from the BMJ and KF schemes are plotted on the same sounding. Note also that the KF scheme is able to respond more to the local environmental conditions. Students may notice that the BMJ scheme does not warm the mid-level environment as much as the KF scheme, but then this example is not a great comparison since the BMJ would not activate for this sounding. Thus, one must be careful in drawing too many conclusions. The difference to highlight is the effect of the schemes on the boundary layer and the smooth vertical structure to the BMJ profiles compared to the KF scheme that responds more to changes in environmental conditions.

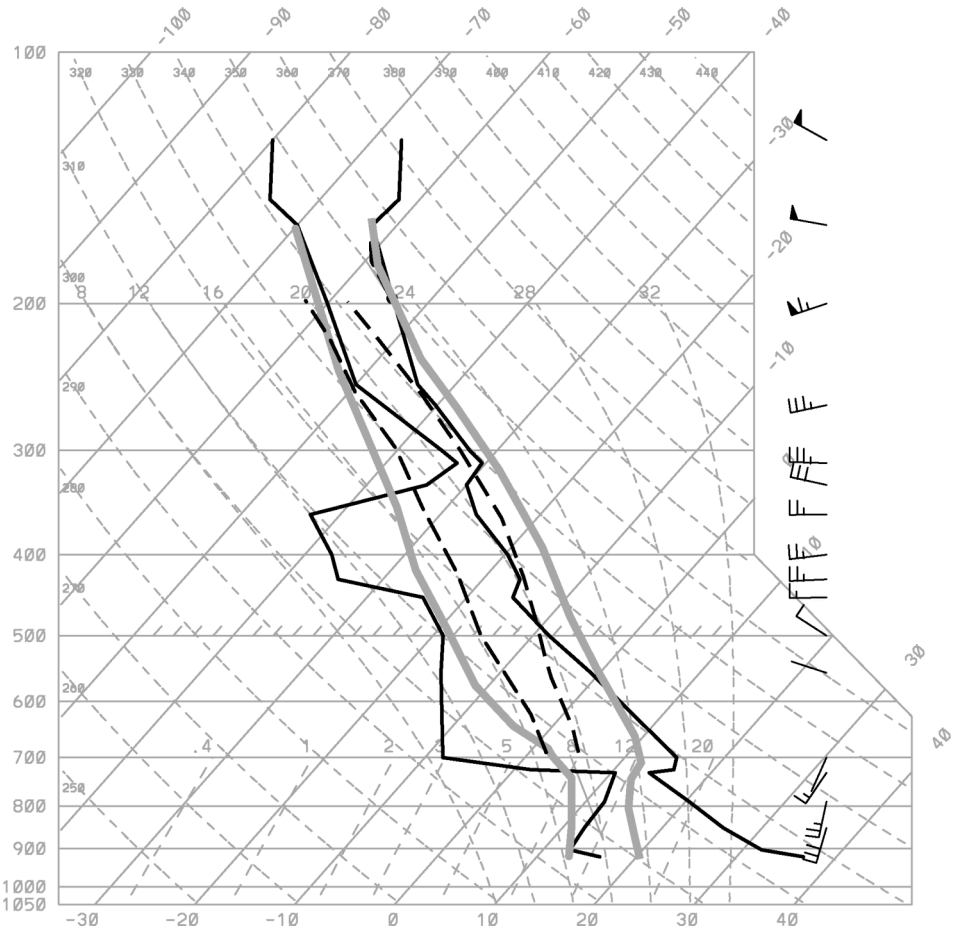

Overlay of the final BMJ (dashed) and KF (thick gray) adjusted profiles for the same sounding. Note the dramatic differences below cloud base.

8] Rework questions 1 through 7 using a sounding from a more tropical environment.

Solution:

This one is up to you. Just follow the basic procedures discussed above. What you typically see when using a more tropical sounding is that the cloud base is much lower and so the differences between the two schemes in the boundary layer are less. The BMJ also is more likely to activate, since most tropical regimes are moister in the cloud layer.

The differences in the final profiles from the KF and BMJ schemes are smaller, but still noticeable.

9] If possible, examine hourly soundings from an operational model forecast in a region of convection. From this examination, find soundings just prior to, during, and after convection has developed in the model. Outline the convective scheme used in this model forecast, and use these soundings to illustrate the behavior of this scheme.

Solution:

As mentioned in the solutions to Chapter 5, I am amazed that it is so hard to find sounding plots from numerical weather prediction models. Horizontal fields abound, but sounding output is rare on the internet and this situation needs to change in my opinion. However, if you have access to such a display system it is helpful for the students to see how rapidly the soundings change once convection is active. Seeing an evolution like that shown in Figure 6.21 is somehow different when you see it yourself. You also will begin to see some characteristic behaviors for some schemes, and this can be helpful in evaluating the environmental conditions and gives you a better understanding of how convection affects the environment.

10] Present an argument for why one would choose a deep-layer over a low-level control convective scheme, or vice versa. Why are both types of convective schemes are in use today?

Solution:

This question is really wide open and almost any reasonable discussion would be acceptable. From my perspective, low-level control schemes more closely mimic our conceptual view of how convection is activated by lifting a parcel to its level of free convection. This is quite appealing to me and is one reason why I tend to favor low-level control schemes. However, convection is a complicated beast and deep-layer control schemes clearly are picking up on some of the processes that influence convection. They tend to focus more on moisture-control instead of instability-control. Both types of schemes are in use today because of the wide variety of needs and the wide variety of model grid spacings. To really begin to handle the processes that lead to convective initiation by a parcel lifted to its level of free convection, model grid spacings need to be in the mesoscale model range (15 to 40 km or so). At larger grid spacings, it is difficult to argue that the model simulation can capture the processes that lead to this type of initiation. Thus, deep-layer control schemes are more reasonable when grid spacings are large and there is a good argument that one should move to low-level control schemes as the grid spacing decreases. But it is clear that both types of schemes capture some signal, and so mixtures of the best parts of the two types of schemes may be the most profitable approach.

Chapter 7

1] Plot the saturation ratio S for pure water as a function of cloud droplet radius.

Solution:

The saturation ratio S for pure water is given by equation (7.2), such that

$$S = \frac{e_s(r)}{e_s(\infty)} = e^{2\sigma / rR_v \rho_w T}.$$

We know that σ is the surface tension (approximately 0.075 kg s^{-2} over the range of meteorologically relevant temperatures), ρ_w is the density of water, R_v is the gas constant for water vapor (461 J kg^{-1} K^{-1}), and T is the temperature of the air. Thus, I simply created an Excel worksheet to calculate S as a function of cloud droplet radius (r). One has to assume a value for temperature, and I choose to use values of 273 and 293 K to explore the effects of temperature on the saturation ratio.

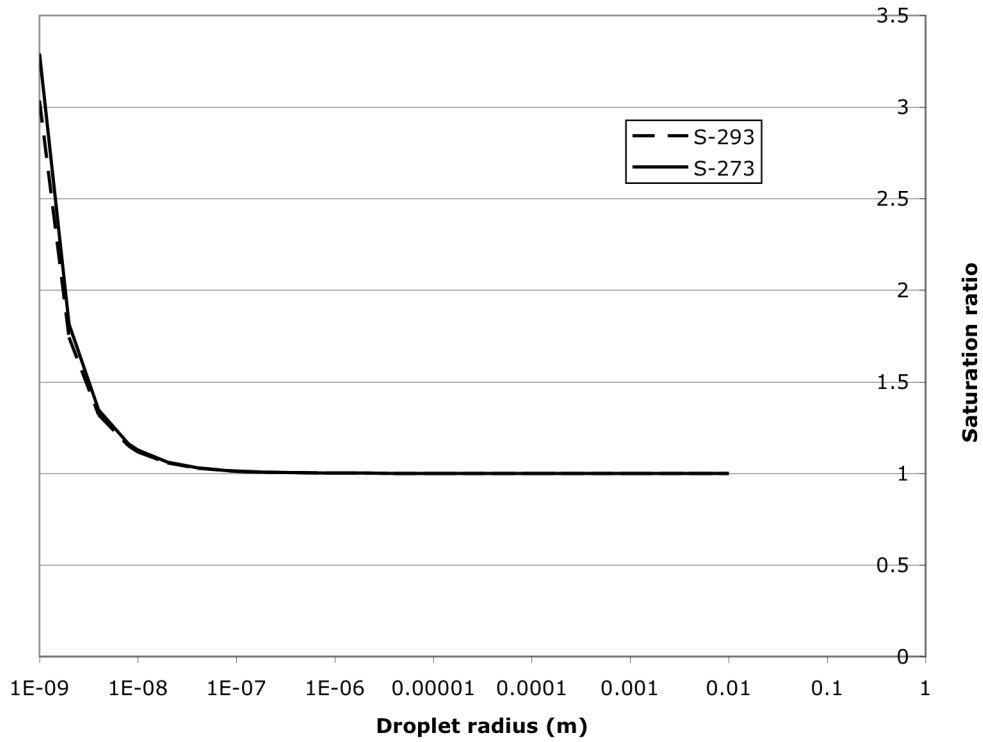

Saturation ratio as a function of droplet radius (m) for temperatures of 293 and 273 K. Note how the curves largely overlap, although the colder temperature requires a slightly higher value of saturation ratio. Also note that for droplets on the order of $1x10^{-9}$ m the values of saturation ratio required exceed 3 or 300% relative humidity.

Calculated values of S also are shown in this Table for reference.

Radius (m)	S-293	S-273
0.000000001	3.035908172	3.293222938
0.000000002	1.74238577	1.814723929
0.000000004	1.31999461	1.347116895
0.000000008	1.148910184	1.16065365
0.00000001	1.117451964	1.126580198
0.00000002	1.057096005	1.061404823
0.00000004	1.028151742	1.03024503
0.00000008	1.013978176	1.015009867
0.0000001	1.011166997	1.011989977
0.0000002	1.005567997	1.005977126

0.0000004	1.002780134	1.00298411
0.0000008	1.001389102	1.001490944
0.000001	1.001111127	1.001192577
0.000002	1.000555409	1.000596111
0.000004	1.000277666	1.000298011
0.000008	1.000138823	1.000148994
0.00001	1.000111057	1.000119194
0.00002	1.000055527	1.000059595
0.00004	1.000027763	1.000029797
0.00008	1.000013881	1.000014898
0.0001	1.000011105	1.000011919
0.0002	1.000005553	1.000005959
0.0004	1.000002776	1.00000298
0.0008	1.000001388	1.00000149
0.001	1.000001111	1.000001192
0.002	1.000000555	1.000000596
0.004	1.000000278	1.000000298
0.008	1.000000139	1.000000149
0.01	1.000000111	1.000000119

2] In the calculation of saturation ratio *S*, include the effects of a solute and replot the curve for various amounts of solute mass. Assume the solute is sodium chloride (NaCl) and that the solute has mass values of $1x10^{-16}$, $1x10^{-15}$, $1x10^{-14}$, $1x10^{-13}$, $1x10^{-12}$, $1x10^{-11}$, and $1x10^{-10}$ g.

Solution:

Using the same basic Excel spreadsheet, add columns for *S* based upon solute mass. Note that since solute mass in given in grams, then the density of water used in the *b* term also must have units of grams to be consistent (or vice versa). The equation needed is (7.3), in which

$$S = \frac{e_s(r)}{e_s(\infty)} = \left[1 - \frac{b}{r^3}\right] e^{2\sigma / rR_v \rho_w T}$$

where $b = 3im_S M_W / 4\pi\rho_L M_S$, m_S is the solute mass (kg), M_s is the molecular weight of the solute, M_W is the molecular weight of a water molecule (18.016), and i is the degree of ionic dissociation (e.g., i=2 for a dilute NaCL solution). For NaCL the molecular weight is 58.44. The only other variable is thus the droplet radius r.

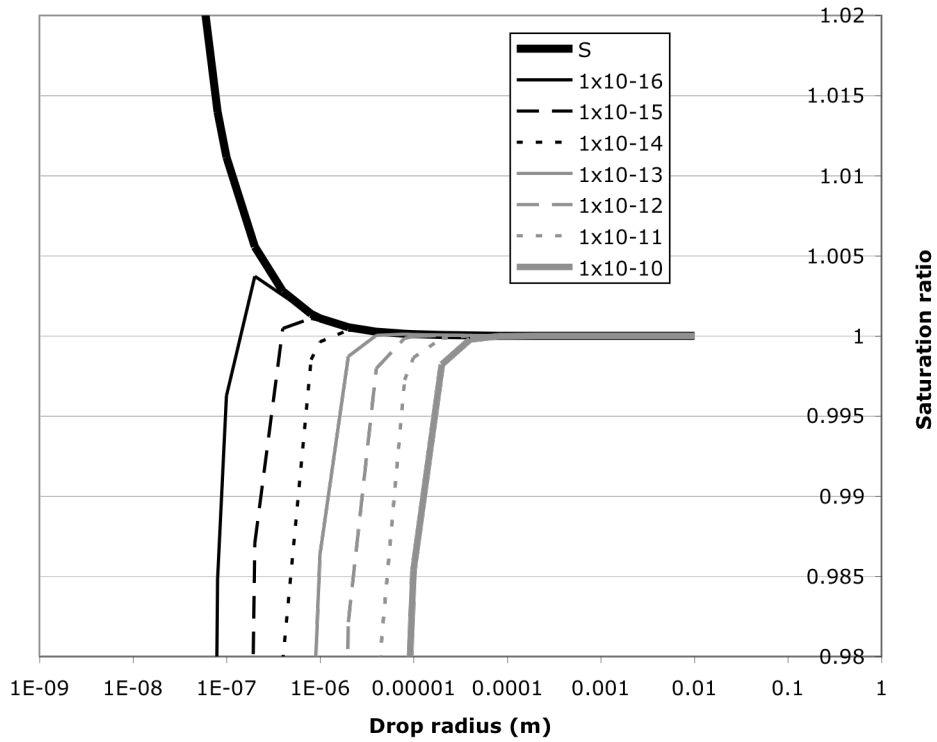

Saturation ratio as a function of NaCL solute mass. Note that the maximum value of saturation ratio (high point on the curves) occurs for the smallest solute mass and decreases towards 1 as the mass of the solute is increased. However, the maximum value of S for a droplet in solution is always greater than 1 for some critical drop radius and then decreases as the drop radius increases. Haze particles can occur for small drop sizes for relative humidities less than 100% (or S less than 1.0). As the solute mass increases, the size of these haze particles also increases.

A few example values are shown in this table for NaCL solute mass values of $1x10^{-16}$ and $1x10^{-15}$ g.

Radius (m)	S	1x10-16	1x10-15
0.000000001	3.035908172	0	0
0.000000002	1.74238577	0	0
0.000000004	1.31999461	0	0
0.000000008	1.148910184	0	0
0.00000001	1.117451964	0	0
0.00000002	1.057096005	0	0
0.00000004	1.028151742	0.791698112	0
0.00000008	1.013978176	0.984828926	0.722485672
0.0000001	1.011166997	0.996283957	0.862336603
0.0000002	1.005567997	1.003717918	0.98706721
0.0000004	1.002780134	1.002549515	1.000473947
0.0000008	1.001389102	1.001360315	1.001101229
0.000001	1.001111127	1.001096392	1.000963777
0.000002	1.000555409	1.000553569	1.000537001
0.000004	1.000277666	1.000277436	1.000275366
0.000008	1.000138823	1.000138795	1.000138536
0.00001	1.000111057	1.000111043	1.00011091
0.00002	1.000055527	1.000055525	1.000055509
0.00004	1.000027763	1.000027763	1.000027761
0.00008	1.000013881	1.000013881	1.000013881
0.0001	1.000011105	1.000011105	1.000011105
0.0002	1.000005553	1.000005553	1.000005553
0.0004	1.000002776	1.000002776	1.000002776
0.0008	1.000001388	1.000001388	1.000001388
0.001	1.000001111	1.000001111	1.000001111
0.002	1.000000555	1.000000555	1.000000555
0.004	1.000000278	1.000000278	1.000000278
0.008	1.000000139	1.000000139	1.000000139
0.01	1.000000111	1.000000111	1.000000111

3] Plot the Marshall-Palmer rain drop size distributions for $n_{0r} = 1x10^{-4}$ m^{-4}, $\rho = 1.0$ kg m^{-3}, and rain water mixing ratios between $1x10^{-8}$ kg kg^{-1} and $1x10^{-3}$ kg kg^{-1}. Plot the curves at regular intervals of rain water mixing ratio. At what value of rain water mixing ratio do more than 10 drops with diameters greater than 5 mm occur for a bin size of 1 mm?

Solution:

The Marshall-Palmer distribution is defined by (7.4) such that

$$n(D) = n_O e^{-\lambda D}$$

where D is the particle diameter (m), n is the number of particles per unit volume (m^{-4}), λ is the slope parameter that defines the fall off of particles as the diameter increases (m^{-1}), and n_O is the intercept parameter that defines the maximum number of particles per unit volume at $D = 0$ size. As mentioned in section 7.4, when the intercept parameter is defined the slope parameter λ_x varies as the mixing ratios change, such that from (7.5) we have

$$\lambda_x = \left(\frac{\pi \rho_x n_{0x}}{\rho q_x} \right)^{0.25}.$$

Thus, to solve this problem calculate λ_x as the mixing ratio is varied across the range specified. Again, I create an Excel spreadsheet, calculate the value of λ_x for each value of rainwater mixing ratio and then plot the Marshall-Palmer distribution as a function of particle diameter. This process yields the following plot.

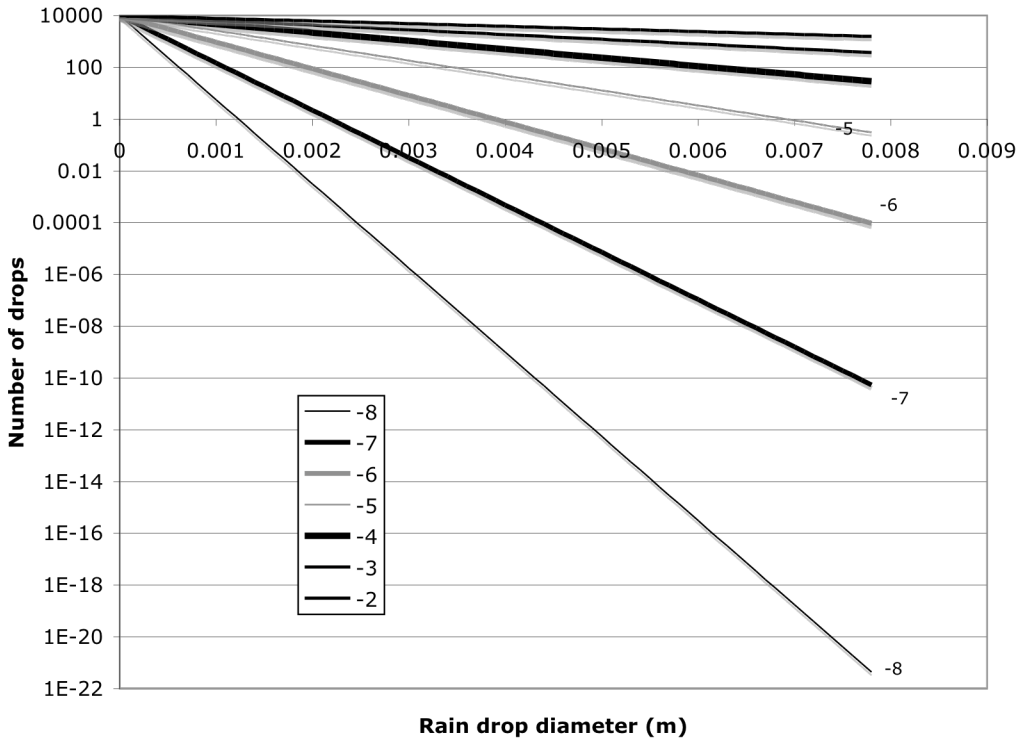

Number of drops as a function of rain drop diameter (m) for various rainwater mixing ratios (-8 implies $1x10^{-8}$ kg kg^{-1}, -7 implies $1x10^{-7}$ kg kg^{-1}, etc).

The plot shows that more than 10 drops of size 5 mm occur when the rain water mixing ratios are larger than $1x10^{-5}$ kg kg^{-1}.

4] Calculate the autoconversion rate using the Kessler, Lin et al, and Tripoli and Cotton expressions over a likely range of cloud water mixing ratios. How large are the differences in autoconversion rates?

Solution:

The expressions for autoconversion are found in the text for the 3 schemes. To answer this question, assumptions are required to specify the air density and temperature. Here I simply choose a value of 1.0 kg m^{-3} for air density and 293 K for temperature. These values are only important for the Lin and Tripoli-Cotton calculations. I again create an Excel spreadsheet with cloud water mixing ratio increasing downward in one column, and then the equations for the 3 autoconversion rates in the other columns. The calculations yield the following information.

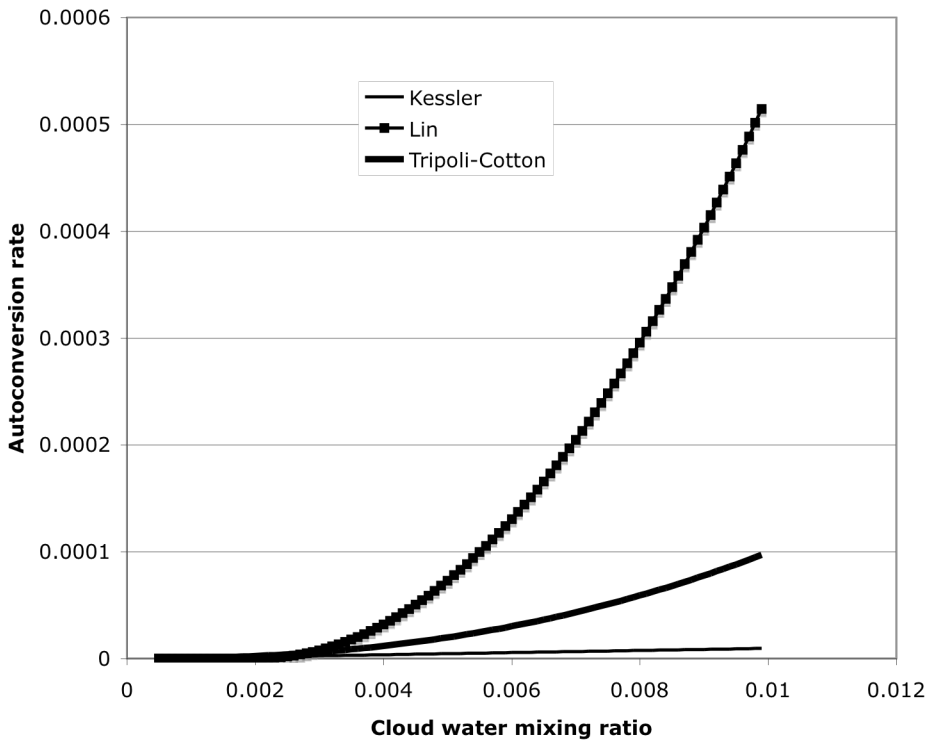

Autoconversion rate versus cloud water mixing ratio (kg kg^{-3}) from the Kessler, Lin et al, and Tripoli and Cotton approaches. The Kessler approach has the smallest values of autoconversion for the larger cloud water mixing ratios, but has smaller autoconversion rates for the lower values of cloud water mixing ratio (not clearly seen in this plot, but easily seen when looking at the actual values).

The differences in autoconversion rate can easily be calculated and plotted as well. This is done by dividing the autoconversion rates of Lin and Tripoli-Cotton by the Kessler value. The results show differences of over 50 between the schemes.

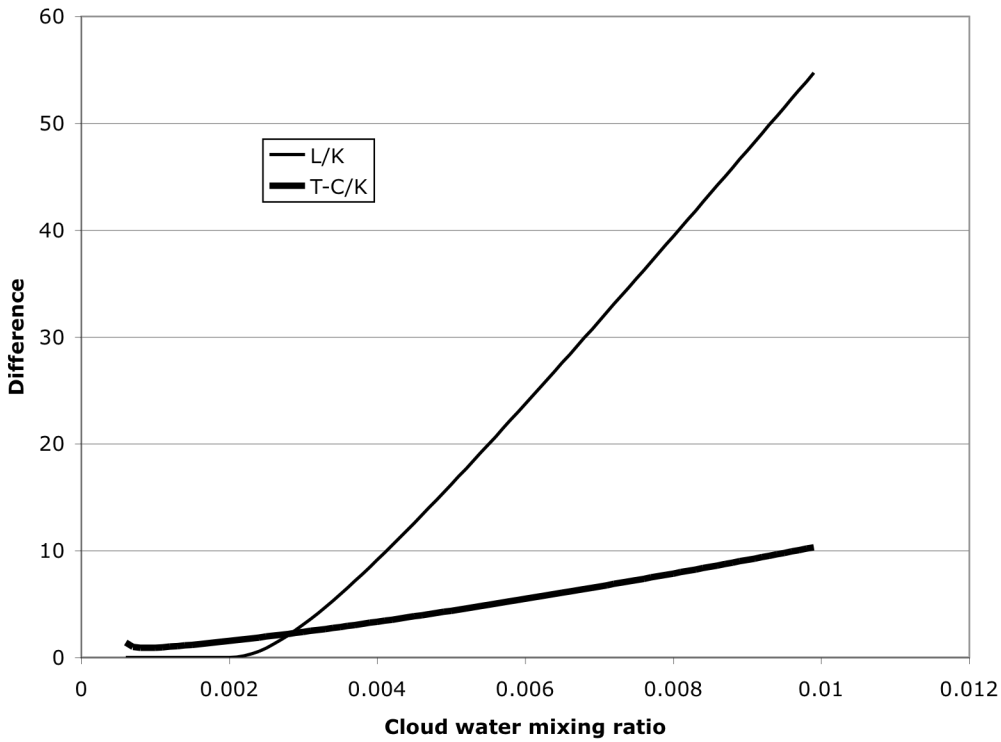

Differences between the Kessler (K), Lin et al. (L), and Tropili and Cotton (T-C) autoconversion rates versus cloud water mixing ratio (kg kg^{-1}). Differences of greater than 50 are found.

5] Derive the Kessler form of the accretion equation (7.23) to (7.25). Show all steps.

Solution:

This is not very hard, but it is often helpful to have the students go through the derivation. Starting with (7.24), we note that

$$P_{ACCR} \equiv \int_0^\infty \frac{d(m(D))}{dt} n(D) dD = \int_0^\infty \frac{\pi D^2}{4} E V_r \rho q_c n_{0r} e^{-\lambda D} dD.$$

If one assumes $V_r = aD^b$, then

$$P_{ACCR} = \int_0^\infty \frac{\pi D^2}{4} a D^b E \rho q_c n_{0r} e^{-\lambda D} dD = \frac{\pi}{4} a E \rho q_c n_{0r} \int_0^\infty D^{2+b} e^{-\lambda D} dD,$$

assuming that density and cloud water mixing ratio are constant.

The gamma function is defined as

$$\Gamma(n) = \int_0^\infty t^{n-1} e^{-t} dt \qquad n > 0,$$

and so

$$\Gamma(b+3) = \int_0^\infty t^{b+2} e^{-t} dt.$$

If we now replace t by λD, then we have

$$\Gamma(b+3) = \int_0^\infty \lambda^{b+2} D^{b+2} e^{-\lambda D} d(\lambda D) = \int_0^\infty \lambda^{b+3} D^{b+2} d^{-\lambda D} dD = \lambda^{b+3} \int_0^\infty D^{b+2} d^{-\lambda D} dD$$

since λ is a constant. Thus, using this expression for the gamma function, we simply need to divided by λ^{b+3}. This yields

$$P_{ACCR} = \frac{\pi}{4} aE\rho q_c n_{0r} \int_0^\infty D^{2+b} e^{-\lambda D} dD = \frac{\pi}{4} aE\rho q_c n_{0r} \frac{\Gamma(b+3)}{\lambda^{b+3}}.$$

6] Compare the Kessler, Tripoli and Cotton, and Schultz accretion rates. Assume that a = 841.996 $m^{1-b}\,s^{-1}$ and b = 0.8 in the fall speed equation. At what value of rain water mixing ratio are the schemes the most different?

Solution:

First convert the Kessler accretion equation so that it depends upon rainwater mixing ratio by using equation (7.5), such that

$$P_{ACCR} = \frac{\pi}{4} aE\rho q_c n_{0r} \Gamma(b+3) \left(\frac{\rho q_r}{\pi \rho_L n_{0r}} \right)^{(3+b)/4}.$$

For b = 0.8, this becomes

$$P_{ACCR} = \frac{\pi^{0.05}}{4\rho_L^{0.95}} aE\rho^{1.95} q_c q_r^{0.95} n_{0r}^{0.05} \Gamma(b+3) \approx 1.478 \rho^{1.95} q_c q_r^{0.95} n_{0r}^{0.05},$$

assuming that E = 1.0 and plugging in values for water density and the variable *a* as given in the question.

With knowledge of the definition of specific content for the Schultz formulation, the accretion rate becomes

$$P_{ACCR} = 17 l_r l_c = 17 \rho^2 q_c q_r .$$

Finally, for Tripoli and Cotton one must first determine the Stokes number and the efficiency *E* before moving to the accretion rate equation. The discussion in the text indicates that the efficiency often is near 1.0, so for simplicity assume *E* = 1.0. Thus,

$$P_{ACCR} = 0.884\left(\frac{g\rho_0}{\rho_w R_m}\right)^{1/2} q_c q_r = 0.884\left(\frac{9.81}{1000 * 2.7x10^{-4}}\right)^{1/2} q_c q_r = 5.328 q_c q_r ,$$

assuming an atmospheric density of 1.0 for simplicity.

An Excel spreadsheet is used to plot the values of these 3 equations assuming $\rho = 1.0$, $q_c = 0.004$. and n_{0r} = 1x10-4 m^{-4}. These calculations yield the figure below.

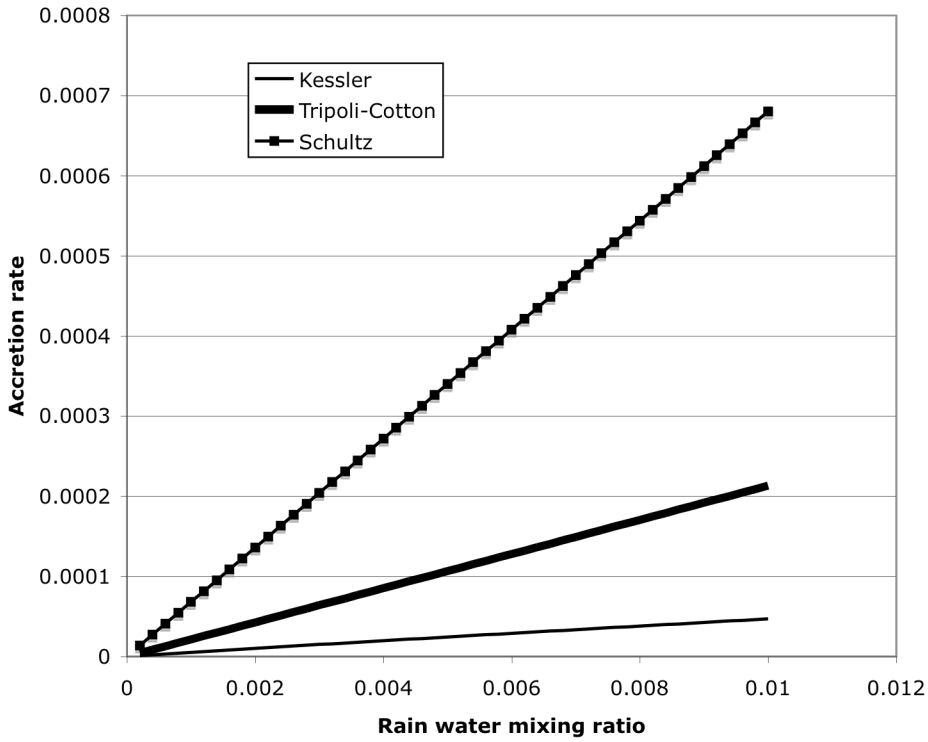

Accretion rate versus rain water mixing ratio (kg kg^{-1}) for the Kessler, Tripoli and Cotton, and Schultz parameterizations. Note that all three are approximately linear with respect to rain water mixing ratio, but with magnitudes that differ by roughly an order of magnitude. Even the Kessler and Tripoli and Cotton approaches differ by nearly a factor of 5.

The schemes are most different at the largest rain water mixing ratios and will continue to become more different as rain water mixing ratio increases.

7] Calculate a distance a rain drop can fall in an environment with a constant relative humidity of 80% and a constant temperature of 278 K for drop sizes of 0.5 mm, 2 mm and 5 mm. Assume the ventilation factor $F = 1$ to simply the calculations. Assume that

the thermal conductivity $K_a = 2.5\text{x}10^{-2}$ J m^{-1} K^{-1} s^{-1} and that the diffusivity of water vapor in the air $D_{diff} = 2.4\text{x}10^{-5}$ m^2 s^{-1}.

Solution:

This question is asking about how long it will take for a drop to evaporate, but with the added complication that one needs to calculate the fall speed and total depth over which the drop falls before it evaporates completely. Start with the equation for evaporation (7.30), which states that

$$\frac{dm(D)}{dt} = \frac{2\pi D(S-1)}{A+B}$$

where S is the supersaturation, and

$$A = \frac{L_v^2}{K_a R_v T^2}, \qquad B = \frac{R_v T}{e_S(T) D_{diff}}.$$

We are given two of the constants in A and B and either know or can determine the rest. For T of 278, the saturation vapor pressure is approximately 872 Pa. Thus, A = 890698.1 m s kg^{-1} and B = 5878807.3 m s kg^{-1}. Their sum is approximately 6.77x10^6 m s kg^{-1}. For a relative humidity of 80%, S = 0.8. Thus, we have as the main equation governing the rate of change of raindrop mass as

$$\frac{dm(D)}{dt} = -\frac{0.4\pi D}{6.77x10^6}.$$

We also know that rain drop mass is related to its diameter D by

$$m(D) = \rho_L V = \rho_L \frac{1}{6}\pi D^3 = 523.6D^3$$

assuming water density at 1000 kg m^{-3}. We can solve this equation for D and substitute this in the equation for *dm*/*dt* to yield

$$\frac{dm(D)}{dt} = -\frac{0.4\pi(m/523.6)^{1/3}}{6.77x10^6}.$$

We also know that the fall speed of a drop can be approximated by aD^b, where a = 841.996 and b = 0.8. If we use a simple 1 second time step to calculate the change in rain drop mass and then calculate how far a rain drop of given size falls in 1 second, converting from rain drop mass to rain drop diameter *D*, then we can step through these calculations until the rain drop has zero mass. This can be done using a computer program or even on a spreadsheet if it can retain enough accuracy (but most don't).

```
      program raindrop
c
c**   Simple program to calculate how long it takes for a falling rain drop to
c**   evaporate in a specified environment.  Also determines the distance this
c**   rain drop will fall before it evaportes.
c
c**   m - mass of rain drop
c**   dm - change in mass of rain drop
c**   d - diameter of rain drop
c**   v - fall velocity of raindrop
```

```
c**     dist - distance rain drop falls
c**     time - total time it takes rain drop to evaporate (seconds)
c**     pi - constant pi
c
      real*8 m,d,v,dist,pi,time,dm
      pi = 4.*atan(1.)
      print *,' pi ',pi
      dist = 0.
      time = 0.
c
      print *,' enter initial rain drop diameter in meters'
      read(5,*) d
c
c**     calculate rain drop mass from diameter
c
      m = 1000.*pi*(d**3)/6.
      print *,' initial rain drop mass (kg) ',m
c
c**     increment over 1 second time intervals, following the drop as it falls and
c**     calculating its decrease in size and change in fall speed
c
      do 10 i=1,100000
c
c**     calculate fall speed of the drop and the amount it falls over 1 second interval.
c**     add this value to the total distance fallen
c
      v = 841.996*d**0.8
      dist = dist + v
      time = time + 1.
c
c**     using 1 second time steps, calculate decrease of raindrop mass as
c**     rain drop falls through environment with T = 278K and 80% RH (or S = 0.8)
c

      dm = -0.4*pi*d/6770000.
      m = m + dm
      if(m.le.0.0) goto 99
c
c**     recalculate diameter d from mass of rain drop
c
      d = (m/523.6)**0.33333
c
 10     continue
      print *,' exited loop 10 without complete evaporation!'
      print *,' rain drop mass ',m
c
```

```
 99    continue
       print *,' time taken for rain drop to evaporate ',time
       print *,' distance rain drop fell ',dist
       stop
       end
```

Results from this program indicate that a rain drop with diameter 0.5 mm will evaporate by the time it falls 1454 m. For a raindrop with 2 mm diameter, the rain drop will fall over 70,000 m before it evaporates! The depth is even greater for a 5 mm rain drop. Play around with drops smaller than 0.5 mm and see that they will evaporate very quickly. Thus, there is a large variation in how quickly drops will evaporate depending upon their size, and this exercise (although imperfect) is an attempt to make the students understand this challenge.

Now imagine what happens for a typical bulk microphysical model with a single fall speed for all drops in the distribution. This gives one a lot of things to ponder.

8] Compare ice aggregation to form snow rate equations from Lin et al., Dudhia, and Murikami for a reasonable range of values for the ice mixing ratio. State any assumptions made. How large are the differences in snow production rate from these three approaches?

Solution:

The expressions for ice aggregation are given by (7.40) to (7.44). However, the expressions depend upon temperature and ice mixing ratio, so these will be varied across a range to see how the values change. I choose to vary the ice mixing ratio from 0.0005

go 0.01 kg kg-1 and at temperatures of 263, 253, and 243 K. Also note that the density of ice is 917 kg m^{-3}.

A few other assumptions are needed. The Murikami scheme requires a number concentration for ice, which is predicted by the scheme. Here I simply assume (perhaps badly) the concentration suggested by the Fletcher curve. Also note that the minus sign in (7.44) typically yields negative rates for this scheme. This minus sign is found in the Reisner et al. paper, but I think that it is intended to mean the rate of ice loss to snow. So the minus sign disappears when you look at snow creation by ice aggregation. So I remove the minus sign from (7.44) in the calculations. For the Dudhia scheme, the aggregation rate is dependent upon the model time step. This is a known concern about using this type of rate equation, and strongly influences the results. Following the original paper, a timestep of 10 second is assumed.

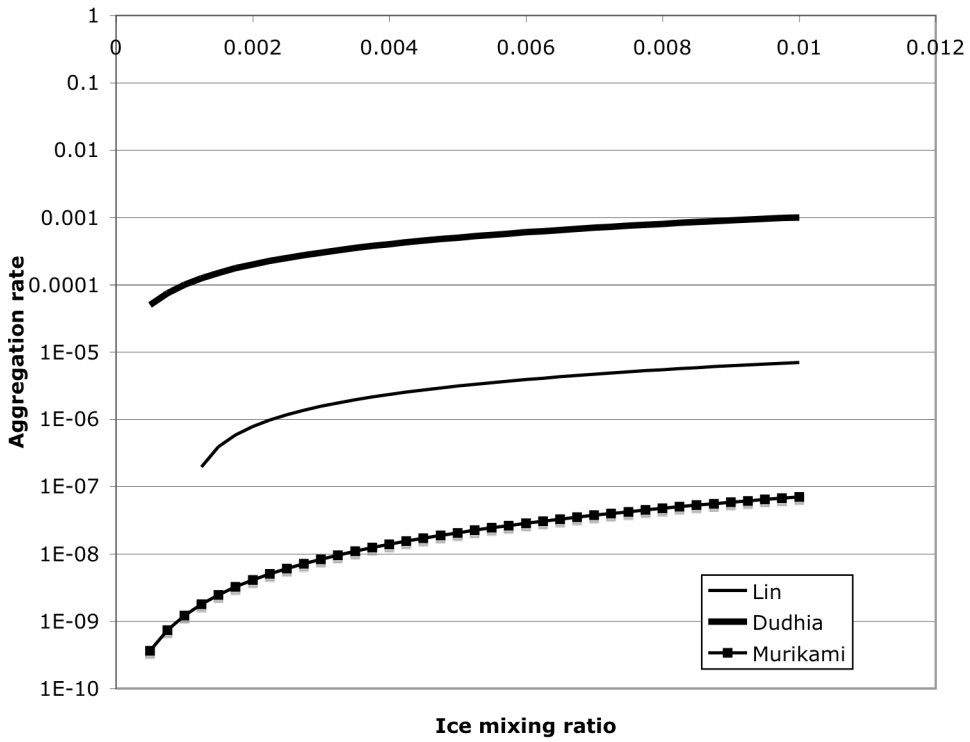

Aggregation rates versus ice mixing ratio for the Lin et al, Dudhia, and Murikami schemes for a temperature of 263 K. Note the large differences in the aggregation rates, varying by several orders of magnitude. While the timestep in the Dudhia scheme plays a role, even the differences between the Lin and Murikami schemes are nearly 2 orders of magnitude.

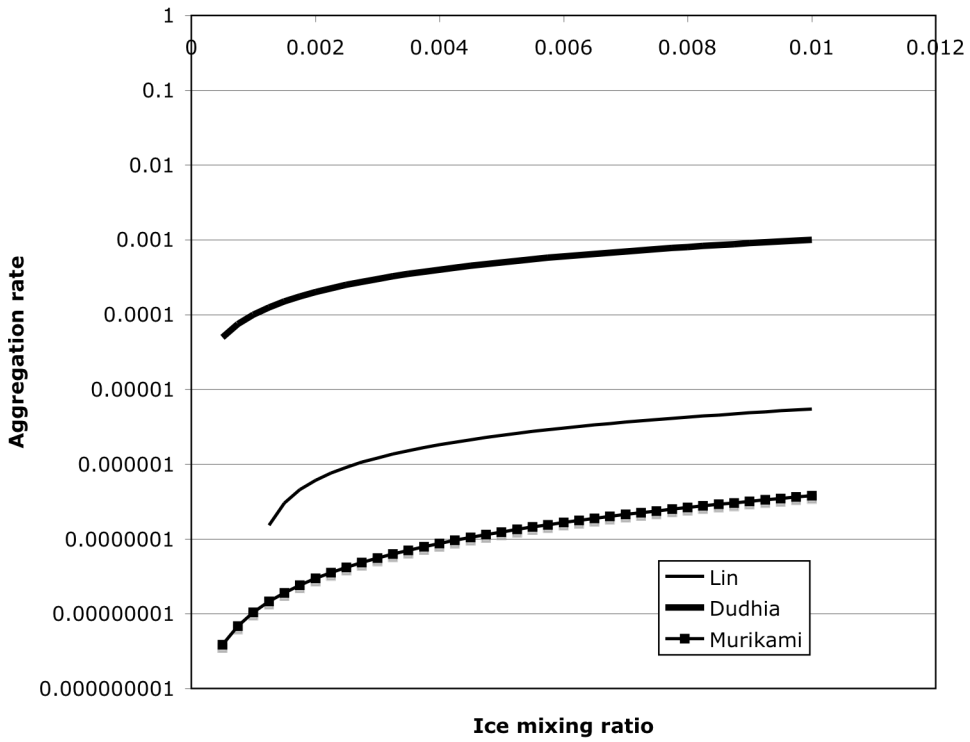

Aggregation rates versus ice mixing ratio for a temperature of 253 K. Similar differences in magnitude are seen as found previously for 263 K. Also note the value of ice mixing ratio for which aggregation is first allowed changes. All 3 schemes have different values of ice mixing ratio that need to be exceeded for aggregation to occur, but these are determined in different ways.

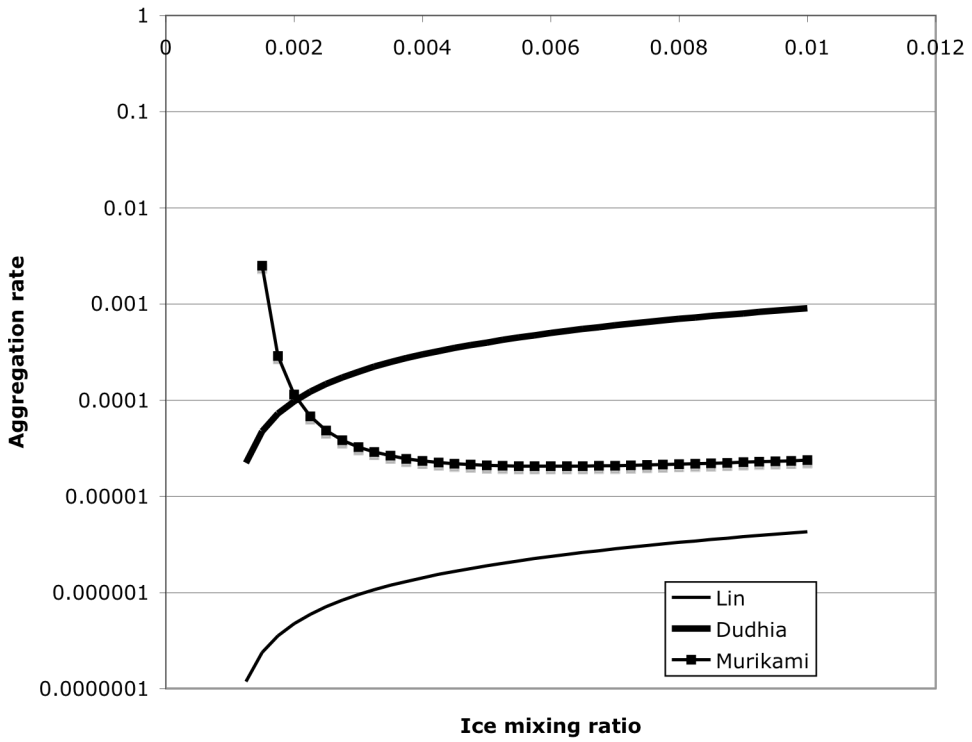

Aggregation rate versus ice mixing ratio for temperature of 243 K. Again, the differences in magnitudes are large, but the Murikami scheme has developed a different shape. I have checked this several times, and for the parameters chosen I think it is correct. When the number of ice crystals is large (hundreds of thousands), then the scheme appears to produce larger aggregation rates for smaller ice mixing ratios.

Chapter 8

The basic ideas behind most of the radiative transfer parameterization schemes are similar, so let us examine the behavior and construction of one of the schemes. Lacis and Hansen (1974) examine how ozone and water vapor influence the total solar flux. The fraction of total solar flux absorbed in the lth layer of the atmosphere by ozone, where l = 1 is the top of the atmosphere and l increases downward, is defined as

$$A_l = \mu_0 \left\{ A(x_{l+1}) - A(x_l) + \overline{R}(\mu_0)\left[A(x_l{*}) - A(x_{l+1}{*}) \right] \right\}, \tag{8.81}$$

where $\overline{R}(\mu_0)$ is the albedo of the reflecting region, x_l is the ozone path traversed by the direct solar beam in reaching the lth layer, and x_l* is the ozone path of the diffuse radiation illuminating the lth layer from below. Ozone absorption is modeled as a purely absorbing region sitting on top of a purely reflecting region. For our purposes, all ozone is generally assumed to lie above the troposphere, or above approximately 100 hPa. The albedo of the reflecting region is defined as

$$\overline{R}(\mu_0) = \overline{R}a(\mu_0) + \left[1 - \overline{R}a(\mu_0)\right](1 - \overline{\overline{R}}a{*})Rg/(1 - \overline{\overline{R}}a{*}\,Rg), \tag{8.82}$$

where Rg is the ground albedo, $\overline{\overline{R}}a{*}$ = 0.144, and the effective albedo of the lower atmosphere is defined as

$$\overline{R}a(\mu_0) = \frac{0.219}{1 + 0.816\mu_0}, \tag{8.83}$$

for clear skies. They also define $x_l = u_l M$, where u_l is the ozone amount in a vertical column above the lth layer, and

$$M = \frac{35}{(1224\mu_0^2 + 1)^{1/2}}, \tag{8.84}$$

is the magnification factor (Rodgers 1967) to account for path slant and refraction. The ozone path traversed by the diffuse radiation illuminating the lth layer from below is defined as

$$x_l{}^* = u_t M + \overline{M}(u_t - u_l), \tag{8.84}$$

where u_t is the total ozone above the main reflecting layer (the ground for clear skies), and $\overline{M}$ = 1.9 is the effective magnification factor for diffuse radiation.

Finally, the fraction of incident solar flux absorbed by the Chappius visible band is defined as

$$A(x_l) = \frac{0.02118x_l}{1 + 0.042x_l + 0.000323x_l{}^2}, \tag{8.85}$$

and the absorption of the ultraviolet region is defined as

$$A(x_l) = \frac{1.082x_l}{(1+138.6x_l)^{0.805}} + \frac{0.0658x_l}{1+(103.6x_l)^3}, \tag{8.86}$$

where the total absorption by ozone in the lth layer is the sum of the individual absorptions from the visible and ultraviolet regions.

If we assume a single layer of ozone above the troposphere with an ozone path x_2 above a single scattering layer, then following Zamora et al. (2003) we find that

$$A = \mu_0\left\{A(x_2) + \overline{R}(\mu_0)\left[A[x_2(M+\overline{M})] - A[x_2M]\right]\right\}. \tag{8.85}$$

1] Calculate the absorption of ozone for a zenith angle of 60 and for ozone path x_2 = 0.2, 0.3, 0.4, 0.5, and 0.6. Assuming a solar constant of 1368 W m^{-2} and ground albedo Rg = 0.10, how much does the presence of ozone decrease the incoming solar radiation?

Solution:

This is basically a coding exercise. All the information needed is found in the equations (8.81) to (8.85). A program to calculate the absorption of ozone is as follows.

```
      program rad_ozone
c
c**   calculate influence of ozone absorption on solar radiation.
cc**  follow variable naming convention in the text.
c
      real pi,zenith,mu,rabar,rbar,rg,rdbar,m
c
      pi=4.*atan(1.)
      zenith=60.*pi/180.
```

```
      rdbar=0.144
      rg=0.10
c
      mu=cos(zenith)
      print *,pi,zenith,rdbar,rg,mu
c
      rabar=0.219/(1.+0.816*mu)
c
      m=35/(1244.*mu**2+1.)**0.5
c
      rbar=rabar+(1-rabar)*(1-rdbar)*rg/(1-rdbar*rg)
      print *,rabar,m,rbar
c
c**    calculate absorption
c
      do i=1,5
       x2=0.1+0.1*i
       print *,i,x2
c
      avis=0.02118*x2/(1.+0.042*x2+0.000323*x2**2)
      aultra=1.082*x2/(1.+138.6*x2)**0.805+0.0658*x2/(1.+(103.6*x2)**3)
      atotal=avis+aultra
c
c**    absorption for x2(M+Mbar)
c
      x3=x2*(m+1.9)
      avis=0.02118*x3/(1.+0.042*x3+0.000323*x3**2)
      aultra=1.082*x3/(1.+138.6*x3)**0.805+0.0658*x3/(1.+(103.6*x3)**3)
      atotalx3=avis+aultra
c
      x4=x2*m
      avis=0.02118*x4/(1.+0.042*x4+0.000323*x4**2)
      aultra=1.082*x4/(1.+138.6*x4)**0.805+0.0658*x4/(1.+(103.6*x4)**3)
      atotalx4=avis+aultra
c
c**    finish calculations
c
      a=mu*(atotal+rbar*(atotalx3-atotalx4))
c
      solar=1368.*(1.-a)
      print *,' end result ',x2,solar
c
      end do
      stop
      end
```

Results from this code indicate that ozone absorption decreases incoming solar radiation by 14.4, 17.4, 20.0, 22.5, and 24.8 W m^{-2} for ozone paths of 0.2 to 0.6. Note that the ozone paths as used here are in units of cm, so that 0.2 cm is equivalant to 200 Dobson units.

2] Now let us turn our attention to the absorption of solar radiation by water vapor. Lacis and Hansen (1974) further discuss water vapor absorption. One formula for water water absorption is

$$A(y) = \frac{2.9y}{(1+141.5y)^{0.635} + 5.925y}, \tag{8.86}$$

where y is the precipitable water vapor in cm. The fractional absorption in the lth layer is then defined under clear skies as

$$A_l = \mu_0 \left\{ A(y_{l+1}) - A(y_l) + Rg\left[A(y_l{}^*) - A(y_{l+1}{}^*) \right] \right\}, \tag{8.87}$$

where the effective water vapor amount traversed by the direct solar beam is

$$y_l = \frac{M}{g} \int_0^{p_l} q \left(\frac{p}{p_0} \right)^n \left(\frac{T_0}{T} \right)^{1/2} dp, \tag{8.88}$$

in units of kg m^{-2}, and where the effective water vapor amount traversed by the diffuse radiation reaching the lth layer from below is

$$y_l^* = \frac{M}{g}\int_0^{p_g} q\left(\frac{p}{p_0}\right)^n \left(\frac{T_0}{T}\right)^{1/2} dp + \frac{5}{3g}\int_{p_{l+1}}^{p_g} q\left(\frac{p}{p_0}\right)^n \left(\frac{T_0}{T}\right)^{1/2} dp, \tag{8.89}$$

where p_g is the ground pressure, g is gravity, p_0=1013 mb, and T_0=273.15 K. One can convert y_l to units of cm by dividing by the density of water (1000 kg m^{-3}) and multiplying by 100 to convert from m to cm. Assuming the atmospheric profile given below, calculate the heating rate in clear sky conditions using n=0, 0.5, and 1 for calculating the effective water vapor. Describe the influence of the pressure scaling on the resulting heating rates.

The sounding to use in calculating water vapor absorption is as follows.

p(mb)	T (C)	q (g/kg)
950.0	36.0	13.0
900.0	32.0	11.0
850.0	26.0	11.0
800.0	20.0	11.0
750.0	15.0	11.0
700.0	15.0	4.0
650.0	10.0	2.0
600.0	5.0	1.5
550.0	0.0	1.5
500.0	-8.0	1.0
450.0	-15.0	1.0
400.0	-20.0	0.4
350.0	-26.0	0.4
300.0	-30.0	0.4
250.0	-44.0	0.2
200.0	-53.0	0.1
150.0	-62.0	0.05

127.4 -67.0 0.05

Solution:

This again is a coding exercise. The following program codes the equations shown above and uses the sounding provided.

```
      program rad_water
c
c**   program to calculate water vapor absorption using a sounding
c
      real p(18),t(18),q(18),a(17)
      real n,m,g,to,po,mu

      data p/950.,900.,850.,800.,750.,700.,650.,600.,550.,500.,
     1       450.,400.,350.,300.,250.,200.,150.,100./
      data t/36.,32.,26.,20.,15.,15.,10.,5.,0.,-8.,-15.,-20.,
     1      -26.,-30.,-44.,-53.,-62.,-67./
      data q/13.,11.,11.,11.,11.,4.,2.,1.5,1.5,1.,1.,0.4,0.4,
     1       0.4,0.2,0.1,0.05,0.05/

      po=101300.
      to=273.15
      cp=1004.
      g=9.81
      pi=4.*atan(1.)
      zenith=60.*pi/180.
      mu=cos(zenith)
      m=35./((1225*mu**2+1.)**0.5)
      rg=0.10
c
c**   convert to units of Pa, Kelvin, and kg/kg.
c
      do k=1,18
       p(k)=p(k)*100.
       t(k)=t(k)+273.15
       q(k)=q(k)*0.001
      end do
c
c**   loop over the three values for n in the scaling approximation.
c
      do i=1,3
```

```
      n=0+(i-1)*0.5
      print *,' results for n = ',n
c
c**   calculate the effective water vapor amount traversed by the direct solar beam
c**   in reaching each of the layers, starting at the top of the atmosphere and moving
c**   downward
c
      yint=0.
      do k=17,1,-1
        qavg=0.5*(q(k)+q(k+1))
        tavg=0.5*(t(k)+t(k+1))
        pavg=0.5*(p(k)+p(k+1))
        yint=yint+(p(k)-p(k+1))*qavg*((pavg/po)**n)*(to/tavg)**0.5
      end do
      yint=(m/g)*yint
      yint=(yint/1000.)*100.
      print *,' total column yl ',yint,' in cm'
c
c**    begin integration over the layers, starting at the top
c
      do l=17,1,-1
c
      yl=0.
      ylstar=0.
      ylp=0.
      ylpstar=0.
c
c**    yl first
c
      do k=17,l,-1
        qavg=0.5*(q(k)+q(k+1))
        tavg=0.5*(t(k)+t(k+1))
        pavg=0.5*(p(k)+p(k+1))
        yl=yl+(p(k)-p(k+1))*qavg*((pavg/po)**n)*(to/tavg)**0.5
      end do
      yl=yl*m/g
      yl=(yl/1000.)*100.
c
c**    ylp next
c
      if(l.ne.1) then
       do k=17,l-1,-1
        qavg=0.5*(q(k)+q(k+1))
        tavg=0.5*(t(k)+t(k+1))
        pavg=0.5*(p(k)+p(k+1))
        ylp=ylp+(p(k)-p(k+1))*qavg*((pavg/po)**n)*(to/tavg)**0.5
```

```
        end do
        ylp=ylp*m/g
        ylp=(ylp/1000.)*100.
       else
        ylp=yint
       end if
c
c**     ylstar next
c
       if(l.ne.1) then
        do k=l-1,1,-1
         qavg=0.5*(q(k)+q(k+1))
         tavg=0.5*(t(k)+t(k+1))
         pavg=0.5*(p(k)+p(k+1))
         ylstar=ylstar+(p(k)-p(k+1))*qavg*((pavg/po)**n)*(to/tavg)**0.5
        end do
        ylstar=yint+ylstar*5/(3.*g)
        ylstar=(ylstar/1000.)*100.
       else
        ylstar=yint+(5./(3.*m))*yint
        ylstar=(ylstar/1000.)*100.
       end if
c
c**     ylpstar next
c
       if(l.gt.2) then
        do k=l-2,1,-1
         qavg=0.5*(q(k)+q(k+1))
         tavg=0.5*(t(k)+t(k+1))
         pavg=0.5*(p(k)+p(k+1))
         ylpstar=ylpstar+(p(k)-p(k+1))*qavg*((pavg/po)**n)*(to/tavg)**0.5
        end do
        ylpstar=yint+ylpstar*5/(3.*g)
        ylpstar=(ylpstar/1000.)*100.
       else
        ylpstar=yint+(5./(3.*m))*yint
        ylpstar=(ylpstar/1000.)*100.
       end if

c
       ayl=2.9*yl/( (1.+141.5*yl)**0.635 + 5.925*yl )
       aylp=2.9*ylp/( (1.+141.5*ylp)**0.635 + 5.925*ylp )
       aylstar=2.9*ylstar/( (1.+141.5*ylstar)**0.635 +
     1         5.925*ylstar )
       aylpstar=2.9*ylpstar/( (1.+141.5*ylpstar)**0.635 +
     1         5.925*ylpstar )
```

```
c
c**    calculate the absorption over an entire day (86400 seconds)
c
      a(l)=1368.*g*mu*(aylp-ayl+rg*(aylstar-aylpstar))/(cp*5000.)
c      print *,aylp,ayl,aylstar,aylpstar
      print *,l,a(l)*86400.
c
      end do
      end do
c
      stop
      end
```

Results from running this program indicate that the scaling factor is important to the end result, especially for longer simulation or forecast time periods.

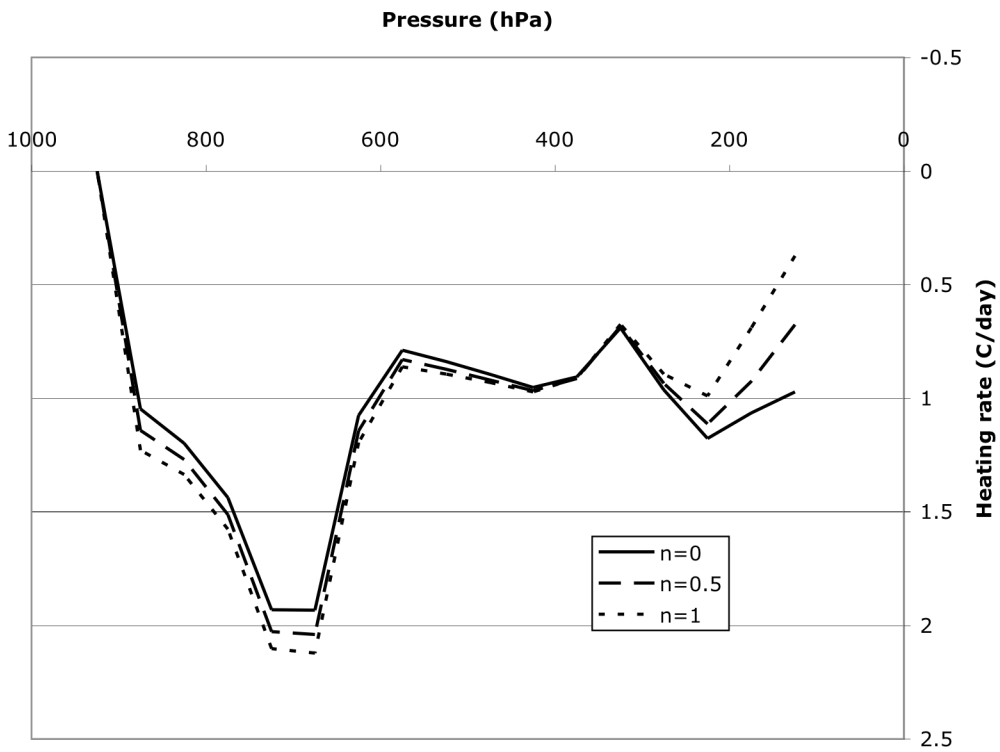

Heating rate calculated from the given sounding as a function of atmospheric pressure using scaling parameter constant values of n = 0.0, 0.5, and 1.0. While the general shape of the heating profile is the same regardless of the value of n, the actual values differ by over 0.5 C/day at the upper levels of the troposphere.

Chapter 9

1] Fill in the details in the derivation of the Sundqvist cloud cover parameterization approach. Starting with (9.17) derive (9.24).

Solution:

Taking directly from the book, we have that beginning with the relationship

$$q = Uq_s, \tag{9.17}$$

where q_s is the saturation specific humidity and taking the derivative with respect to time, one finds

$$\frac{\partial q}{\partial t} = \frac{\partial U}{\partial t} q_s + U \frac{\partial q_s}{\partial t}. \tag{9.18}$$

Using the approximation $q_s \cong \varepsilon e_s/p$ to replace q_s in the last term of (9.18), where e_s is the saturation vapor pressure, p is pressure, and $\varepsilon = 0.622$, yields

$$\frac{\partial q}{\partial t} = \frac{\partial U}{\partial t} q_s + \frac{U\varepsilon}{p}\frac{\partial e_s}{\partial t} - \frac{U\varepsilon e_s}{p^2}\frac{\partial p}{\partial t}. \tag{9.19}$$

Making use of the Clausius-Clapeyron equation, $de_s / dT = \varepsilon L_v e_s / R_d T^2$, where R_d is the specific gas constant for dry air, and L_v is the latent heat of vaporation. The next step is to use the relation $de_s = \varepsilon L_v e_s dT / R_d T^2$ to replace de_s and to multiply all terms on both sides of the equation by $(1/q)$ and remembering that $(1/q) = (1/Uq_s) = (p/U\varepsilon e_s)$. This leads to

$$\frac{1}{q}\frac{\partial q}{\partial t} = \left(\frac{1}{Uq_s}\right)\frac{\partial U}{\partial t}q_s + \left(\frac{p}{U\varepsilon e_s}\right)\frac{U\varepsilon}{p}\left(\frac{\varepsilon L_v e_s}{R_d T^2}\frac{\partial T}{\partial t}\right) - \left(\frac{p}{U\varepsilon e_s}\right)\frac{U\varepsilon e_s}{p^2}\frac{\partial p}{\partial t}.$$

Cancel like terms and you are left with

$$\frac{1}{q}\frac{\partial q}{\partial t} = \left(\frac{1}{U}\right)\frac{\partial U}{\partial t} + \left(\frac{\varepsilon L_v}{R_d T^2}\frac{\partial T}{\partial t}\right) - \frac{1}{p}\frac{\partial p}{\partial t} \tag{9.20}$$

Following Sundqvist et al. (1989), the tendency equations for temperature, specific humidity, and cloud water mixing ratio (q_c) in the case of stratiform condensation and evaporation are

$$\frac{\partial T}{\partial t} = A_T + \frac{L_v}{c_p}Q - \frac{L_v}{c_p}E_0, \tag{9.21}$$

$$\frac{\partial q}{\partial t} = A_q - Q + E_0, \tag{9.22}$$

$$\frac{\partial q_c}{\partial t} = A_{q_c} + Q - (P - E_r) - E_0, \tag{9.23}$$

where the A-terms represent the tendencies due to all processes other than condensation and evaporation, c_p is the specific heat of air at constant pressure, P is the rate of release of precipitation, E_r is the evaporation rate of precipitation, and E_0 is the total evaporation rate due to E_r and the evaporation of cloud water. When the environment is saturated, $U \equiv 1$ and the dU/dt term on the right-hand side of (9.20) is identically zero. If this modified version of (9.20) for saturated conditions is inserted into (9.22), and if (9.21) is then used to eliminate the temperature tendency, one arrives at

$$Q = \frac{M - q_s \dfrac{\partial U}{\partial t}}{1 + \dfrac{U \varepsilon L_v^2 q_s}{R_d c_p T^2}} + E_0, \tag{9.24}$$

where M is the convergence of available latent heat into the grid cell as specified by (9.25). Since this last part of the derivation is very straightforward, I leave it to you.

2] Let us examine the effects of clouds on longwave radiation. Assume a very simple atmosphere of only one layer, with $F_{Dclear} = 315$ W m^{-2} and $F_{Dcloud} = 350$ W m^{-2}. Using (9.37) and (9.38), calculate the downwelling surface longwave radiation as a function of cloud cover. Also vary the cloud aspect ratio from 1 to 5. Describe the results.

Solution:

This is again best examined using a simple spreadsheet. Set it up to vary the cloud cover b, but modify it using (9.38), and then plug this value into (9.37) and display the results.

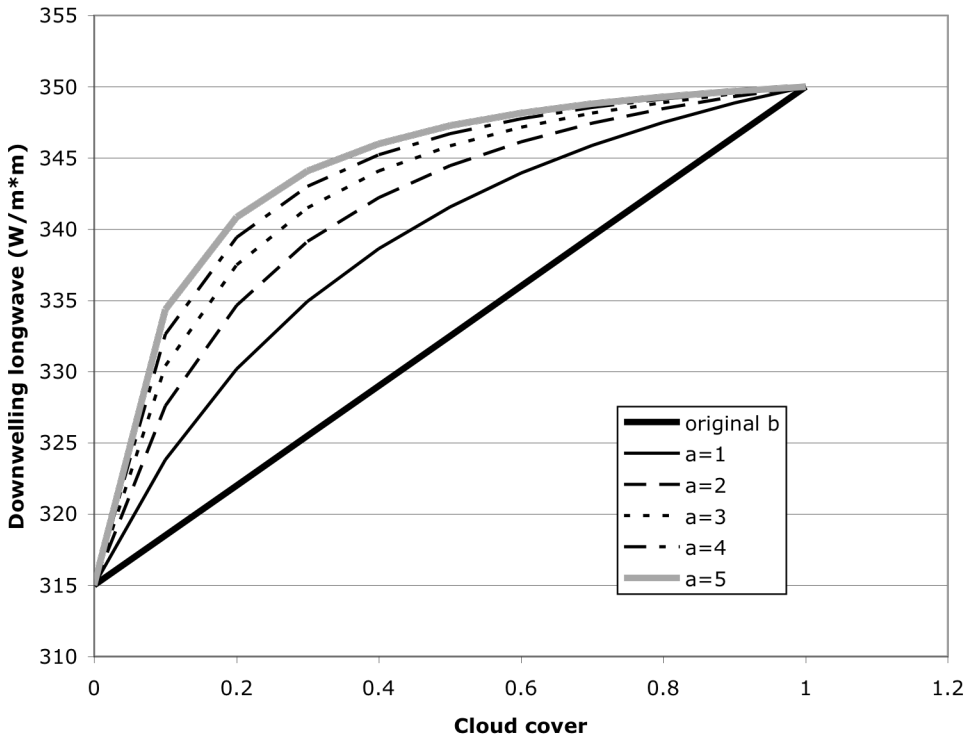

Downwelling longwave radiation as a function of cloud cover using the original linear scaling for cloud cover and the modified version based upon the cloud aspect ratio a. Note that as the cloud aspect ratio increases, meaning that the clouds are deeper than wide, the downwelling radiation is weighted more by the cloudy sky contribution.

3] Using the results of question 2], how large are errors in downwelling surface radiation for uncertainties of 30% in cloud cover? What does this say about the importance of cloud cover parameterization in models?

Solution:

A simple examination of the above plot suggests that 30% errors in cloud cover can easily yield 10 W m^{-2} errors in downwelling longwave radiation. However, this error is larger if the clouds are tall, with errors approaching 30 W m^{-2}. These errors are relatively large, amounting to 10% or so of the typical value, and may influence model forecasts.

4] Turning our attention to shortwave radiation, vary the values of cloud water path from 10 to 10,000 g m^{-2} and calculate the transmissivity using (9.42). Assuming that the incoming shortwave radiation at the top of the cloud is 800 W m^{-2}, plot the values of shortwave radiation exiting the bottom of the cloud as a function of cloud water path using (9.43) - (9.49). Assume that $\mu_0 = 0.87$, $\beta = 0.06$, and $\tilde{\omega}_0 = 0.8$.

Solution:

Solve for the optical thickness using the various values of cloud water path using (9.42). With knowledge of the assumed single scattering albedo, choose the appropriate equations to calculate u^2, τ_{eff}, R, and then Tr. Multiply the calculated value of Tr by 800 W m^{-2} to get the incoming shortwave radiation as a function of cloud water path.

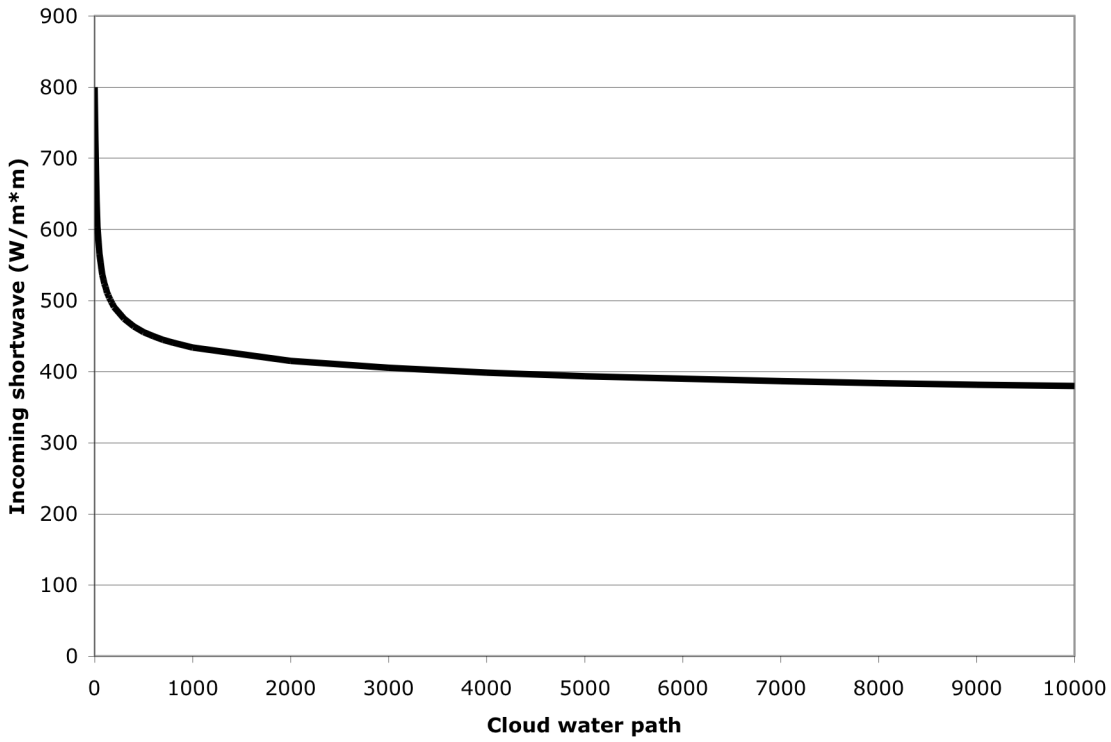

Incoming shortwave radiation as a function of cloud water path. Note that the incoming radiation drops off quickly as the cloud water path increases slowly and decreases by at least 300 W m^{-2} for cloud water paths greater than 170 g m^{-3}.

5] Using the results of 4] with a cloud water path of 1000 g m^{-3}, determine the difference in the shortwave radiation exiting the bottom of the cloud for an uncertainty of 100 g m^{-3} in cloud water path. Since cumulonimbus clouds are associated with cloud water paths of 10,000 g m^{-3}, an error of 10% or 1000 g m^{-3} is probably even more reasonable for this cloud type. Repeat the difference calculations for the exiting shortwave radiation at the bottom of the cumulonimbus cloud. How important are these uncertainties to the resulting calculations of shortwave radiation?

Solution:

For large values of CWP, such as for cumulonimbus clouds, the differences in shortwave radiation exiting the bottom of the cloud are not large. For a 1000 g m^{-3} cloud water path, a difference of 100 yields only slightly more than a 3 W m^{-2} difference in shortwave radiation. At 10,000 g m^{-3}, a 10% error yields differences of around 2 W m^{-2}. Much larger differences are found for the values of cloud water path less than 200 g m^{-3}, where the differences can be much larger for an error of 10%.

Chapter 10

1] Using the sounding data listed below, plot the sounding on a thermodynamic diagram, and calculate the values of N using (10.1) for each height level.

Solution:

Using the sounding data listed at the bottom, plot the sounding on a Skew-T log p diagram.

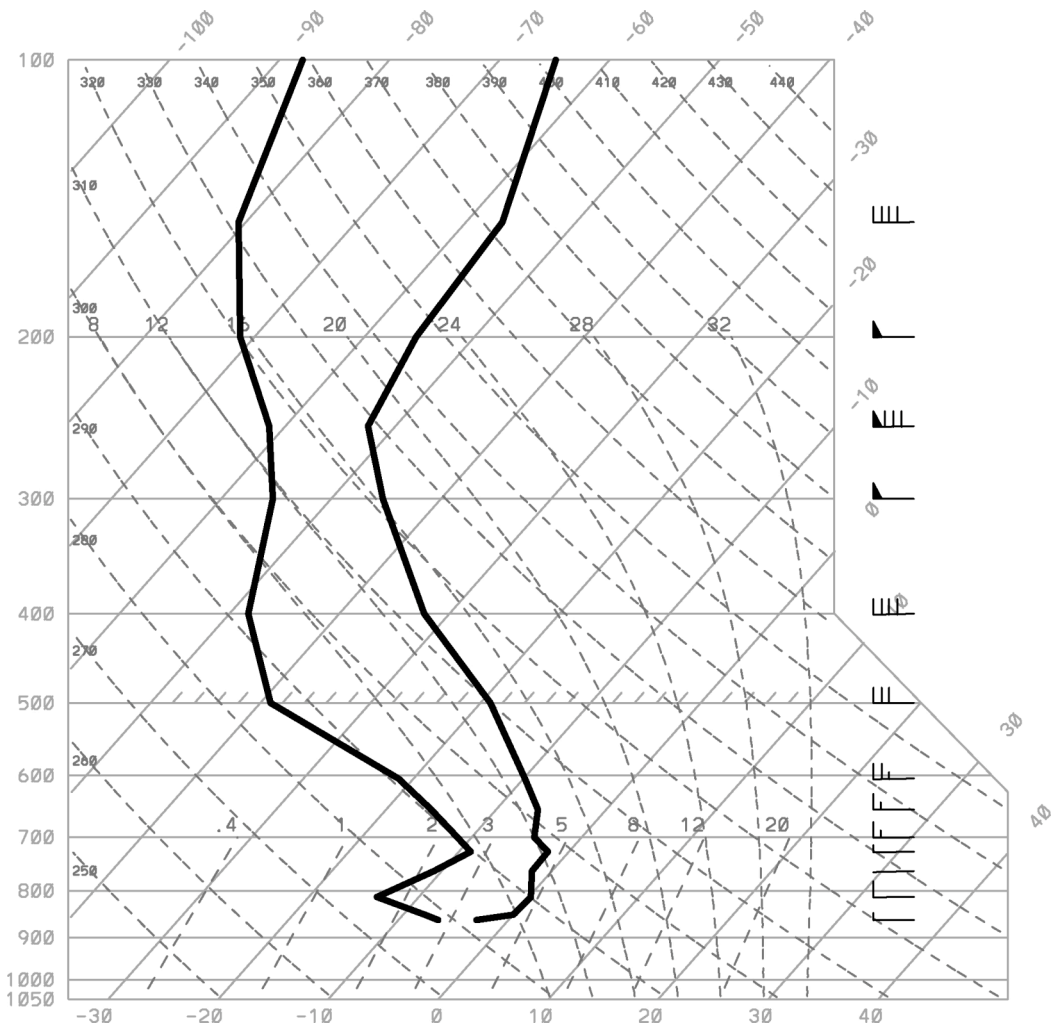

Sounding from data found below.

The next step is to calculate the values of N based upon the sounding data. Recall that

$$N^2 = \frac{g}{\theta}\frac{\partial\theta}{\partial z},$$

and so we can easily find *N* by calculating the potential temperature at each vertical level and then its vertical gradient. Since the number of vertical data points are few, I decided to calculate the vertical gradient of potential temperature from just 2 vertical points instead of a centered difference. These calculations yield the following results.

p	h	t	t(k)	theta	N
861	1475	-2.9	270.26	282.0790752	0.037901286
850	1573	0	273.16	286.1562865	0.019232075
813	1930	0.2	273.36	290.0341052	0.014696734
762	2438	-1.8	271.36	293.2963841	0.018338522
726	2831	-1.9	271.26	297.2746551	0.007238
700	3120	-4.3	268.86	297.7338099	0.015268872
653	3658	-6.2	266.96	301.5650614	0.011599079
604	4267	-9.9	263.26	304.094323	0.011206229
500	5710	-19.1	254.06	309.7639492	0.007985052
400	7320	-32.3	240.86	313.0224775	0.011521169
300	9300	-45.3	227.86	321.5225327	0.012797878
250	10500	-52.5	220.66	328.0294013	0.018777395
200	11920	-55.3	217.86	345.2096445	0.020157006
150	13750	-56.7	216.46	372.4050435	0.017347659
100	16270	-64.9	208.26	402.3517217	

Table showing pressure (hPa), height (m), temperature (C), temperature (K), potential temperature (K), and (s^{-1}).

2] Assume that a mountain exists near this sounding location with a ridge orientation of 180°. Vary the mountain height between 100 and 500 m by 50 m increments and

calculate the inverse Froude number using (10.2). What type of atmospheric response would be expected from this obstacle to the flow?

Solution:

The Froude number is defined using (10.2) as

$$Fr = \frac{Nh}{U}.$$

We already have calculated N, and the problem provides value for h, and the value of U is defined by the sounding. All that is left is to calculate Fr for various values of h. The only challenge is to determine the appropriate values of U and N for given obstacle height values. Here I simply average the values of U and h over the given depth, in an approximate fashion. The corresponding flow behavior is indicated. Note that for the value of Fr = 1.71, I am uncertain if the stratification is strong enough that the flow would only go entirely around the obstacle, or if some of the flow would go over the obstacle. I have opted to be cautious and indicate that the flow would both go around and over the obstacle.

h	Fr	Flow behavior
100	0.57	Over
200	1.14	Over and around
300	1.71	Over and around
400	2.29	Around
500	2.24	Around

3] Given a surface stress of 1.0 $kgm^{-1}s^{-2}$ and $B = 0.2$, calculate δh and Ri_{min} for each height level using (10.22)-(10.23). Explain the mechanics of this calculation and any assumptions made. Would wave breaking occur?

Solution:

Use (10.22) and (10.23) to first calculate the height displacement due to gravity waves (δh) and then calculate the minimum Richardson number for each height level.

h	N	U	t(k)	rho	dh	Ri	Rimin
1475	0.037901286	2	270.26	1.110042182	7.708560586	0.383228274	0.275217345
1573	0.019232075	8	273.16	1.084226268	5.474783849	11.78497638	10.64610663
1930	0.014696734	6	273.36	1.036271808	7.397110592	1.984345909	1.852614423
2438	0.018338522	0.7	271.36	0.978424331	19.95217254	9.818792943	0.673489458
2831	0.007238	3	271.26	0.932543215	15.71377751	0.273472002	0.252973767
3120	0.015268872	7	268.86	0.907172651	7.181042974	67.48052912	52.14180621
3658	0.011599079	8	266.96	0.852285482	7.951255562	1.386050608	1.33362483
4267	0.011206229	14	263.26	0.799411083	6.314022928	65.37198313	60.03489644
5710	0.007985052	16	254.06	0.685727891	7.554578385	10.32968929	10.04580951
7320	0.011521169	20	240.86	0.578646609	6.123715664	20.81533931	20.09003492
9300	0.012797878	25	227.86	0.458744917	5.836606116	0.921294428	0.913295826
10500	0.018777395	41	220.66	0.394761234	4.056095368	2.777201504	2.754958856
11920	0.020157006	25	217.86	0.319867856	5.569506186	54.42697539	50.76336163
13750	0.017347659	20	216.46	0.241452501	7.725626623	76.44389614	67.7591633
16270		15	208.26	0.167306279			

Note that the minimum Richardson number never decreases below it's critical value of 0.25, although it comes close at the surface and again at 2831 m.

4] Increase the values of N in the column by 10%. How does this change the expectations for wave breaking?

Solution:

Simply multiply *N* by 1.1 and recalculate.

h	N	U	t(k)	rho	dh	Ri	Rimin
1475	0.041691415	2	270.26	1.110042182	7.349824136	0.463706211	0.321972382
1573	0.021155282	8	273.16	1.084226268	5.220001584	14.25982142	12.70403509
1930	0.016166408	6	273.36	1.036271808	7.052868218	2.40105855	2.22260863
2438	0.020172374	0.7	271.36	0.978424331	19.02365009	11.88073946	0.64282294
2831	0.0079618	3	271.26	0.932543215	14.98249899	0.330901123	0.30369206
3120	0.01679576	7	268.86	0.907172651	6.846855827	81.65144023	60.89015856
3658	0.012758987	8	266.96	0.852285482	7.581224716	1.677121236	1.606149685
4267	0.012326852	14	263.26	0.799411083	6.020184649	79.10009959	71.75569542
5710	0.008783557	16	254.06	0.685727891	7.203007867	12.49892404	12.10858281
7320	0.012673286	20	240.86	0.578646609	5.838733792	25.18656057	24.18683984
9300	0.014077666	25	227.86	0.458744917	5.564985579	1.114766258	1.103955718
10500	0.020655134	41	220.66	0.394761234	3.867335192	3.36041382	3.330037694
11920	0.022172706	25	217.86	0.319867856	5.310315788	65.85664022	60.80929016
13750	0.019082425	20	216.46	0.241452501	7.366095964	92.49711433	80.58482521
16270		15	208.26	0.167306279			

Increasing *N* moves the values of minimum Richardson number farther away from it's critical value. At 2831 m, it increases from 0.252 to 0.30, which is more than a 10% change in value. Thus, small changes in *N* can lead to different expectations. Try again with a 10% decrease in *N* and see what happens!

5] Increase the values of wind speed normal to the ridge orientation by 10%. How does this change the expectations for wave breaking?

Solution:

Simply multiply *U* by 1.1 and recalculate.

h	N	U	t(k)	rho	dh	Ri	Rimin
1475	0.037901286	2.2	270.26	1.110042182	7.349824136	0.316717582	0.241037705
1573	0.019232075	8.8	273.16	1.084226268	5.220001584	9.739649898	8.977880935
1930	0.014696734	6.6	273.36	1.036271808	7.052868218	1.639955297	1.551177031
2438	0.018338522	0.77	271.36	0.978424331	19.02365009	8.114704912	0.845844385
2831	0.007238	3.3	271.26	0.932543215	14.98249899	0.226009919	0.211909989
3120	0.015268872	7.7	268.86	0.907172651	6.846855827	55.76903233	45.34948519
3658	0.011599079	8.8	266.96	0.852285482	7.581224716	1.145496371	1.110176387

4267	0.011206229	15.4	263.26	0.799411083	6.020184649	54.02643234	50.48613486
5710	0.007985052	17.6	254.06	0.685727891	7.203007867	8.536933295	8.348837787
7320	0.011521169	22	240.86	0.578646609	5.838733792	17.20275976	16.723296
9300	0.012797878	27.5	227.86	0.458744917	5.564985579	0.761400354	0.756007706
10500	0.018777395	45.1	220.66	0.394761234	3.867335192	2.295207855	2.280373171
11920	0.020157006	27.5	217.86	0.319867856	5.310315788	44.98097139	42.55506593
13750	0.017347659	22	216.46	0.241452501	7.366095964	63.17677367	57.38855281
16270		16.5	208.26	0.167306279			

Changes in the value of *U* by 10% lead to two heights with minimum Richardson numbers below it's critical value, right off the surface and at 2831 m.

6] Decrease the value of *B* from 0.2 to 0.1. Describe the changes to the values of Ri_{min}.

Solution:

Change the value of *B* in the equation and recalculate.

h	N	U	t(k)	rho	dh	Ri	Rimin
1475	0.037901286	2	270.26	1.110042182	10.90155093	0.383228274	0.239012135
1573	0.019232075	8	273.16	1.084226268	7.74251357	11.78497638	10.21808646
1930	0.014696734	6	273.36	1.036271808	10.46109412	1.984345909	1.801126543
2438	0.018338522	0.7	271.36	0.978424331	28.21663301	9.818792943	0.232821485
2831	0.007238	3	271.26	0.932543215	22.22263727	0.273472002	0.244884829
3120	0.015268872	7	268.86	0.907172651	10.15552837	67.48052912	47.23203775
3658	0.011599079	8	266.96	0.852285482	11.24477345	1.386050608	1.312581049
4267	0.011206229	14	263.26	0.799411083	8.929376857	65.37198313	58.0066728
5710	0.007985052	16	254.06	0.685727891	10.68378721	10.32968929	9.931316277
7320	0.011521169	20	240.86	0.578646609	8.660241743	20.81533931	19.79991279
9300	0.012797878	25	227.86	0.458744917	8.254207527	0.921294428	0.910005043
10500	0.018777395	41	220.66	0.394761234	5.73618508	2.777201504	2.745810463
11920	0.020157006	25	217.86	0.319867856	7.876471183	54.42697539	49.34885505
13750	0.017347659	20	216.46	0.241452501	10.92568595	76.44389614	64.57508635
16270		15	208.26	0.167306279			

Decreasing the value of *B* by half leads to a general decrease in the minimum Richardson number. There now exist 3 levels where the minimum Richardson number is below 0.25, with the additional level at 2438 m.

7] Using the results of questions 3 through 6, discuss the sensitivities of the parameterization scheme to the model forecasts of the environment the schemes use to predict orographically-produced gravity waves.

Solution:

It is clear that changes of 10% in *N* and *U* can have significant implications for our expectation of gravity wave development from soundings. This type of behavior is very consistent with what we have seen in other parameterizations, namely that small environmental differences can lead to large changes in expected behavior. Thus, one would expect a fair amount of uncertainty in whether or not gravity waves would be expected above a given location if the values of *N* and *U* conspire to place the minimum Richardson number close to it's critical value.

Sounding data for use in questions 1 through 7.

P (hPa)	H(m)	T(°C)	TD(°C)	U(ms^{-1})
861	1475	-2.90	-6.40	2.00
850	1573	0.00	-8.00	8.00
813	1930	0.20	-13.80	6.00
762	2438	-1.80	-10.73	0.70
726	2831	-1.90	-8.90	3.00
700	3120	-4.30	-11.30	7.00
653	3658	-6.20	-15.94	8.00
604	4267	-9.90	-21.35	14.00
500	5710	-19.10	-39.10	16.00
400	7320	-32.30	-48.30	20.00
300	9300	-45.30	-55.30	25.00
250	10500	-52.50	-61.50	41.00
200	11920	-55.30	-71.30	25.00
150	13750	-56.70	-80.70	20.00
100	16270	-64.90	-87.90	15.00